NUMERICAL DYNAMIC STRESS SIMULATION ON BATTERY PACK HOLDER FROM A SINGLE BUMP ROAD TOPOLOGY

PIYAWAT PAETANOM

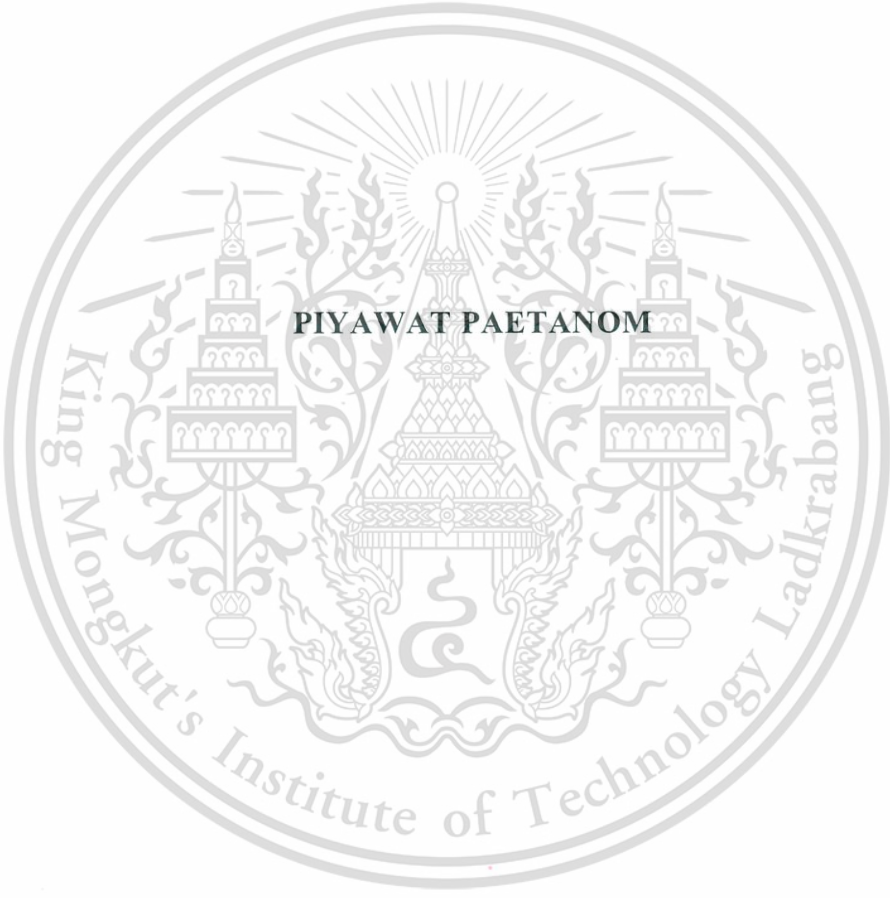

A THESIS REPORT SUBMITTED IN PARTIAL FULFILLMENT
OF THE REQUIREMENTS FOR THE DEGREE OF
MASTER OF ENGINEERING IN AUTOMOTIVE ENGINEERING
INTERNATIONAL COLLEGE
KING MONGKUT'S INSTITUTE OF TECHNOLOGY LADKRABANG
ACADEMIC YEAR 2018

KMITL-2018-IC-M-004-007

NUMERICAL DYNAMIC STRESS SIMULATION ON BATTERY PACK HOLDER FROM A SINGLE BUMP ROAD TOPOLOGY

PIYAWAT PAETANOM

A THESIS REPORT SUBMITTED IN PARTIAL FULFILLMENT
OF THE REQUIREMENTS FOR THE DEGREE OF
MASTER OF ENGINEERING IN AUTOMOTIVE ENGINEERING
INTERNATIONAL COLLEGE
KING MONGKUT'S INSTITUTE OF TECHNOLOGY LADKRABANG
ACADEMIC YEAR 2018
KMITL-2018-IC-M-004-007

THESIS TITLE	Numerical Dynamic Stress Simulation On Battery Pack Holder From A Single Bump Road Topology
STUDENT NAME	Mister Piyawat Paetanom
STUDENT ID	58610003
DEGREE	Master of Engineering
PROGRAME	Automotive Engineering
ADVISOR	Asst.Prof.Dr.Panya Kansuwan
CO-ADVISOR	Dr.Chi-na Benyajati
CO-ADVISOR	Prof.Dr.Masaaki Okuma

ABSTRACT

The electric vehicle is an emerging technology which uses sustainable and renewable energy. It is an alternative option to reduce emissions in the transportation system. However, the major challenge facing an electric vehicle industry is the duration that can operate per charging. Hence, the researchers have installed as many battery packs as possible on an electric bus. Consequently, finding appropriate locations becomes a challenge in both performance and functionality-wise. This will be an issue for a low-floor bus configuration due to the service requirements for the disability and elderly accompanied by a limited installation space in the lower area. The installation of the battery packs on the roof is considered in this study. The objective is to evaluate and to analyze the damage that occurred at the battery pack holder on each design. The method of analysis is a dynamic suspension system. The system cooperates the full bus model travelled over the interested road profile to the finite element analysis of the battery pack holder. The virtual bus model was created and simulated using multi-body systems software, i.e. MSC.ADAMS/Car. The dynamic suspension system was applied as the boundary condition in finite element model, where the finite element model of bus structure was modeled and simulated using the software (HyperMesh via HyperWorks). The non-linear dynamic loading simulation of the finite element model was done by RADIOSS solver. The dynamic displacement of the suspension system from the multi-body simulation shows a strong correlation with the road profile. Furthermore, the dynamic stress of each design of the battery pack holder during the speed bump maneuvers of the electric bus demonstrate a great performance. The results of dynamic acceleration, the displacement of battery packs, and the stress on the roof structure can conclude that the battery holder design is the most appropriate design.

ACKNOWLEDGEMENT

The author gratefully acknowledge support from Thailand Advanced Institute of Science and Technology and Tokyo Institute of Technology (TAIST-Tokyo Tech) by National Science and Technology Development Agency (NSTDA) for providing full scholarship. This study has been conducted as part of a research project in the Light Weight Engineering Laboratory, National Metal and Material Technology Center (MTEC), and KMITL International College.

The author would like to express his sincerest thanks and appreciation to his major advisor, Dr.Chi-na Benyajati, Light Weight Engineering Laboratory, MTEC, Asst.Prof.Dr.Panya Kansuwan, department of Mechanical Engineering, KMITL and Prof.Dr.Masaaki Okuma, department of Mechanical Engineering, Tokyo Tech. for their advice and support, as well as helping to guide the problems and providing the valuable opportunities for this research.

Piyawat Paetanom

December, 2018

TABLE OF CONTENTS

LIST OF TABLES

Table **Page**

LIST OF FIGURES

Figure **Page**

LIST OF SYMBOLS

a, $\ddot{x}$	Acceleration
C	Damping value
x	Displacement
F	Force
g	Gravity force
X	Longitudinal direction
Y	Lateral direction
M	Mass
K	Spring Constant
t	Time
Z	Vertical direction
W	Weight
F_s	Spring force
M_i	Modal mass for the i^{th} mode
K_i	Modal stiffness for the i^{th} mode
F_i	Modal force for the i^{th} mode
M_{bb}	Mass coupled between boundary d.o.f.
M_{bi}	Mass coupled between boundary and internal d.o.f.
$\dot{x}$	Velocity
ω_f	Eigenfrequency
φ	Mode shape
∂	Modal coordinate
ω	Natural frequency
Δt	Time increments
$[\phi_c]$	Constraint Modes Matrix
$\{\phi_f\}$	Free-interface Vibration Modes
$\{\phi_r\}$	Rigid body modes
$\{\phi_i\}$	Set of Eigenvectors
$\{\lambda\}$	Set of Eigenvalues

LIST OF DEFINITIONS

CG	Center of Gravity
CAD	Computer Aided Design
CAE	Computer Aided Engineering
CAM	Computer Aided Manufacturing
CMS	Component Mode Synthesis
DoF	Degrees of Freedom
FEA	Finite Element Analysis
FEM	Finite Element Method
MBS	Multi-Body System / Multi-Body Simulation
MF	Magic-Formula
NVH	Noise, Vibration and Harshness
VPG	Virtual Proving Ground
WFT	Wheel Force Transducers

CHAPTER 1

INTRODUCTION

1.1 Background

Nowadays, designs of a vehicle structure are of fundamental importance to a vehicle performance. The structure must be strong and durable. It has to be optimized and tested several times. Automotive companies need to reduce cost and time of development for a new product. The durability test is a time-consuming process. It is impossible to test a lot of different road surfaces. The cost will be very high and shows only visible results. The heavy vehicle manufacturer tried numerous methods to test the durability. The Computer Aided Engineering (CAE) methods were employed during the design process to help cutting-down the time and cost involved in physical proving-ground or durability test. Such methods include vehicle and component testing on public roads, proving grounds and in various types of test rigs. The computer simulation using Finite Element Method (FEM) has a role in the design section and the durability testing process.

The design of battery pack holder that can support the weight and the movement of the battery packs during various driving situations were the main purposes. One of the most challenging design was to ensure the strength and durability of the holder when it experiences a dynamic behavior of the bus. The virtual testing is being given a more influential role in component development. Replacing physical durability testing with virtual testing procedures necessitates analyses able to consider full vehicle surroundings. The lifetime of components can be determined by magnitude of the loads acting on it. Vehicle durability is one of the many important aspects of the vehicle development. The durability testing is a time-consuming and a high-cost process.

The method of a Multi-Body System (MBS) was employed to study the dynamic behavior of interconnected rigid or flexible interconnected bodies observing about the translational and rotational displacements. An advantage of the multi-body system is the calculation of the mechanical systems that moves under the influence of forces. Virtual Proving Ground (VPG) approach involves driving the model over a virtual 3D-road to obtain the dynamic stress. It corresponds to the road profile of the test track segment at which the physical testing was performed.

This application can be used in many fields to improve or to develop the design of the vehicle. It can reduce the time and cost to predict the components lifetime.

1.2 Research Objectives

- This thesis aims to study the durability and the stress distribution of designed battery packs holder through dynamic analyses using Finite Element Method and Multi-body simulations.
- To investigate the effect of virtual proving ground condition through bus structure model to the battery packs holder.

1.3 Scopes of the research

- Full bus model was created by ADAMS/Car (MSC.Software Corporation, 2012a), consisted of tires, front and rear suspension systems, power train, steering systems, chassis and skeleton structure. Tire was expressed as a subsystem, to calculate the displacement on the suspension mounting point via determination of the acting forces from the tire contacts with road surface to the structure.
- The parts such as windshield, doors, seat, and the interior components have been included in the vehicle structure.
- The road chosen is a single bump condition. To show the period that the displacement exerted on the structure causes the highest stress on the battery packs holder on the roof of bus structure.
- The limitation of the study is the investigation of the stress distribution on the battery packs holder in the finite element model via HyperWorks: HyperMesh (Altair Engineering, Inc., 2016). The durability analysis of the vehicle subsystems such as suspension components, transmission, engine and the interior parts are out of scope of this study. In addition, the fatigue life is not investigated.
- The investigation of the type of finite element model and their properties such as mesh type are not covered.

CHAPTER 2

LITERATURE REVIEW

2.1 Fundamentals of metal failure

Metal structure when subjected to repeated loading exhibit damage by fatigue. The magnitude of stress in each cycle is not sufficient to cause failure with a single cycle. Large numbers of cycles are therefore needed for failure by fatigue. Therefore, for accurate prediction of fatigue failure in structural components, accurate prediction of dynamic stress time histories is required.

Fatigue manifests in the form of initiation or nucleation of a crack followed by its growth till the critical crack size of the parent metal under the operating load is reached leading to rupture. The crack can be either safe or unsafe. The component under cyclic load works satisfactorily for years, even with the growth of hidden cracks, but ruptures suddenly without any pre-warning (Frost,K. J., 1976). Such characteristics make cyclic load dangerous. The fatigue analysis is based on the assumption that most damage areas are experiencing stress (Engineering Technology Associates, Inc., 2009), for vehicle behavior, the various loads are caused by road conditions or vibration from a driveline. The growth of these cracks in material will lead to fatigue in the components of vehicle.

2.2 Durability testing in the automotive industry design

Nowadays, the testing of vehicle design can be done in several methods. In each method have different advantages; it can be selected to suitability of the test design. The main purpose of the vehicle testing is to determine the strength, durability, handling or performance, including noise, vibration and harshness (NVH). The vehicle durability testing for the strength of a vehicle component or structure, the methods are usually performed in testing on comprehensive proving ground, Laboratory test rigs or Computer simulation (CAE, FEM, and MBD). For the load prediction and the indications of defects in design about strength and fatigue, advanced computer simulation has played a role in designing stage and computing the durability of components.

The virtual prototype for testing needs to design iterations by virtual testing to get the best of design. In order to reduce the production of virtual prototypes is expensive and time-consuming. As (Ferry, Frise, Andrews, & Malik, 2002) mentioned, the component

design iterations with virtual testing without the need of a physical prototype is a great advantage due to reduce the production time consumption and cost savings in prototyping. (Kyung-Won Suh, Suh, & Hong, 2000) was describe, in the side of vehicle durability, it is surely impossible of a car to be tested on a lot of pattern road in the field. One test takes away a lot of time and money and provides only visible results. Of laboratory durability tests the road simulator test and the multi-axial test are best similar to the proving ground test, but those are different in the input load and constraint terms. The method brings fast and accurate results only in few laboratory tests where the body is under the equal condition in the load and constraint to the durability analysis, but has some limitations in being applied to the vehicle durability test in the proving ground. The reliance of simulation testing results is often questioned. So physical testing will still be an important part of the product design stage.

Wherewith physical testing has been applied for decades in the automotive industry, these methods have been progressively developed over the years. The results of the stress that caused the fatigue damage from the test. The stress occurred depends on the number of load cycles on the component and the duration of the test. The physical testing usually takes a long time-consuming. Therefore, reducing the time spent on physical durability testing is important. As (Zwaanenburg, 2002) mentioned that the more advanced development stages are demonstrated design based on virtual testing with few physical prototype data.

2.3 Types of physical durability testing

There are many different types of physical durability testing. The duration and conditions are different. The manufacturer will be select the types of test as appropriate the conditions of testing. Different types of physical durability tests are discussed in detail below.

2.3.1 Long-term road testing

The test is usually done by running a vehicle on a public real road or test tracks. This test is aim to study the full vehicle driven with fully loaded to achieve real driving situation. Long-term testing ensures that accurate data is being replicated during customer usage such as the weight of the load or the driving behavior (Chien & Kuchipudi, 2003). This type of test can effectively display results, but in the other hand,

the disadvantage of this test is that it has a lot of testing equipment and it is spent extremely time consuming. This testing method can apply to making short-term route predictions for vehicle drivers (Krumm, 2008).

Figure 2.1 2015 Honda Odyssey EX Long-Term Test: 19,000 Miles (T. Cain, 2017)

2.3.2 Proving ground testing

The proving ground testing is the track used for testing vehicle. The purpose is to determine the durability and probable life of components. The enforcement of standards through component was testing to find weaknesses that need to be resolved, and the effects of equipment under various conditions, including extreme temperatures and weather conditions, difficult terrain, and excessive use (Aakanksha Gaur, 2014). The proving ground test track have various durability test tracks such as obstacle courses that corresponding to various rough roads condition. The obstacles have specific characteristics about the damage to vehicle that are likely to be dealt with under similar conditions to normal road. Proving ground testing also classifies as a full vehicle test. But the test is limited by repetitive run over tracks in durability testing. And it also shows only the visibility of serious damage from these obstacles (Halfpenny & Pompetzki, 2011).

Figure 2.2 Japan Automobile Research Institute Proving ground, Japan. (JARI, 2013)

2.3.3 Components testing

The component testing is another important step in vehicle durability testing. In case of the assumptions of structural durability analysis, the differences in driving behavior and vehicle usage as well as variations in road characteristics and environmental conditions. The structural integrity analysis is based on statistical methods, which are considering the variation of component strength and road loading. The component testing is playing a role in the design of the vehicle components with the need to cut-off the processing time and cost as well as the increasing of the reproduction of prototype components in developing stage (Pötter, 2012). In this type of testing those test components can be tested independently as a component without the other components. The test consists of a structural load test that conforms to a specific configuration standard. It is a test technique using occasional loads with a small test rig to perform tests on components like a bracket or chassis component. Test specimens are confined to the test rig and are repeatedly loaded by predefined displacement or frequency spectrum in the case of a vibration test until failure occurs. In principle, several samples are tested for durability. This test can be used as a basis for the prediction of components or subsystems that have been tested. The study of (Bonato & Goge, 2016)'s illustrate a set of tools can be

used to compare the vibration signals used to determine the mechanical durability of vibration-damping in vehicle components.

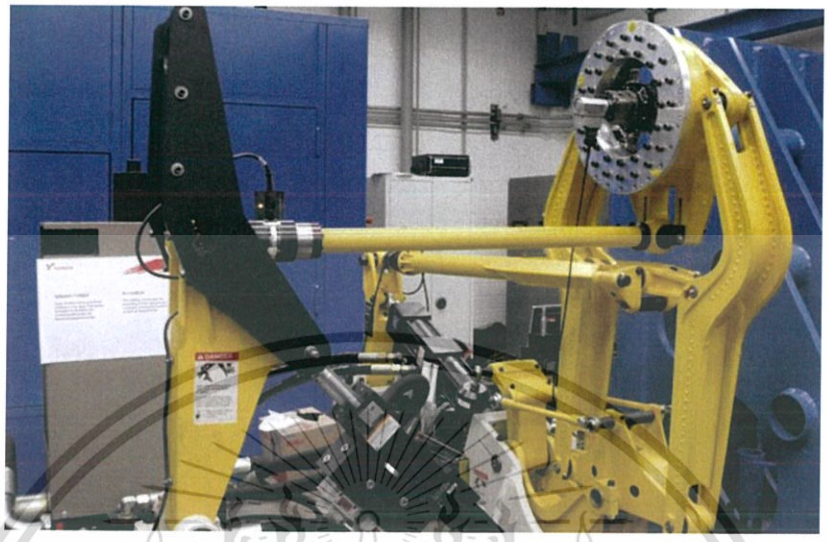

Figure 2.3 Multi axis suspension test rig (VETR, 2014)

2.4 Virtual prototype durability testing

The growing of the automotive industry makes it imperative to reduce development time and consequently. One of the most expensive steps in the vehicle development process is the durability field testing, in terms of the number of prototypes used and the time required to complete the course. The fatigue life prediction methods are an important part in the durability analysis via Computer-Aided Engineering (CAE). In order to be reliable and also reduce development time and costs, the precision of loads acting on the structure that can accurately represent the field durability tests is very important. Virtual durability testing can include common stress and strain analysis in Multi-body dynamics system analysis and finite element method to predict load (Mahendra A. Petale, 2016). The main advantages of this approach include that the design can be evaluated before a prototype is available and virtual testing results can be easily validated by subsequent physical testing. The virtual prototyping process has been shown in the Figure 2.4.

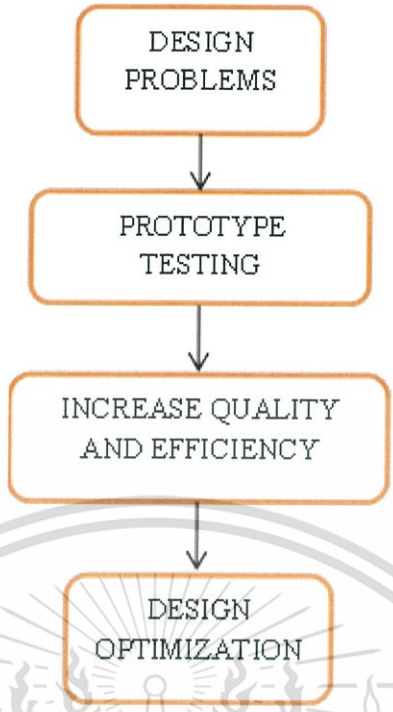

Figure 2.4 Virtual Prototyping Process

The literature on estimation of fatigue life, both in modeling and evaluation, is available in the CAE or FEM applications (Bishop, 2012; Niemi, 1995). Therefore, it is referred to in the theories and methods.

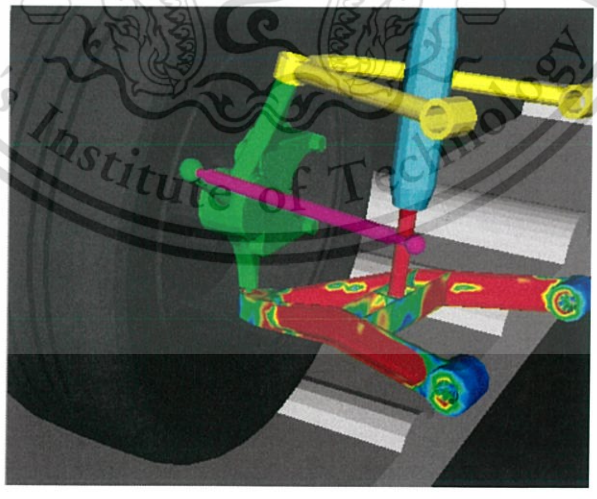

Figure 2.5 Life prediction of lower a-arm via ADAMS/Car simulation (MSC.Software Corporation, 2012a)

2.5 Static analysis

The Fatigue assessment of subsystems or automotive components requires the completion of a virtual vehicle durability test. The fatigue prediction is based on static analysis of the subsystem or components. Static loads are derived from different dynamic theoretical calculations based on the type of load. These loads are applied to calculate the durability and fatigue of the components in the design process through the finite element method. The estimation of the fatigue for the structural response can be the superimposed (Lee, Barkey, & Kang, 2011).

Analysis of the structure of the components has different conditions and techniques to analyze the suitability of the components. Static structure analysis can be divided into two techniques. The boundary conditions of an analytical structure often determine which technique is most appropriate. The conventional static analysis requires a constrained structure. While the second technique is static analysis with inertia relief is used for unconstrained structures.

According to (Kuo & Kelkar, 1995), the disadvantage of static analysis is the interpretation of dynamic with static load. There is a tendency to lack precision due to free vibration considerations and dynamic effects are not taken into account in calculations.

2.5.1 Static analysis with inertia relief

Unconstrained structure analysis is exemplified in a variety of ways, such as the driving of vehicles on the road or the movement of aircraft in the air. In general, the automotive industries, there is an unconstrained structural analysis under static or quasi-static load. The equilibrium state in inertia relief analysis is the calculation of sum of applied force and moment in the systems. The calculation of the distribution of nonlinear internal forces can be done by the inertia relief method (Liao, 2011). In the calculations, it is necessary to use the load duration that is greater than the time interval of a rigid body mode to achieve more accurate in the inertia relief calculation. However, due to the singularities in the stiffness matrix introduced from rigid body motion, finite element static analysis cannot be used in the case of unconstrained structures. So, static analysis with the inertia relief technique will play a role in solving this problem. This technique will consider the external load used and calculates the acceleration of the solid body relative to the reference point.

The selected constraints for inertia relief calculation eliminated rigid body motions and didn't generate associated constraint forces while actual structural supports had constraint forces. Thus, the topology optimization was different for the case with inertia relief effects in comparison with the case without inertia relief.

The theory and simple equation of inertia relief method will be explained in this section. The basic equations of the static analysis with inertia relief method are derived from the dynamic theory as (Lee et al., 2011) described.

The example of inertia relief method is explained by (Liao, 2011), two masses with different weight ($W_1 > W_2$), are connected together with a spring that having the constant elastic value (K) with apply the external force (F) to mass 1 (m_1). The assumption of this example is the movement of mass 1 and 2 (m_1 and m_2) and also the spring can move in vertical direction only (Z axis). The external force is applied larger than the weight of mass 1 (m_1), thus the mass 1 will move along the axis, while the mass 2 is heavier will going down with gravity. The spring that connected to both of masses is compressed. When the force acting to spring is greater, the spring is compressed enough to cause a reaction force greater than the weight of the two masses, ($W_1 + W_2$), the mass 2 (m_2) is pushed to moved up in vertical direction. After a while, the system goes into steady-state, this means that mass 1 and 2 are move in the same direction with constant a11cceleration, the system is shown in Figure 2.6.

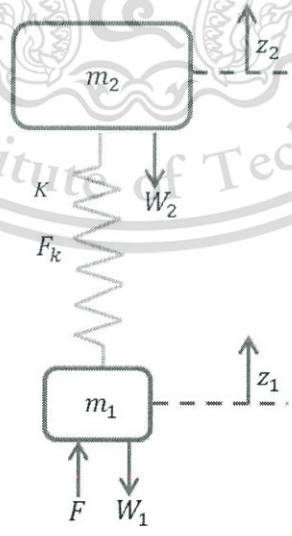

Figure 2.6 Mass-Spring systems model

The constant acceleration of the linear mass-spring systems can calculate by eq. (2.1).

$$a = \frac{F - W_1 - W_2}{m_1 + m_2} = \frac{F - W_1 - W_2}{(W_1 + W_2)/g} \tag{2.1}$$

When the system is going to steady-state, the spring force equation can calculate by eq. (2.2)

$$F_s = K(z_1 - z_2) \tag{2.2}$$

Where, the external force of the systems will be calculated separately for each mass. This is shown in eq. (2.3) and (2.4).

At mass 1; $$F - F_s - W_1 = m_1 a \tag{2.3}$$

At mass 2; $$F_s - W_2 = m_2 a \tag{2.4}$$

After getting the equation of external force and spring force, so the equation of motion will be derived as show in eq. (2.5)

$$a\begin{bmatrix} m_1 & 0 \\ 0 & m_2 \end{bmatrix} + \begin{bmatrix} k & -k \\ -k & k \end{bmatrix} \begin{Bmatrix} z_1 \\ z_2 \end{Bmatrix} = \begin{Bmatrix} F - W_1 \\ -W_2 \end{Bmatrix} \tag{2.5}$$

To determine the position of two masses when the system is not constrained, the relative displacement can use in this condition by restraining either z_1 or z_2. The equation of relative displacement will be derived as eq. (2.6) and (2.7)

If $z_1 = 0$; $$z_2 = \frac{(-m_2 a - W_2)}{k} = \frac{\left(-\frac{W_2}{ga - W_2}\right)}{k} \tag{2.6}$$

If $z_2 = 0$; $$z_1 = \frac{(m_2 a + W_2)}{k} = \frac{\left(\frac{W_2}{ga + W_2}\right)}{k} \tag{2.7}$$

From the equation above, it can be noticed that the relative displacements of z_1 and z_2 are the same for both constraints. This means that, the selection of constraints in the inertial relief analysis does not affect the results of acceleration and deformation of the structural system.

However, the application of inertia relief techniques in the case of structural stresses analysis is rather limited. The inertia relief method can be applied to the condition of a structural system with dynamic loading conditions only if the system has a natural frequency below the natural frequency of structure as (Kuo & Kelkar, 1995) explained.

2.6 Dynamic analysis

The structure of model is subjected by input loading, which the load is respect to time-frequency domain. The transient response of the structure can be calculated by the Dynamic analysis. The basic elements of the dynamic system are consisting of 4 elements, mass, energy distribution (damper), resistance (spring) and applied load. As the model is subjected to input load cause the model has moves in response to applied load. The dynamic motion of the model is described by the equilibrium equation with the equation of motion. From the description of (Cook, 2001), the most common dynamic analysis in finite element method are discussed below.

2.6.1 The equation of motion

The equation of motion is the equation that describes the equilibrium condition of the motion of physical systems in terms of time domain (Siemens Industry Software, 1993). The equation of motion is represented as eq. (2.8)

$$M\ddot{x}(t) + C\dot{x}(t) + Kx(t) = F(t) \qquad (2.8)$$

The equation to motion described the input load acting on the system respect with time domain. Which M is the mass, C is the damping that approximates the energy distribution in the structure, and K is the static stiffness where the $\ddot{x}$, $\dot{x}$ and x are the nodal accelerations, velocities and displacement.

For the static analysis, the acceleration and velocity are considered to be very small value compared to displacement. Therefore, the inertia and damping forces are

neglected. The objective of a dynamic analysis is to determine the solution of the equation of motion such as accelerations, velocities, displacement and/or stresses which is in time domain.

In automotive industry, the dynamic analysis is applied to the structural dynamics calculation method with finite element analysis application. These calculations method improve in calculating the structural dynamic problems.

2.6.2 Modal analysis

Modal analysis is the calculation and analysis of dynamic responses of structures or systems in engineering during testing or excitation. In structural engineering, Modal analysis uses to analyze the structure to determine the various time period that will naturally resonate (Dr. C. M. Ramesha, Singh, & Chetan S Naik, 2015). The overall mass and stiffness of structure will be relevant in this analysis. The structure frequency must keep away from natural frequencies (Mahmoodi-k & Davoodabadi, 2014). If both frequencies have matching, the structure may experience structural damage.

The vibration of the system without external forces, unconstrained and no response changes by just only natural behavior. In this type of system, the damping will not have involved. A free system mentioned above will describe by the eq. (2.9)

$$M\ddot{x}(t) + Kx(t) = 0 \tag{2.9}$$

The response of system is given in eq. (2.10)

$$x = \varphi_i sin(\omega_i t) \tag{2.10}$$

$$\omega = \sqrt{\frac{K}{M}} \tag{2.11}$$

Where, φ_i represent the mode shapes, ω_i is the natural frequency of system, t is the time and the i^{th} is the eigenvalue and eigenvector; $i = 1,2,3 \ldots n$

From eq. (2.9) and (2.10), the equation can be rewrite as eq. (2.12)

$$(K - \omega_i{}^2 M)\varphi_i = 0 \tag{2.12}$$

2.6.3 Transient response analysis

Transient response analysis is a common method to compute dynamic responses. In order to determine the behaviour of the structure that is induced by time. Input load applied as load at each time interval. These loads are in the form of applied force that determines the motion of an object in direction. Calculation with the method of transient response analysis will obtain the results are displacements, velocities, and accelerations of each node, and also contain of forces, stresses and strains energy in elements. Analysis with this technique is appropriate for analysing interest in the full response history of the vehicle structure with each load of road profiles. This method of analysis techniques is recommended for transient response prediction of a non-linear structure correspond to those for non-linear elements under the same condition (Burgress, 1988). This analysis method is divided into 2 different numerical methods, according to the characteristics of the structure and input load as (Cook, 2001) described.

2.6.3.1 Direct transient response analysis

The direct transient response analysis is the calculation method of the response of a system with load over time. This analysis method is more efficient when analyzing with high frequency excitation that required a large number of modes. The direct transient response analysis is performed by direct integration (Siemens Industry Software, 1993). The responses in the structure are typically calculated at different time intervals, separated by time increments Δt. The expression for velocity $\{\dot{x}(t)\}$ and acceleration $\{\ddot{x}(t)\}$ at the current time increment will derive in eq. (2.13) and (2.14) at any time n.

For velocity;
$$\{\dot{x}_n\} = \frac{1}{2\Delta t}(x_{n+1} - x_{n-1}) \tag{2.13}$$

For acceleration;
$$\{\ddot{x}_n\} = \frac{1}{\Delta t^2}(x_{n+1} - 2x_n + x_{n-1}) \tag{2.14}$$

From the equation above, these are then substituted into the equations of motion in eq. (2.15).

$$\left[\frac{M}{\Delta t^2}\right](x_{n+1} - 2x_n + x_{n-1}) + \left[\frac{C}{2\Delta t}\right](x_{n+1} - x_{n-1}) + \left[\frac{K}{3}\right](x_{n+1} + x_n + x_{n-1}) = \frac{1}{3}(F_{n+1} + F_n + F_{n-1}) \quad (2.15)$$

Separate the equation into individual variables and rewrite in eq. (2.16).

$$[P_1]\{x_{n+1}\} = [P_2] + [P_3]\{x_n\} + [P_4]\{x_{n-1}\} \quad (2.16)$$

Where;

$$[P_1] = \left(\frac{M}{\Delta t^2} + \frac{C}{2\Delta t} + \frac{K}{3}\right)$$

$$[P_2] = \frac{1}{3}(x_{n+1} + x_n + x_{n-1})$$

$$[P_3] = \left(\frac{2M}{\Delta t^2} - \frac{K}{3}\right)$$

$$[P_4] = \left(-\frac{M}{\Delta t^2} + \frac{C}{2\Delta t} - \frac{K}{3}\right)$$

The mathematical algorithms used in the finite element software will be divided into implicit and explicit integration. In terms of application, the explicit method is almost used in the simulation of crash and rollover testing under various conditions. On the side of structure dynamics problem, the input loads are varying slowly with times change and only lower modes has important in the response of the structure, the implicit approach would be more appropriate for this problem (Kim Bladh, 2012). However, the explicit method will be more computationally in each time step. The larger of finite element model like full vehicles finite element models results in larger d.o.f. systems, which in turn influences the computing resources required as (Cook, 2001) described.

2.6.3.2 Modal transient response analysis

Another method for computing the transient response of a structure is the modal transient response analysis. This method is use to reduce the size in the mode shapes of structure where normal mode shapes are overlapped to characterize the dynamic response of a linear structure (Siemens Industry Software, 1993). Model size reduction is performed to reduce the cost of computation. When the equations of motion are uncoupled, this analysis will make the numerical integration more efficient. The modal transient response analysis is a natural extension of a normal mode analysis which the mode shapes of structure are generally calculated as part of the structure.

The modal transient response analysis is based on the mode superposition method. As the first step in formulation, transform the variables from physical coordinates $x(t)$ to modal coordinate $\partial(t)$ shown in eq. (2.17)

$$x(t) = (\varphi)\{\partial(t)\} \tag{2.17}$$

The mode shapes (φ) are used to change the problem in terms of behavior of the mode is opposed to the behavior of the grid point. The eq. (2.17) denotes equality if it is calculated and uses all modes.

From the eq. (2.9) show the damping is ignored, then substitute eq. (2.17) into eq. (2.9) as eq. (2.18)

$$[M][\varphi\{\ddot{\partial}(t)\}] + [K][\varphi\{\partial(t)\}] = F(t) \tag{2.18}$$

As eq. (2.18) is the coupled of the equation of motion. To uncouple this equation, need to multiply by $[\varphi]^T$ as shown in eq. (2.19)

$$[\varphi]^T([M][\varphi\{\ddot{\partial}(t)\}]) + [\varphi]^T([K][\varphi\{\partial(t)\}]) = [\varphi]^T\{F(t)\} \tag{2.19}$$

Where; $[\varphi]^T[M][\varphi]$ = Modal mass matrix

$[\varphi]^T[K][\varphi]$ = Modal stiffness matrix

$[\varphi]^T\{F(t)\}$ = Modal force vector

The uncoupled of the equation of motion will be rewritten in a set of single degree of freedom systems form as eq. (2.20).

$$M_i\ddot{\partial}_i(t) + K_i\partial_i(t) = F_i(t) \tag{2.20}$$

Where; M_i = Modal mass for the i^{th} mode

K_i = Modal stiffness for the i^{th} mode

F_i = Modal force for the i^{th} mode

2.7 Component mode synthesis

The component mode synthesis (CMS) is common method to analyses the complex structural system having different connected of subsystems with dynamic response. The CMS approach is a very useful tool in dynamically structured analysis and evaluating stress in structural engineering problems. This technique is suitable for modeling and simulation of large and complex systems (Ulf Sellgren, 2003). The CMS also play a role in the multi-body systems simulation (MBS). The Finite element model of subsystem in MBS which using the CMS can be formulated and imported as a flexible body. This will lead to dynamic system analysis, taking into account the flexibility of components. It also includes an analysis of specific components when in a system environment, coupled with MBS components with linear and nonlinear features. The common techniques for flexible body in multi-body system are the Craig-Brampton method and the Craig-Chang method that will be discussed by (S. Vizzini, 2014).

2.8 The Craig-Brampton method

The Craig-Brampton method is one of the reduction methods to re-characterize large finite element models into relatively small matrices. These methods consist of two types of modes; the fixed-interface modes and the constraints modes (S. Vizzini, 2014). The corresponding displacement and acceleration are represented by x and $\ddot{x}$. The applied forces in time domain are represented by $F(t)$. The resulting of the equation of motion for the free unconstrained modes is same as eq. (2.9) shown in eq. (2.21)

$$M\{\ddot{x}\} + K\{x\} = F(t) \tag{2.21}$$

2.8.1 The fixed-interface modes

The fixed-interface normal modes are the vibration modes of structure. These modes contain of vibrational of structure with the fixing of all boundary point, degree of freedom (d.o.f.). In the calculation, the Craig-Brampton method require the boundary d.o.f. (x_b) and internal d.o.f. (x_i), it is convenient to partition these systems into matrices (S. Vizzini, 2014).

From x in eq. (2.21);

$$\{x\} = \begin{bmatrix} x_i \\ x_b \end{bmatrix} \tag{2.22}$$

So, eq. (2.21) becomes;

$$\begin{bmatrix} M_{ii} & M_{ib} \\ M_{bi} & M_{bb} \end{bmatrix} \begin{Bmatrix} \ddot{x}_i \\ \ddot{x}_b \end{Bmatrix} + \begin{bmatrix} K_{ii} & K_{ib} \\ K_{bi} & K_{bb} \end{bmatrix} \begin{Bmatrix} x_i \\ x_b \end{Bmatrix} = \begin{Bmatrix} F_i \\ F_b \end{Bmatrix} \tag{2.23}$$

From the eq. (2.23), the boundary and internal are representing in b and i. The mass coupled between boundary d.o.f. is in M_{bb} and M_{bi} as the mass coupled between boundary and internal d.o.f. The boundary fixed-interface mode is the result from solving the eigenvalue of the internal set with boundary fixed. Then, the constrain of boundary d.o.f., $\{x_b\} = 0$;

$$[M_{ii}]\{\ddot{x}_{ii}\} + [K_{ii}]\{x_{ii}\} = 0 \tag{2.24}$$

The basic of Eigenvalue equation will be present in eq. (2.27) with the set of eigenvalues $\{\lambda\} = {\omega_n}^2$ and eigenvectors $\{\phi_i\}$.

$$([K] - \{\lambda\}[M])\{\phi_i\} = 0 \tag{2.25}$$

As the equation above, the equation that gives the result of eigen modes and eigen frequencies of the fixed-interface vibration modes will derived in eq. (2.26).

$$([K_{ii}] - \omega_i{}^2[M_{ii}])\{\phi_i\} = 0 \quad (2.26)$$

The full matrix of eigen modes represents the fixed-interface vibration modes is show in eq. (2.27)

$$[\phi_i] = [\{\phi_{i1}\}\{\phi_{i2}\}\{\phi_{i3}\} \dots \{\phi_{in}\}] \quad (2.27)$$

2.8.2 The constraint modes

The mode of static deformation by the displacement of unit used with one of the boundaries d.o.f. while other boundaries are inhibited and no force is applied to the interior d.o.f. (Bampton & Craig, Jr., 1968) It can be said that the constraint modes are the static displacement of the structure that caused by the deflection of the unit defined at the interface d.o.f.

With the zero inertial effects for the static modes, $F_i = 0$, the calculation of the constraint mode from eq. (2.23) will show in eq. (2.28).

$$[M_{ii}]\{\ddot{x}_i\} + [M_{ib}]\{\ddot{x}_b\} + [K_{ii}]\{x_i\} + [K_{ib}]\{x_b\} = 0 \quad (2.28)$$

It can be neglect the inertia forces from the static displacement of the structure. Therefore, the constraint modes equation can rearrange in eq. (2.29)

$$\{x_i\} = -[K_{ii}]^{-1}[K_{ib}]\{x_b\} \quad (2.29)$$

From the equation above, the term of $-[K_{ii}]^{-1}[K_{ib}]$ is consider as static mode. So, the constraint mode matrix with respect to the entire substructure can be written in eq. (2.30).

$$\begin{bmatrix}\{x_i\}\\ \{x_b\}\end{bmatrix} = [\phi_c]\{x_b\} = \begin{bmatrix}-[K_{ii}]^{-1}[K_{ib}]\\ [I]\end{bmatrix}\{x_b\} \quad (2.30)$$

Where, $[\phi_c]$ is the constraint modes matrix.

2.9 The Craig-Chang method

The Craig-Chang method is the approach to use the free-interface normal mode which the basic of reduction (S. Vizzini, 2014). The component will be considered in unconstrained condition.

2.9.1 The free-interface modes

The free-interface normal modes are the vibration modes that simply with the structure modes with unconstrained condition. The calculation of this method can be done by solving the eigenvalue of the total mass and stiffness matrix. The equation of the free-interface mode is the same with the eq.(2.26). with free-interface vibration modes, $\{\phi_f\}$ and eigen frequencies ${\omega_f}^2$ that will rewrite in eq.(2.31).

$$([K_f] - {\omega_f}^2[M_f])\{\phi_f\} = 0 \tag{2.31}$$

2.9.2 The rigid body modes

The rigid body modes are the vibration modes of free-interface vibration mode in the structure that can be translate in any direction without shape deformation. The eigen frequencies those related to these modes can be neglected in the analysis, $\{{\omega_f}^2\} = 0$ and the set of rigid body modes are represented as $\{\phi_r\}$. The equation of rigid body normal modes can be derived in eq.(2.32).

$$[K_f]\{\phi_r\} = 0 \tag{2.32}$$

2.10 The analysis of multi-body system

The finite element method is very beneficial in design process of automotive industry. However, this method of simulation requires input load values to apply to the structure or models in the simulation. Therefore, the input load calculation is very important. For the calculation of the input values for efficient and reliable. The method of calculation is presented in several ways. One of the most popular methods is multi-body system. In the automotive industry, the multi-body system is used in predicament to perform load prediction in a virtual durability test (Kim Bladh, 2012).

The multi-body system is a group of bodies connected by joints that are influenced by the input loads and restricted by the constraints. This system causes the behavior of displacement and movement of structure. The motion of mechanical properties is called multi-body dynamics (Darshan Vijay Wale, 2015). The multi-body system is used to modeling the dynamic behavior of structures that are interconnected by rigid or flexible bodies to study the large movement of components respect with another, the motion of multi-body system can be viewed as Figure 2.7. Generally, the movement of the multi-body system is explained with their kinetic behavior. The results of the dynamic behavior are described from the static equilibrium and the rate of change of momentum (Jens Wittenburg, 2008).

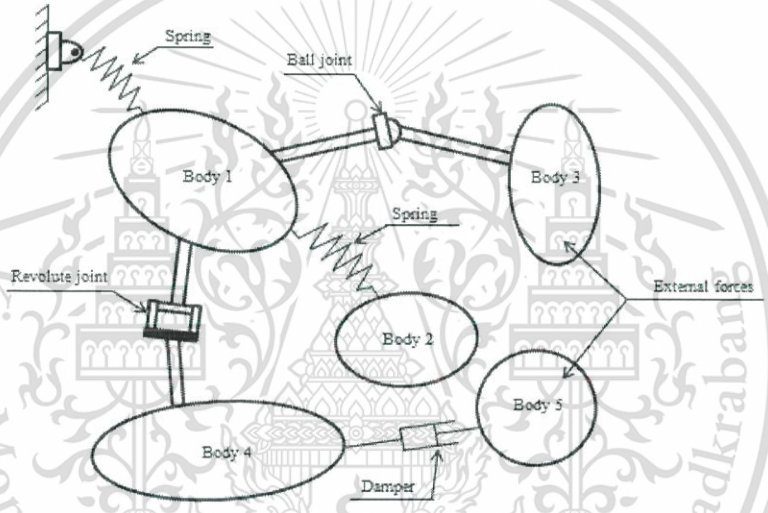

Figure 2.7 Schematic of general multi-body system

2.10.1 Rigid body simulation

The rigid body in multi-body system simulation is a simulation model of a system that consisting of several solid bodies interconnected to the components with limiting motion by the type of joint, spring or bushing that restricts the movement behavior of each body (Kim Bladh, 2012). This technique allows to obtains the load parameters, displacement, velocity and acceleration of each component in a vehicle subsystem to be used as input parameter in the next step of calculation. The ability of this technique is widely used in mechanical problems (Cardona, Geradin, & Doan, 1991) and research to study the durability of components by using the rigid multi-body parameters as input to finite element analysis simulation to compute the stress, strain and fatigue prediction

of vehicle components (Conle & Mousseau, 1991). The result of rigid multi-body system can be used as input in static or dynamic analysis techniques.

2.10.2 Flexible body simulation

Nowadays, the development of computational capabilities, the development of sophisticated system analysis can be accomplished in the simulation of the complex components efficiently. Due to the limitation of the rigid body in the calculation of durability in multi-body analysis, the flexible body is takes on role play in durability and fatigue prediction of vehicle component in the multi-body simulation (Iyidiker Cagri, Yilmaz Anil, & Otokar Otobus Karoseri A.S, 2010). The flexible multi-body simulation is not only used to compute the precise load predictions on component, but also enhances the ability to analyze stress and strain on the flexible components.

The flexible body theory is based on the Craig-Brampton method. To increase the appropriateness of the dynamic multi-body simulations, the formulation of the flexible body has been modified. The stress and strain calculation of flexible body is performed in modal stress and strain recovery (Bampton & Craig, Jr., 1968). The method of modal stress and strain during the flexible body was generated provide the stresses and strains when combined with modal coordinates from multi-body system simulation.

(Tebbe et al., 2006) has classified the different of multi-body system for vehicle durability testing into semi-analytical and fully analytical approaches divided by the structural load calculation method. For the sake of classifying the multi-body system, this method is organized as semi-model and fully model.

2.10.2.1 Semi-model analysis

The semi-model analysis is the method used input load from the measurement data from virtual proving ground testing. The input loads that will be used to calculation with the structure depends on the scope of the different works, such as, spindle loads, velocity, acceleration or displacement, the acceleration of the vehicle structures. This approach is a way to apply the measured input to the unconstrained model directly. However, the input load that measured from the virtual testing is difficult. The input values obtained from the measuring equipment cannot respect with the real-time requirement (Wang, Lin, & Zhang, 2015). These inputs will result in error of simulation results.

(Tebbe et al., 2006) mentioned a technique of load from wheel force transducers (WFT) that applied directly to vehicle spindle of unconstrained model. The technique causes the unstable simulation on condition, such as, rollover conditions, with unconstrained model. This will result in the mismatch of multi-body system model and virtual prototype vehicle model. The main factor that that influence to the motion of the multi-body model is the external environment caused by the error of measurement equipment, vibration and noise. Due to derive the input value is tough, another technique has been introduced. Use the same load input as described above, but change the limitation of movement of the model by constrained the vehicle model. Because of the movement of model is limited by constrained. The unwanted movement of model is eliminated from the simulation. On the other hand, due to the limitations of constrained model, the inertia of sprung mass is eliminated, meaning that loads of the model may be dissimilar with the virtual prototype model. The Figure 2.8 is illustrated the unconstrained and constrained model with loads input applied at front and rear spindle.

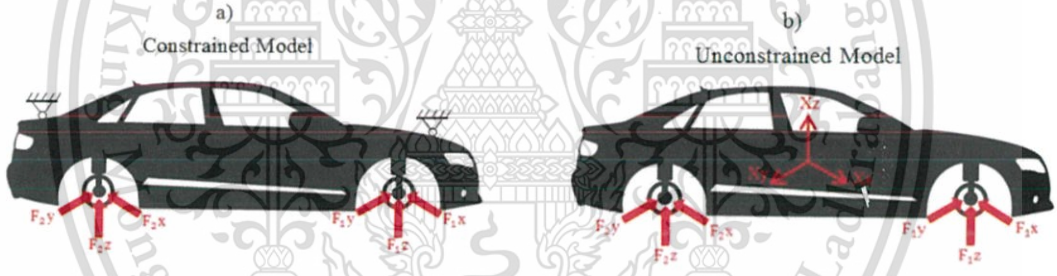

Figure 2.8 a) Constrained model concept, b) Unconstrained model concept

2.10.2.2 Fully model analysis

The fully model analysis is general analysis of vehicle behavior. This analysis technique is related to the multi-body systems vehicle model, which consists of major components of the vehicle, tires properties, suspension and steering systems, including the digitized road profile. The models are driven independently by driving characteristics with unconstrained model. This technique of simulation will obtain the various loads that affect the structure of the model. In 2003, (Gi Seob Choi & Jung, 2003) did experiment simulation about full vehicle model run over single bump test and road load simulation. To determine the reaction force and torque at each joint of the suspension components that acting to chassis. (Kim, Hwang, & Yoon, 2000) use this technique to study about

the effective method for dynamic stress analysis of structural components of bus systems or general mechanical systems.

This simulation technique is widely used in the automobile industry. The technique can reduce the duration and cost of the design process and also simulate the durability of vehicle components and behavior of vehicle under various conditions. The advanced simulation can improve the design and analysis capabilities with efficiently.

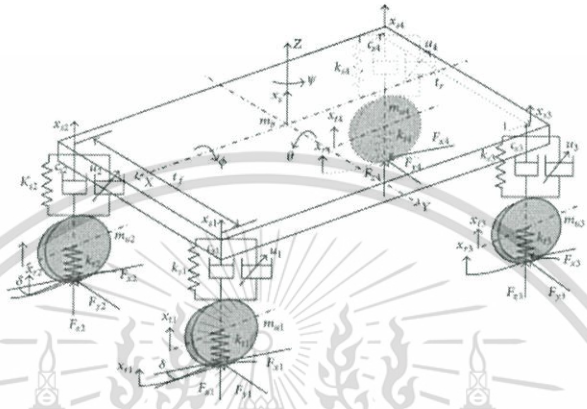

Figure 2.9 Illustration of degree of freedom of the full vehicle dynamic model (Zhao, Li, & Qu, 2014)

2.11 Virtual Proving Ground Technique

In the automotive industry, the vehicle durability and design testing are a major section of the research and development of vehicle lines. After design process, part durability testing is required, which can be tested with various techniques. The virtual proving ground is a new technique for analytical approach to vehicle component durability test which the automotive industry is widely used and also many literatures use this method to apply to their applications for study the vehicle behavior. This technique has been developed for simulation of dynamic nonlinear events which to analyzing the durability under road load from the virtual proving ground test environment. In study of Dynamic and Durability Analysis using Virtual Proving Ground (Edara, Shih, Tamini, Palmer, & Tang, 2008), they investigated the 18 Wheel Truck by using virtual proving ground. the spindle load as well as the component loads and stress/strain time histories are predicted. (Farhang Aslani, 1994) did the study of fatigue life under proving ground events to predict the stress for heavy truck caps by using software of MSC.ADAMS.

The simulation of full vehicle model consists of vehicle structure, chassis, suspension systems, engine and also tire models with combination of finite element model to

perform nonlinear dynamic analysis will providing a reasonable basis of prediction of the vehicle fatigue life. There are limitations in the real testing due to the designing time and the prototype testing, it is also impossible for a vehicle to be tested with various patterns road test. So, this method was introduced on the aim of reduce the testing time and cost of the proving ground testing.

Apart from the durability simulation, the applications of the virtual proving ground can also be used for noise, vibration and harshness (NVH), crashworthiness and safety testing, and handling analysis (Arthur Tang, 2000).

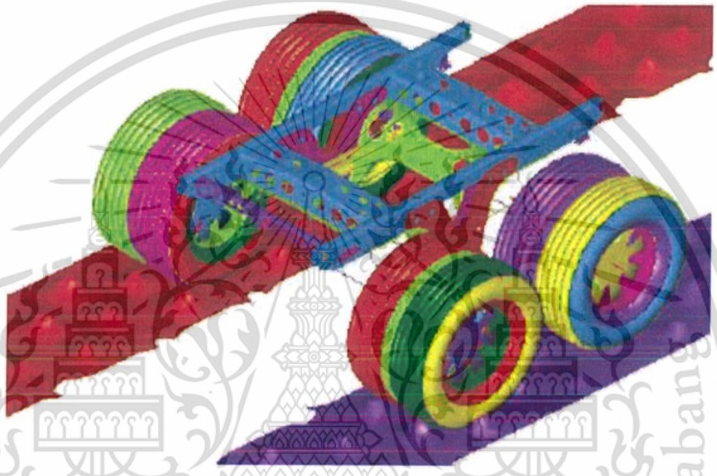

Figure 2.10 Trailer assembly on cobblestone proving ground surface 18 Wheel Truck dynamic (Edara et al., 2008)

2.12 Simulation

A simulation is a set of hardware and software systems that mimic the behavior of an entity or a certain phenomenon. Usually, the entity or phenomenon that is simulated comes from the domain of the object or work piece. Simulations may be used to analyze and validate theoretical models, which may be difficult to understand on a regular basis. There is a representation of a system or process. It can be modeled without limitation, creating complex situations. These capabilities help to analyze and understand how each part interacts and how it impacts the simulated environment. Simulation plays an important role in every industry including the academic.

Despite of the increasing of the use of simulation to be a viable and necessary research tool, many of the problems are related to the limitations of the calculation of the existing

hardware, but have been overcome quickly when the replacement of the device is more powerful.

2.12.1 Computer Aided Engineering (CAE)

With computer technology advancing rapidly, making it a major player in the automotive industry. Nowadays, more and more CAEs are being used, which can help to reduce costs and errors from traditional work. Computer Aided Engineering (CAE) is based on the use of CAD (Computer Aided Design) technology to work with CAM (Computer Aided Manufacturing), which is used to control industrial machinery, thus becoming a technology that can tell the designed object can be used. Calculation with CAE software will yield faster and more accurate results. So, CAE is an advanced tool for calculating and predicting performance, as well as the lifetime of components. This technique plays an important role in the application to enhance and improve the efficiency of product development (Pankaj Chandna & V.P. Singh, 2008).

Although CAE is well-known as a troubleshooting, and analysis tool, there are also conflicts that the results are accurate to design. This can be expected to become a problem for modern and highly sophisticated products.

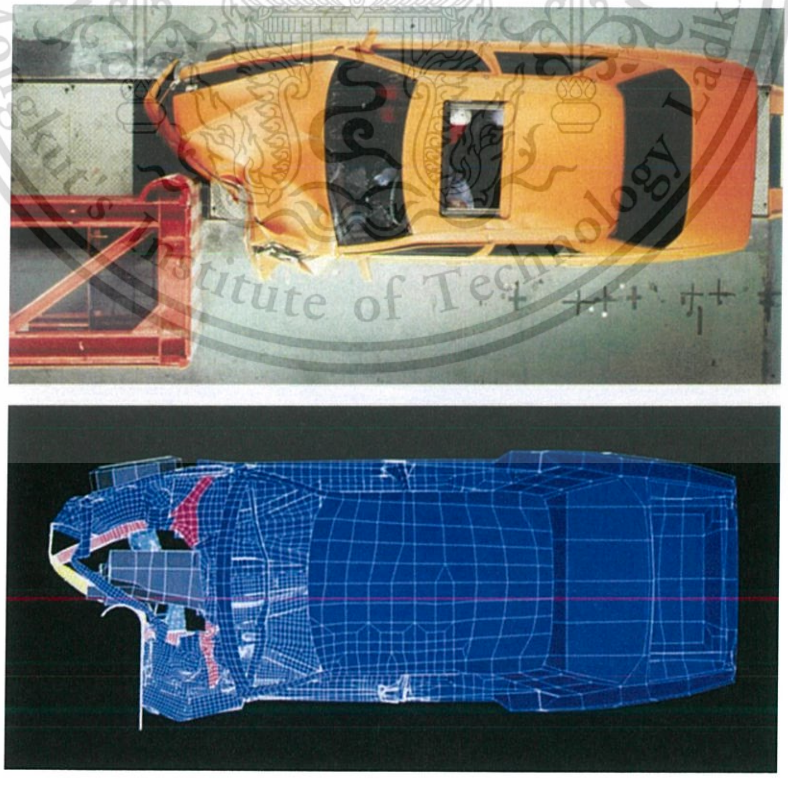

Figure 2.11 Real and simulated vehicle crash test (Cray Research Inc., 2018)

2.12.2 Advantages of CAE

One of the main advantages of the simulation is that they can provide useful feedback to users in the design process of components or devices. This allows the users to determine the authenticity and performance of the design before creating it. Therefore, they can take advantage of alternative designs without actually physically components. The investigation of the impact of the design during the design section results in a significant reduction in the overall cost of construction.

Another advantage of simulation is that users can study different levels of problem. At a complex component, users can better understand the behavior and interactions of components within the system. This complexity can create problems for them if the problem is approached from a basic component. After users have understood the complexity of the components through the simulator, they may be able to design basic components and simulate them for use in the verification, evaluation and optimization of complex components. Therefore, it is better able to meet the overall complexity of the system (Donald C. Craig, 1996).

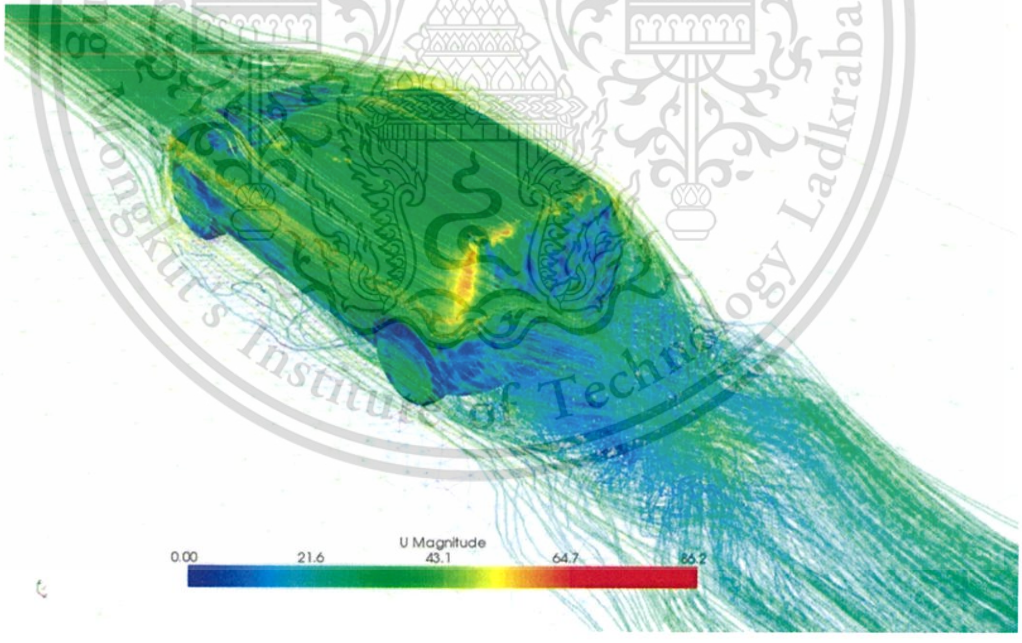

Figure 2.12 Aerodynamics simulation of Volvo Car Corporation (Cray Research Inc., 2008)

2.12.3 Multi-body systems simulation: MSC ADAMS/Car software

With the dramatic development of computational software, the multi-body dynamics (MBD) systems plays a role in engineering calculations and computer-aided engineering (CAE) fields. It can help with thorough investigation of complex mechanical systems. The multi-body dynamics systems can be applied to the mechanism of components that vary in shape and size with their movement. This associated with geometric change will cause the components to change shape from the original system in different directions (MSC.Software Corporation, 2012a). Movement may involve the complex combination of large and small deformation and solid body interaction.

Multi-body dynamics (MBD) systems is a system that consisting of several bodies connected by constrained joints to the relative motion of these components. The MBD is an analysis of the mechanical system under the influence of continuous dynamic force, translational and rotational displacements. The dynamic system of the interconnected body is based on the principles of Euler and Lagrange dynamics equations (Brian D. Jensen & Timothy W. McLain, n.d.). In general, the movement of the body is explained by kinetic behavior. The effect of dynamic movement behavior is based on the equilibrium of applied force and the rate of change of momentum as mentioned in above chapter.

ADAMS/Car is one of the most popular Multi-body dynamic systems software solutions in the automotive industry for modeling and simulation of semi or full vehicles. In ADAMS/Car, users can create the virtual prototype models and perform with realistic simulation. It also performs in highly complex vehicle dynamic analysis and analysis of suspension, steering and full vehicle maneuvers. In addition, it can also be used to generate a digitized virtual proving ground for various driven conditions.

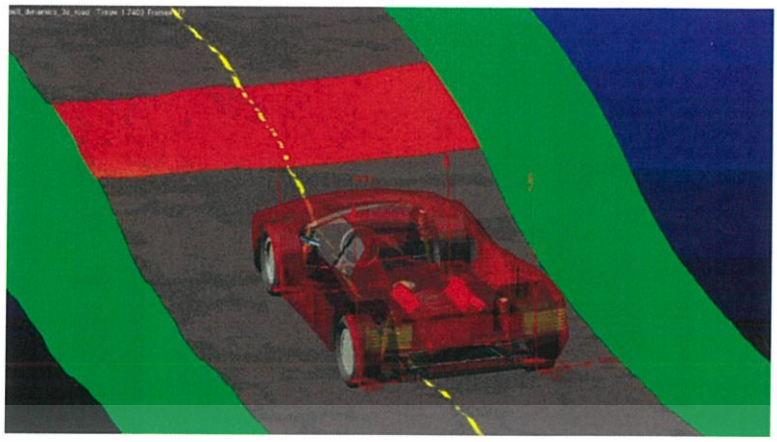

Figure 2.13 Full vehicle model simulation on VPG via MSC ADAMS/Car software (MSC.Software Corporation, 2012a)

2.12.4 Finite element analysis simulation: Altair HyperMesh

The finite element method (FEM) is a numerical method for solving problems of complex engineering problems and unmethodical mathematical physics. The most common engineering problems present in the finite element method include structural analysis, fluid and mass flow, heat transfer and mass transportation. The solutions of these problems that are related to the analysis, solving boundary value problems for partial differential equations is highly necessary. The boundary value problem is a mathematical problem that requires the use of differential equations within a domain that is independent and domain specific using at least one variable (Altair Engineering, Inc., 2016). The formulations of the finite element method are results in the algebraic equation for steady state problems and the ordinary differential equations for transient problems. This method provides an estimate of the unknown value at various points across the domain.

The finite element analysis (FEA) has become an integral part of Computer Aided Engineering (CAE) and is widely used to performing the real time engineering analysis. The technique of creating a mesh for dividing complex problems into small components has been used in the FEA approach.

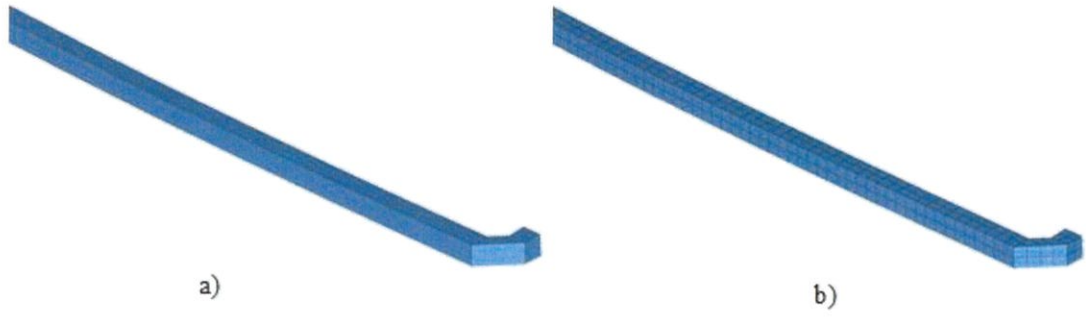

Figure 2.14 a) Tube model b) Tube model after meshing

There are powerful software tools and packages for finite element analysis that available in various industries. Altair; HyperMesh is one of the software used to analyze the widespread. This software is a multi-disciplinary finite element pre-processor which manages the generation of the largest, most complex models with high quality mesh in a short time. The models are divided into specific areas as nodes and element delicately and starting with the geometry to exporting to run solver file.

To solve the highly non-linear problems under dynamic loadings of structural analysis, the RADIOSS solver is applied. It is a finite element solver using implicit and explicit integration schemes for the solving the engineering problems (Altair Engineering, Inc., 2016; Ashish Kumar Choudhary & Rakesh Grover, 2017; Atul Kumar, 2015). It can be used to simulate structures and mechanical systems. This solution allows manufacturers to maximize durability, noise and vibration, crashworthiness and safety.

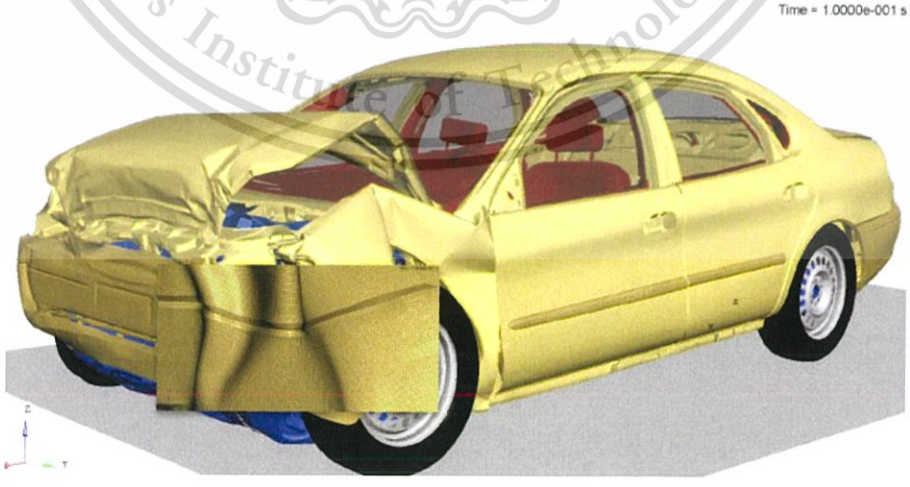

Figure 2.15 Highly efficient crash simulation via HyperWorks: RADIOSS solver (Altair Engineering, Inc., 2016)

2.12.4.1 Numerical procedures of HyperMesh: RADIOSS solver

The RADIOSS numerical solver can be summarized for each time step in a particular analysis, the algorithm used to compute results is follow the steps below and the flow chart will show in Figure 2.16. (Altair Engineering, Inc., 2009)

1. The input parameter; the displacement, velocity and acceleration, or the external force will be applied as boundary condition.

2. The looping of the elements being carried out by computing the internal force and the hourglass force of element along with the next time step sizes. The loop over element was produces by:

2a. The displacements in the intrinsic coordinates system to the physical system will be computed by the Jacobian matrix, as eq. (2.33).

$$\left.\frac{\partial \Phi}{\partial x_j}\right|_t = F_\xi^{-1} \left.\frac{\partial \Phi}{\partial \xi}\right|_t \tag{2.33}$$

2b. The strain rate is calculated by eq. (2.34).

$$\dot{\varepsilon_{ij}} = \left(\frac{\partial \Phi_I}{\partial x_j}\right)\dot{x} = \frac{1}{2}\left(\frac{\partial v_i}{\partial x_j} + \frac{\partial v_j}{\partial x_i}\right) \tag{2.34}$$

2c. The stress rate is calculated by eq. (2.35).

$$\dot{\sigma_{ij}} = f(\dot{\varepsilon}, material - law) \tag{2.35}$$

2d. The Cauchy stresses are computed by using explicit time integration as eq. (2.36).

$$\sigma(t + \Delta t) = \sigma(t) + \dot{\sigma}\Delta t \tag{2.36}$$

2e. The internal and hourglass force vectors, and also the next time step size is computed.

3. After the internal and hourglass force on each element are calculated, the algorithm will be computing the contact forces between any interfaces.

4. After complete the calculation of forces, the mass matrix and the external and internal force vectors will be performed to calculate the new accelerations, the equation of calculation will show in eq. (2.37).

$$\dot{v}_i = M^{-1}(f_{external} - f_{internal}) \tag{2.37}$$

5. Finally, time integration of velocity and displacement is performed using the new value.

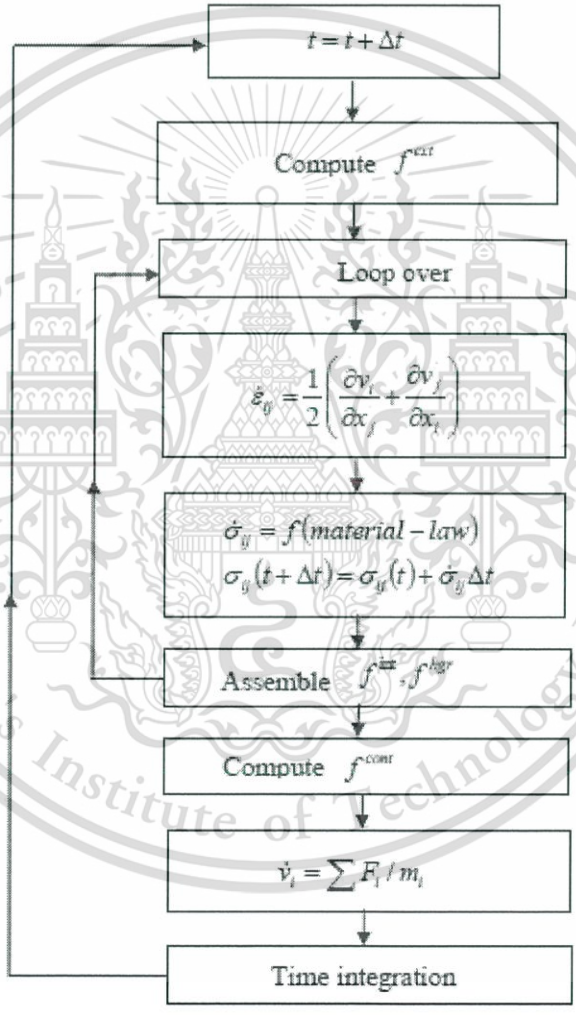

Figure 2.16 Numerical procedures (Altair Engineering, Inc., 2009)

The direct integration method is usually choosing in the transient dynamic analysis. In RADIOSS, the method is derived from the Newmark time integration. The state of this method at a given time $t_{n+1} = t_n + h$ is computed using Taylor's formula (Altair Engineering, Inc., 2009).

The computation of displacements and velocities of the system at time $t_n + 1$ of the Newmark's method is show in eq. (2.38) and (2.39).

$$\dot{u_{n+1}} = \dot{u}_n + \int_{t_n}^{t_{n+1}} \ddot{u}(\tau)d\tau \tag{2.38}$$

$$u_{n+1} = u_n + h\dot{u}_n + \int_{t_n}^{t_{n+1}} (t_{n+1} - \tau)\ddot{u}(\tau)d\tau \tag{2.39}$$

The central difference algorithm corresponds to the Newmark algorithm and the equation will show in eq. (2.40) and eq. (2.41) and the flow chart show in Figure 2.17.

$$\ddot{u}_{n+1} = \ddot{u}_n + \frac{1}{2}h_{n+1}(\dot{u}_n + \dot{u}_{n+1}) \tag{2.40}$$

$$u_{n+1} = u_n + h_{n+1}\dot{u}_n + \frac{1}{2}h^2{}_{n+1} + \ddot{u}_n \tag{2.41}$$

With h_{n+1} is the time step between t_n and t_{n+1}.

At time $t = 0$, the displacement u and velocity $\dot{u_0}$ are known from the initial conditions. The equations of motion are solving the acceleration $\ddot{u_0}$ and time step h_1.

$$h_0 = 0 \tag{2.42}$$

$$\dot{u_{-\frac{1}{2}}} = \dot{u}_0 \tag{2.43}$$

$$\dot{u_{\frac{1}{2}}} = \dot{u}_0 + h_{\frac{1}{2}}\ddot{u}_0 \tag{2.44}$$

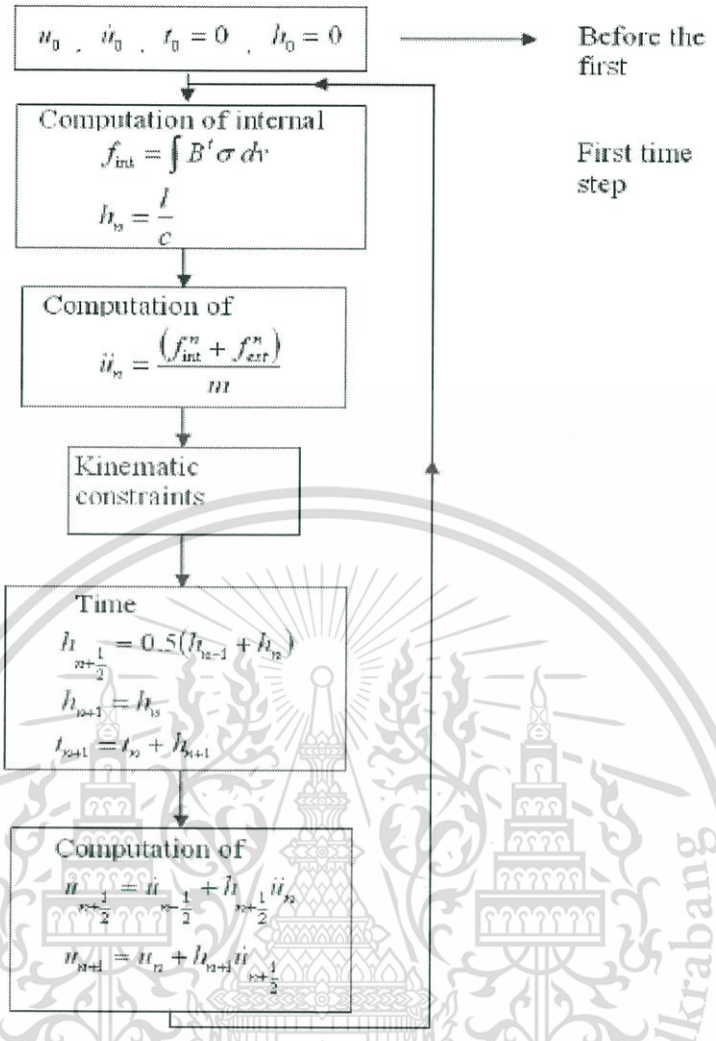

Figure 2.17 The flow chart of the central difference algorithm (Altair Engineering, Inc., 2009)

CHAPTER 3

RESEARCH METHODOLOGY

3.1 Vehicle model

3.1.1 CAD model

First step to make finite element model of bus structure, a full skeletal model of 12-metre bus infrastructure will be built first in computer-aided design (CAD) software. The CAD model consists of member of beam structure with different thickness depends on area of structure and thin plate. In this study, CAD model of structure of 12-metre bus model has been generated using SolidWorks software (Dassault Systèmes SolidWorks Corporation, 2015) shown in Figure 3.1.

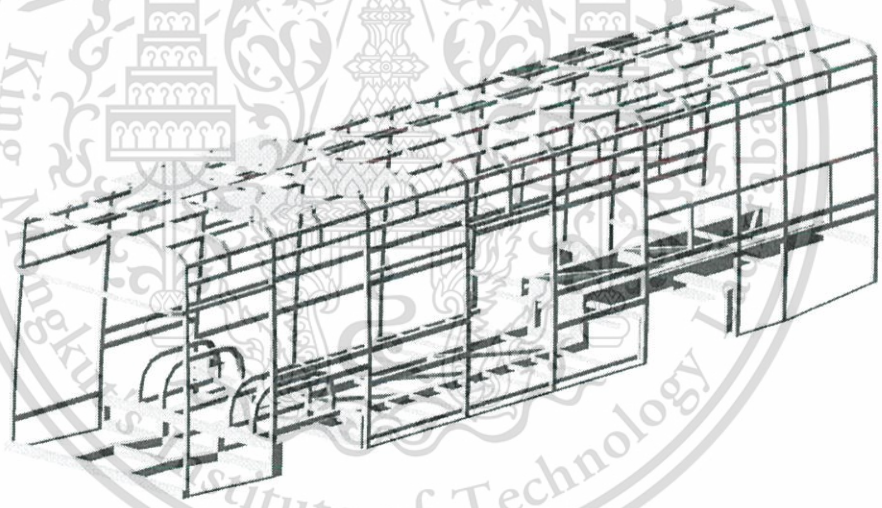

Figure 3.1 The bus structure CAD model

The CAD model also consists of battery packs and battery packs holder, which have been assembled to full structure of bus model.

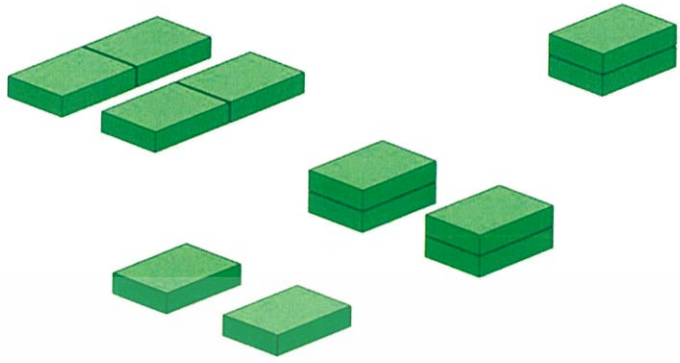

Figure 3.2 CAD model of battery packs

3.1.2 MSC.ADAMS/Car modeling

Full bus model was created in the multi-body dynamic systems software, (MSC.Software Corporation, 2012), consisted of tires, front and rear suspension systems, power train, steering systems, chassis and skeleton structure. All the vehicle components were assumed as rigid bodies. Some subsystems have been modified to fit the model to be specific to the scope of this study.

3.1.2.1 Suspension model

Front suspension system is Low beam front mount type with air-spring systems, where are 3 functional components (air-spring, damper and bump stopper) on each side. And rear suspension system is 4-bar type with double air-spring systems. The functional components were 6 functional components (double components) on each side. Using 4 air springs to support the weight of the car and absorb the force from the suspension. The air spring suspension systems are used to improve the suspension system to reduce the vibration from the road load through the suspension systems to the structure of the vehicle that influence the driving factors (Marco W. Holtz & van Niekerk, 2008). The air spring damper suspension, the spring can be changed according to the height of the car that referred to by the ride height sensor that attached to the suspension system; this sensor will measure the height of the car. The K value was generated in the air springs to absorb the force and maintain the height of the car. Reduce the frequency of the structure when the height is changed. The characteristics of suspension components;

air-spring, shock absorber, and bushing, are specified using non-linear force displacement which based on data measurements was taken from the manufacturer.

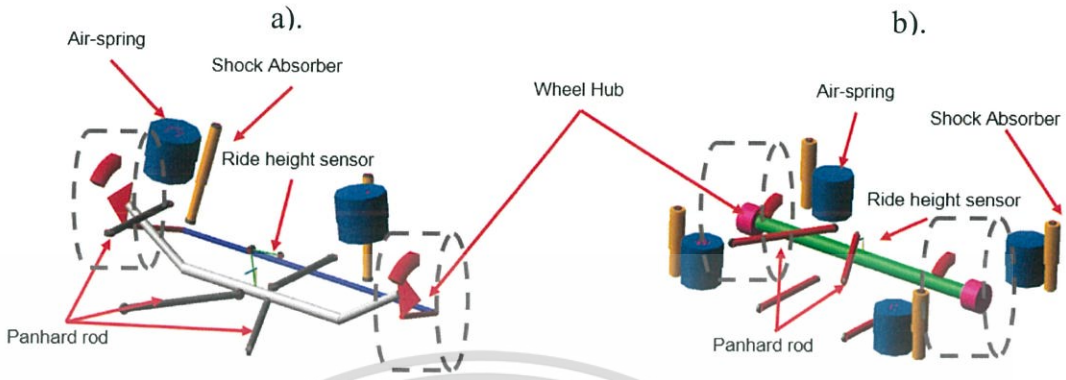

Figure 3.3 a) Front low beam suspension with air-spring system, b) Rear 4-bar suspension with double air-spring system.

3.1.2.2 Tire model

This study is a technique of virtual proving ground simulation. Tire was expressed as a subsystem, to calculate the stresses that occurred on the battery packs holder via determination of the acting forces from the tire contacts with road surface to the structure through suspensions. The PAC2002 tire model was used in the front suspension. The Magic-Formula (MF) model is the most advanced model for modeling propulsion interaction between tires and roads in vehicle dynamics applications, the tire handling forces and moments. The PAC2002 tire model has been developed by (MSC.Software Corporation, 2012a) based on Tyre and Vehicle Dynamics (Pacejka, 2006). Generally, the tire model MF describes the tire behavior for smooth roads. (Road obstacle wavelength is longer than the radius of the tire). However, the PAC2002 has extended functionality that increases the validity towards short road obstacle wavelengths (with use of the 3D Enveloping Contact). For the rear suspension, the Fiala tire model was used to deal with road obstacles for ride and comfort and durability analysis (Darshan Y. M. Reddy, 2017). The Fiala tire model can describe the 3D tire dynamic response up to 120 Hz and beyond, due to its flexible ring approach for the tire belt. So, it can handle any road obstacle (MSC.Software Corporation, 2012b).

The tire model is compatible with vehicle handling and stability simulation. The vehicle dynamics application, the accuracy of the tire interactions is important because the movement of vehicles mainly depends on the force on the road with tires. These

reaction forces depend on the properties of the road and the tire, including the movement of the tire with respect to the road. The tire model calculates vertical loads and slip quantities based on the position and wheel speed with road surface. The forces and moments in the contact patch between tire and road will calculate by the set of MF parameters through the MF equations, which are derived from the tire testing data (MSC.Software Corporation, 2005). However, in this study not to focus about the performance detailed of the tire that affected to the movement behavior of the vehicle, so some parameters are not mentioned; Tire temperature and pressure.

3.1.2.3 Battery packs model

The installation of the battery packs on the roof is considered. Due to a configuration of this design, an overall center of mass of the bus would be shifting to a higher location. The battery packs were assumed to be solid bodies by adding weight to the model. The weight of each battery pack is 175 kg, which in the full model has 12 battery packs, there are 4 battery packs were located on the roof structure and 8 packs inside the bus structure. The battery packs holder is focused in this study. It was designed in CAD model and generated to finite element model later.

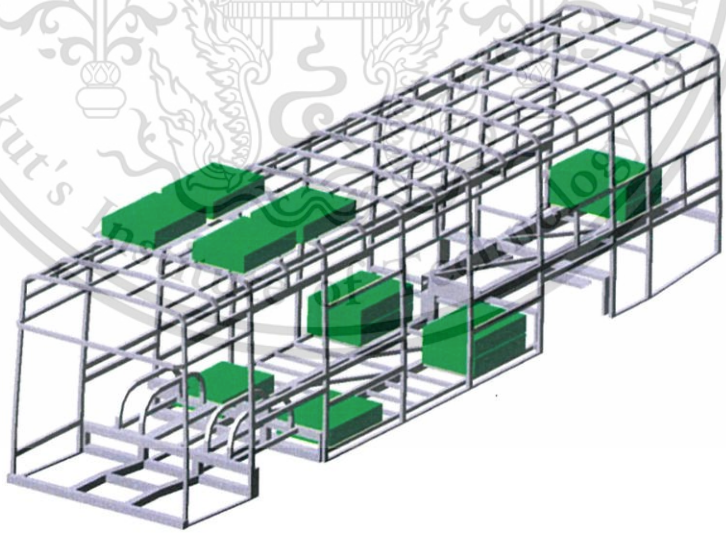

Figure 3.4 Bus structure with battery packs (rectangular boxes) assembled

3.1.2.4 Full bus model

Suspension modeling and inertial properties of powertrain are influencing the dynamics of the coach structure. The powertrain, steering systems, and brake systems have been modeled as rigid with mass and inertial properties relative to the commercial bus. The full bus model assembled from any subsystems; tire was also fit in; the model shows in Figure 3.5. The mass of model and position of CG were obtained by software.

Figure 3.5 Full bus model with battery packs assembled in MSC.ADAMS/Car software

The other components such as windshield, doors, seat, and various interior components are out of scope of full bus model. However, their mass distributions have been included in the bus structure subsystem.

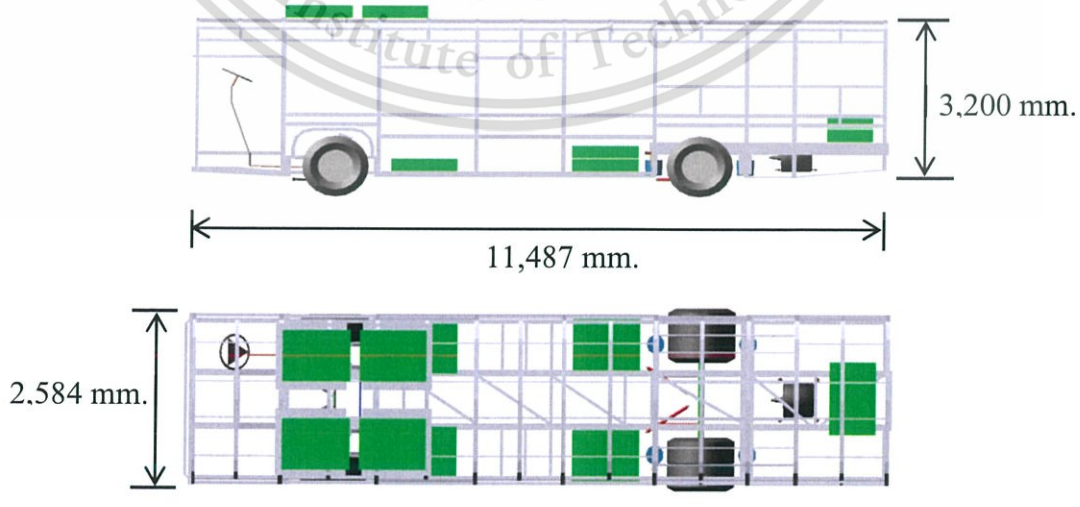

Figure 3.6 The dimension of the full bus model (mm.)

Table 3.1 Full bus property with battery packs assembled

Full bus model with battery packs	Properties		
Mass (kg)	1.4608 E+04		
	X	Y	Z
Center of Mass (mm.)	7296.4434	-3.9358	1520.9283
Orientation (deg.)	90.6220	1.6269	269.8002

3.2 Finite element model

The design of the bus frame depends on the factors that influence the strength of the operation under load conditions and the types of operations that result from road conditions. The road loads are carried out from different circumstance such as quasi static load, acceleration and braking loads condition (Rayakar & Bhat, 2014). The finite element modelling for bus structure is performed evaluate the durability and NVH analysis of bus structure at different conditions with normal static load.

The finite element model of bus structure model in this study was generated using HyperMesh in HyperWorks software (Altair Engineering, Inc., 2016). The model has been modeled with relatively high detail to give a close representation of the properties and weight distribution of the models in MSC.ADAMS/Car software. The finite element model should import by the cad model in Parasolid format, in this study will import from Solidworks software. The CAD model has been processes of geometric checkup and remodel in order to get better mesh quality. The efficiency of an element type is dependent on the surface geometry and application.

3.2.1 HyperWorks modeling

The major element of the model was generated by first order element. The finite element model was consisting of 2 element types; 2D-element (Shell element) and 3D-element (Solid element). According to the objective of this study, the stress distributions of the battery packs holder have been interested, so 3D element was chosen because this point requires high accuracy of simulation results. Boundary conditions including forces and displacements of this element type can be treated more

realistically and the finite element mesh visually looks like the physical system (Carlos Felippa, 2017). The size of solid element on the battery packs holder is around 10-15 mm. On the other hand, the accuracy of this element type requires a lot of resources and a longer calculation time. To keep these things in reasonable limit, it may be necessary to use coarser mesh with two-dimensional model. The scope of this study is investigating only the battery packs holder. To reduce the use of limited simulation resources, 2D-element was chosen for other components. In order to reduce time consumption of simulation, this type of element is a simple method to interpret of finite element analysis results due to the organized and grouped into individual stresses and displacement (C. M. Wai, Rivai, & Bapokutty, 2013). The bus structure that representative of the components that transmit the force generated by the virtual proving ground simulation was taken for 2D-element. The chassis, roof, battery packs, and battery plate also take shell element with their thickness properties. The size of the entire element has been taken not over 35 mm. for maximum size and 10 mm. for minimum size with different thickness properties. The complete meshed of bus structure is shown in Figure 3.7.

A full-scale modeling durability assay will require detailed modeling along with small element size to provide accurate fatigue estimates. Although, not within the scope of this work to carry out such fatigue analysis. But this comprehensive finite element model can be used to investigate the feasibility and limitations of fatigue life prediction.

Figure 3.7 Finite element model of bus structure with battery packs assembled

The property of each component is divided according to the structure. this will determine the thickness of the element profile in each component. The structure model has 7 thickness. In this work, the bus structure is divided into two sections, the primary and secondary structure. The primary structure has 3 thickness for the main bus structure and 4 thickness for the secondary structure. The primary structure consists of 3 sizes of thickness; 3 mm, 6 mm, and 15 mm. and 4 other thickness sizes for secondary structure; 1 mm, 1.6 mm, 2 mm, and Solid property that thickness will depends on the geometry of component.

The chassis, Figure 3.8, is the primary structure of bus model. This component is composed of two parts which is the main chassis and the sub-chassis. The main chassis was used of 6 mm in size, which is equivalent to the thickness in the CAD model. For the thickness of sub-chassis was 3 mm. Due to it is not directly impacted of force and use a smaller size to get a lighter weight.

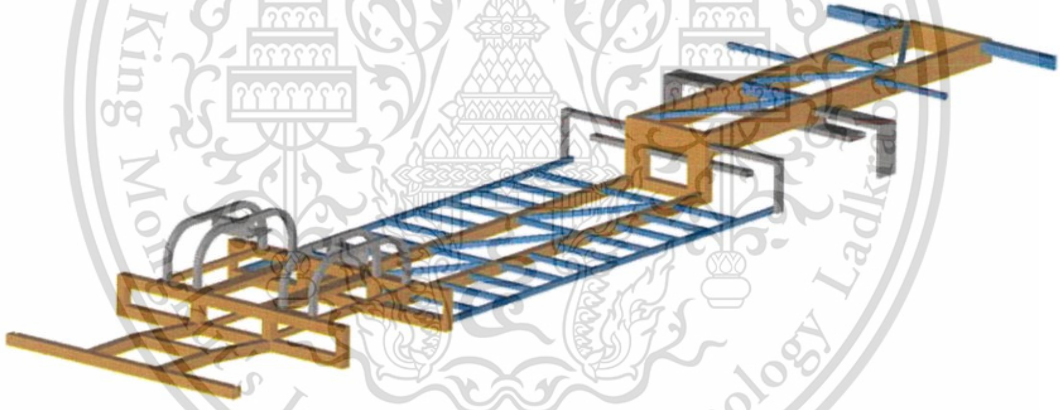

Figure 3.8 Finite element model of chassis structure

The left, right structure, Figure 3.9, and also roof structure, Figure 3.10, were used the thickness size of 2 and 3 mm. The side structure also divided in the same way as chassis, the main and sub-structure. The main structure was used of 3 mm and 2 mm for sub-structures that are not high load.

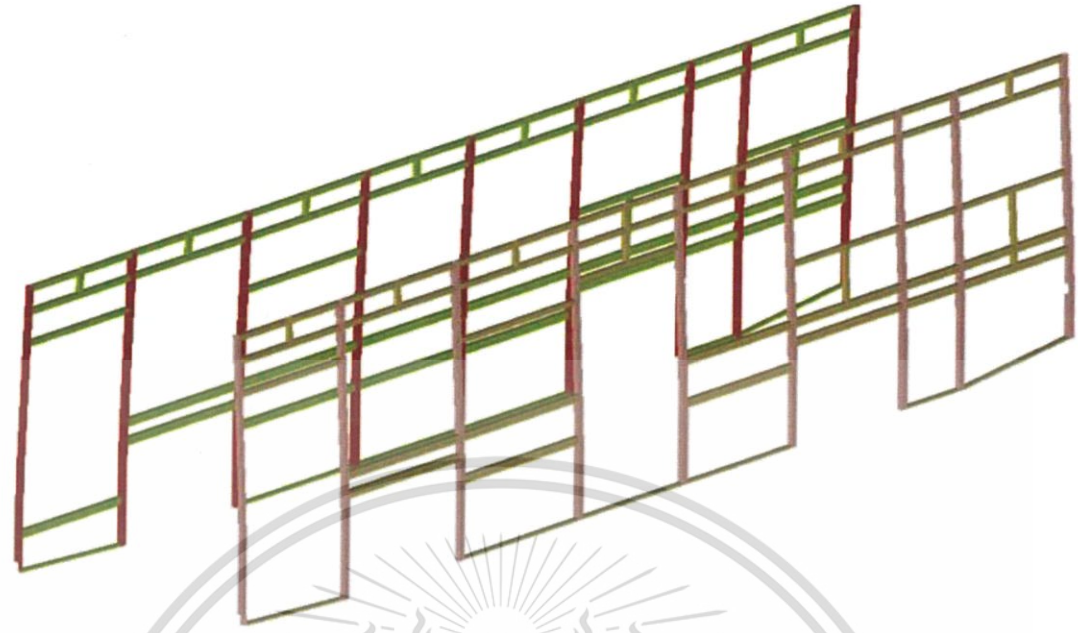

Figure 3.9 Finite element model of left and right structure

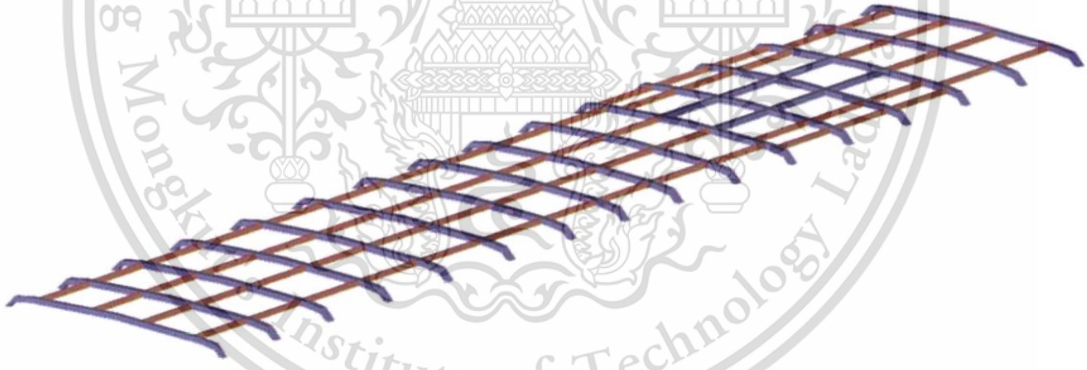

Figure 3.10 Finite element model of roof structure

The battery plate tube, Figure 3.11, is secondary structure. This component was used the thickness of element as 1.6 mm. The battery plate was used in the largest thickness profile as 15 mm for supports the weight of the battery packs including the load that causes the movement behavior and also the gravity force from each battery pack. While the battery packs are made into a rigid element, the rigid element is only interested in the geometry of component to maintain and prevent the deformation. The thickness of this area is not necessarily detailed.

Figure 3.11 Finite element model of battery plate and battery plate tube

Table 3.2 The thickness of components of finite element model

Components	Thickness (mm)
Primary structure	
Chassis	6
Left main structure	3
Right main structure	3
Roof main structure	3
Battery plate	15
Secondary structure	
Sub-Chassis	3
Left sub-structure	2
Right sub-structure	2
Roof sub-structure	2
Front tube	2
Battery plate tube	1.6
Battery packs	1
Battery packs holder	Solid

The material of this model was applied as elastic plastic linear material (M36_PLAS_TAB) by curve as Figure 3.12. The material properties and number of shell elements and nodes of the bus structure finite element model were shown in Table 3.3 and Table 3.4.

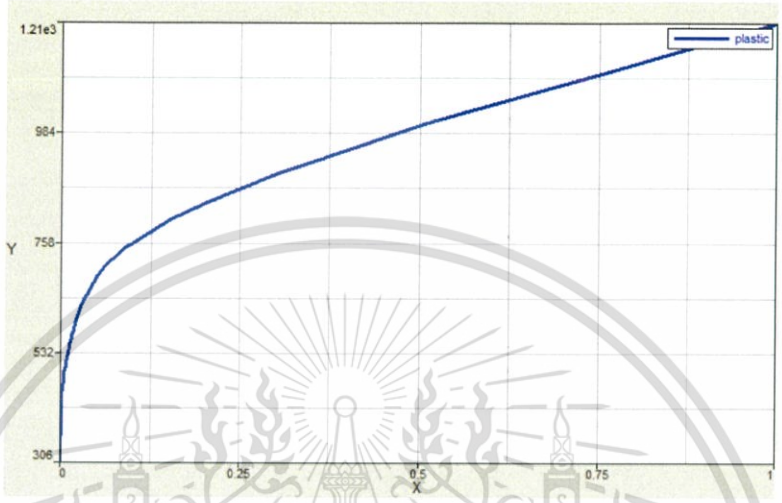

Figure 3.12 The elastic plastic linear curve

Table 3.3 The material properties of finite element model

Material	Steel
Density (kg/m^3)	7.80 E+03
Poisson's Ratio	0.3
Modulus of Elasticity (MPa)	2.10 E+05

Table 3.4 The number of shell elements and nodes in full structure finite element model

Components	Shell elements	Nodes
Chassis	34,299	34,093
Left structure	20,686	20,721
Right structure	20,213	20,289
Roof structure	19,993	19,917
Front tube	686	693
Battery plate	10,047	10,647
Battery plate tube	160	266
Battery packs	24	32
Full bus structure	106,108	106,658

The number of solid elements and nodes on battery pack holder will discuss and show in the investigation of design on battery packs holder section.

3.3 Road profile modeling

The virtual proving ground (VPG) method for durability testing is a simulation of full vehicle to be driven on a digitized road. Normally, the simulation of the full vehicle model is usually fed the load input or any specific measured data to the systems for simulate the behavior of components that occurs in the full vehicle model. With this method, the simulation can perform without any input but required the full vehicle model and the digitized road surface condition. The VPG approach utilizes road elevation as input data from tire contact patches through suspension systems, and also observe the continuous stress distribution at every timestep on structure components using graphic animation of the stress distribution (Choi, Min, & Paik, 2000).

The digitized 3D shell road model is a three-dimensional tire-to-road contact model that calculates the intersection between a road and tire. This model can simulate a vehicle that is hitting a bump, travel over pothole, and moving on rough or irregular road surfaces.

3.3.1 Single bump road surface model

According to the objective of this study is to study the stress distribution on design of battery packs holder and investigate the effect of virtual proving ground condition through bus structure model to the battery packs holder. The road surface used in this approach is three-dimensional finite element models of actual road surfaces. The road surface was introduced and performed by the MSC.ADAMS/Car via Road builder module; it is representing the structural strength of the vehicle. The road surface chosen for this analysis was a non-periodic single event obstacle, single bump curb condition (Darshan Y. M. Reddy, 2017), to measure the displacement of the suspension mounting in 3 directions; longitudinal, lateral and vertical direction, and also to show the period that the force exerted on the structure that caused the highest stress.

Figure 3.13 Overall geometry of digitized speed bump

3.4 Simulation procedures

This study divides the simulation into two sections, to take advantages of software to obtain the input data for further analysis. In the first section is to study on vehicle dynamic and multi-body systems through MSC.ADAMS/Car software. And the second section is study about finite element analysis with dynamic condition by using HyperWork; RADIOSS solver. The simulation procedures are show as flow chart in Figure 3.14.

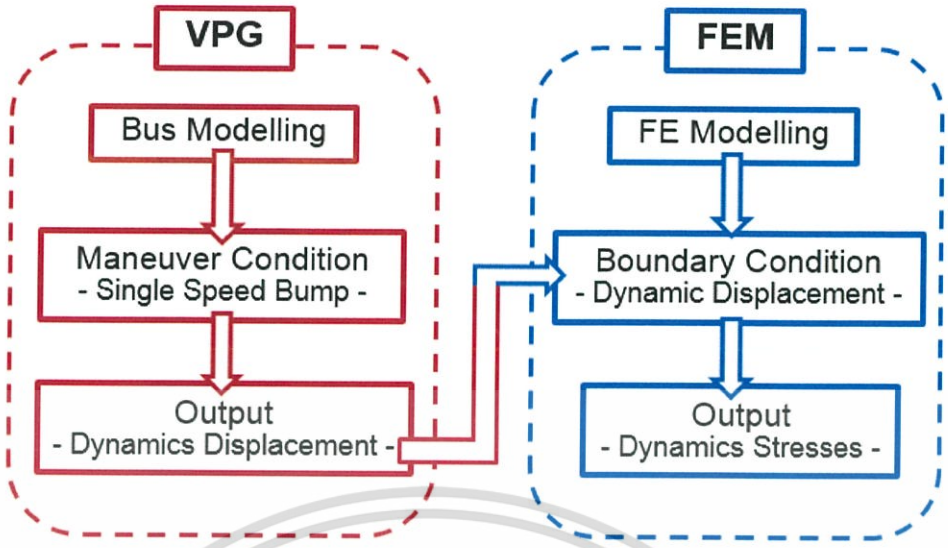

Figure 3.14 The procedures flow chart of simulation

3.4.1 Virtual proving ground simulation using MSC.ADAMS/Car

First simulation section was done by commercial software, MSC.ADAMS/Car (MSC.Software Corporation, 2012), which is the multi-body dynamic system simulation engine. A three-dimensional virtual proving ground with obstacle, single bump is performed in simulation. The full bus model was assigned to traverse over and interact with a digitized road surface of interest at initial velocities 25 km/hr., according to an appropriate speed of bus to run over the bump for nearly the worst case of speed bump (Granlund & Brandt, 2008). The simulation results were carried out the displacement of suspension on the suspension mounting point resulting from the tire contacts with road surface to the body structure via suspensions systems. Appropriate settings for steering control are controlled by the software module to keep the full bus model traveling in a straight path even over the bump during simulations.

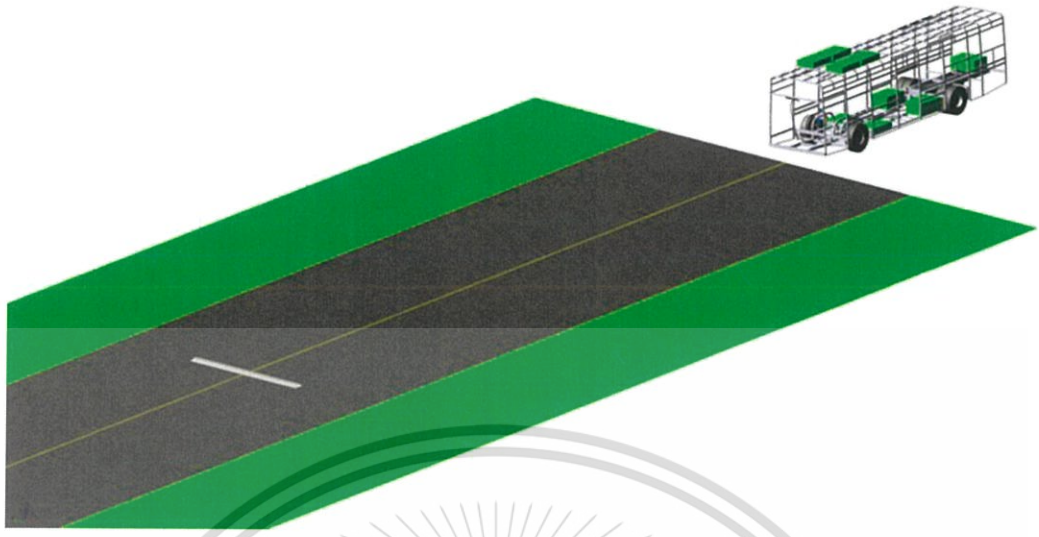

Figure 3.15 The full bus model was travel over single bump road surface condition

3.4.2 Finite element simulation using HyperWorks: RADIOSS

In this section, the dynamic stresses on battery pack holder were determined by finite element analysis. The commercial solver, HyperWork RADIOSS (Altair, 2017), was used to solve a large number of high non-linear dynamics problems, with large displacements, large strains, contact and material non-linearity. The non-linear quasi-static analysis was carried out to find the location of highest dynamic stresses occurred on different designs of the battery packs holder.

The Finite Element model in HyperMesh was applied the gravity force acting on the rigid link element of each battery packs component that shown in Figure 3.16.

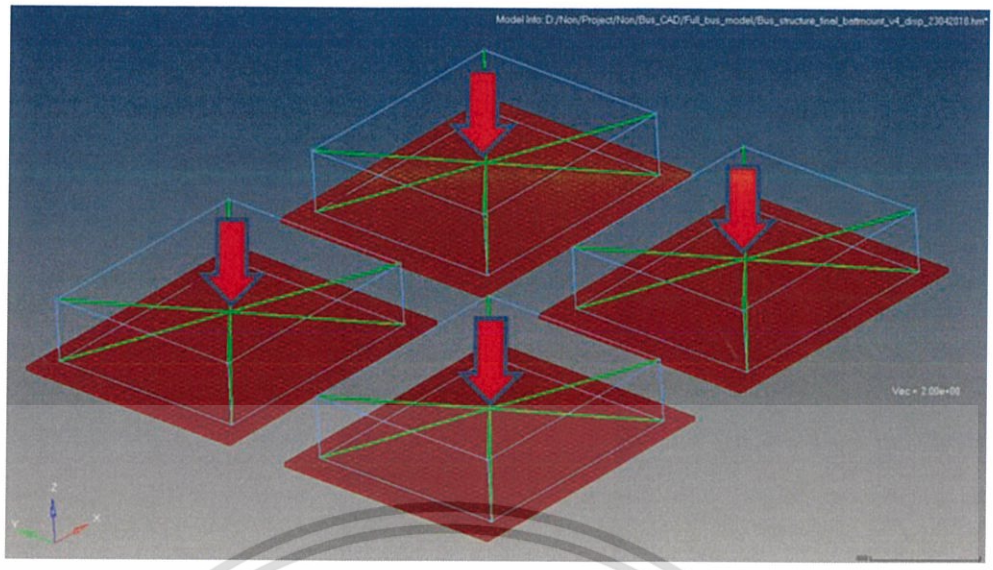

Figure 3.16 The gravity force on each battery packs CG position

The resulting dynamic displacement on the suspension mounting, Front, and Rear suspension systems, during the speed bump maneuvers of the electric bus model obtained from the multi-body systems simulation, ADAMS/Car software, were filtered and converted to the bus structure finite element model via Cure Editor module in HyperMesh software, the suspension displacement was shown in Figure 3.17. The dynamics displacement was assigned as input to the finite element model via Load Collector in function of IMPDISP (Imposed Displacement) to test-rig that attached to each suspension mounting in the finite element bus model that shown in Figure 3.18.

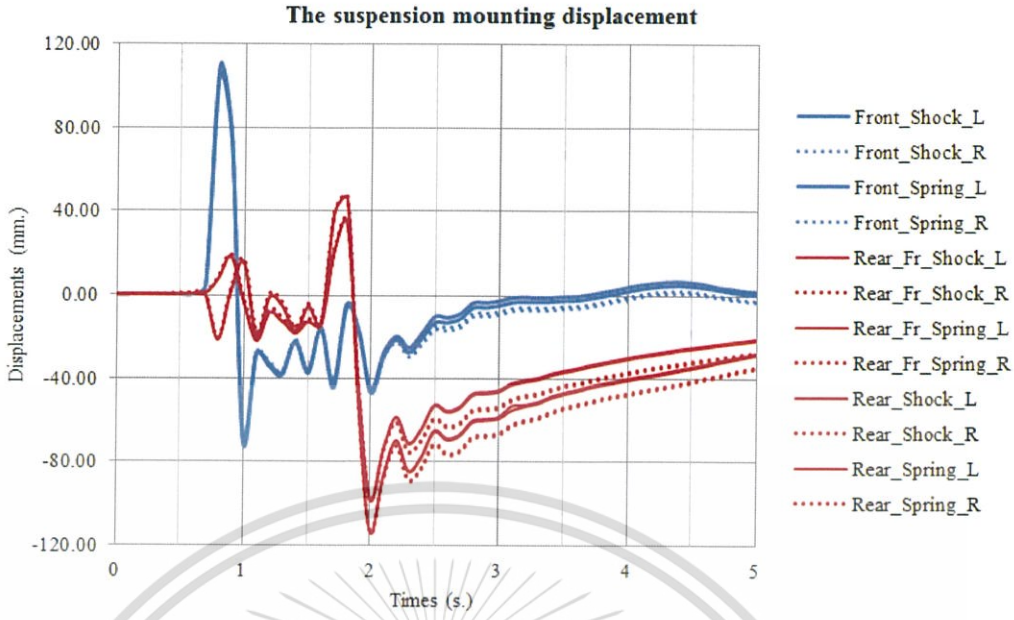

Figure 3.17 The displacement of suspension mounting

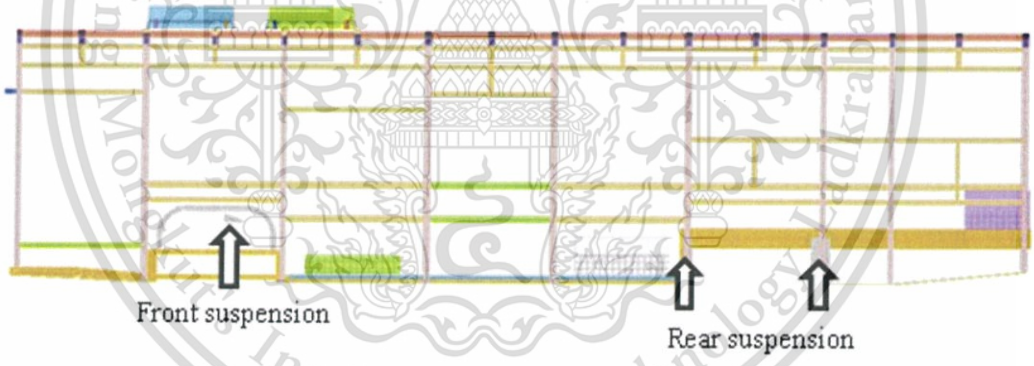

Figure 3.18 The position of test-rig on suspension mounting of chassis

The components of the battery packs are assumed to be placing on the battery plate with contact function as TYPE24 (Sliding Contact), Figure 3.19. This contact of battery packs and battery plate has a friction value about 0.2. This implies that the battery packs have movement and rotation in 3-axis belong to the movement behavior of the bus structure via the displacement of suspension.

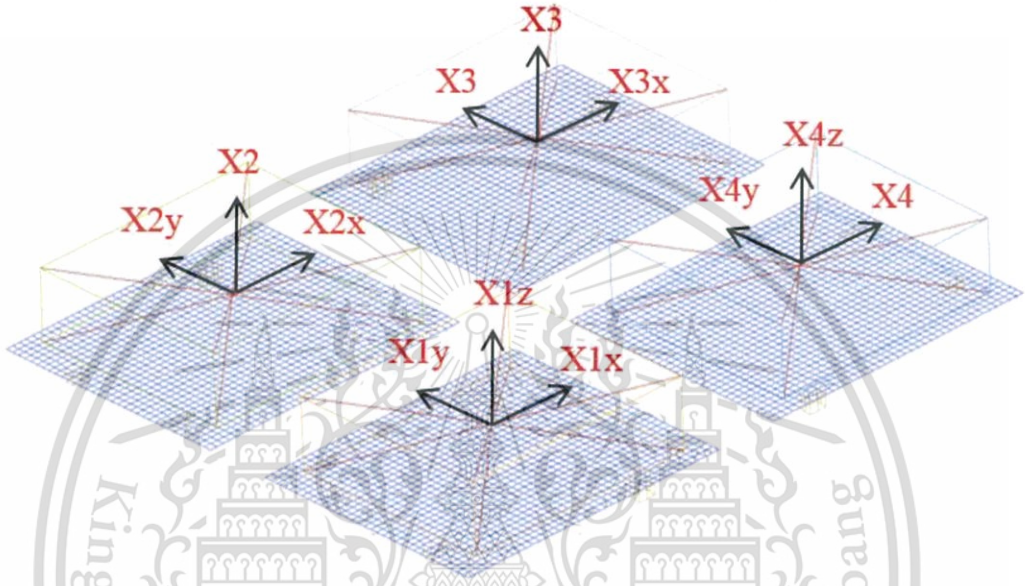

Figure 3.19 The battery packs free-body diagram

3.5 The design of battery packs mounting

The investigation of design to find the differences and the most appropriate design for the battery packs mounting. This study presents three different models of battery packs holder under the same simulation conditions.

3.5.1 Battery mounting bracket with fastener

First design of battery packs mounting will use the brackets mount to the battery packs and lock up with fastener. Each battery pack has a total of 8 brackets to prevent the movement of the battery pack in the axle under the load condition. For the battery bracket is presumably installed by a nut that locks through the bold holes as shown in Figure 3.20. and the properties of the structure bus model is show in Table 3.5.

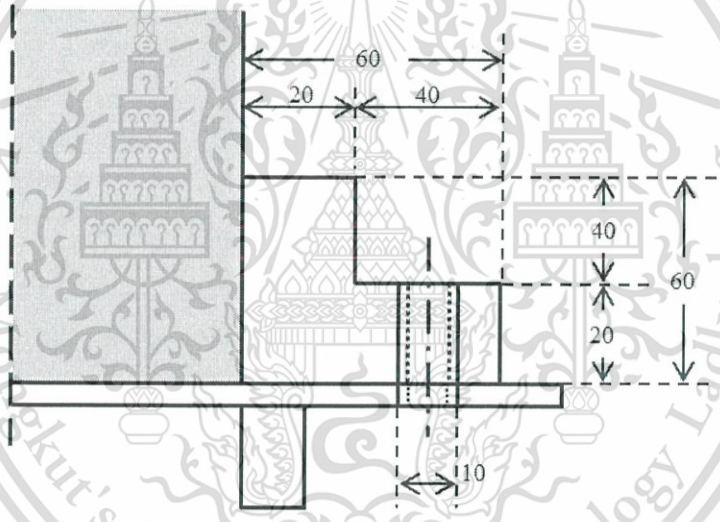

Figure 3.20 The mounting brackets geometry and dimension (mm.)

Table 3.5 The properties of the bus structure finite element model

Design	Holder mass (Kg.)	Volume (mm^3)	Total Mass (Kg.)
Mounting brackets	14.92	3.738 E+08	5,050

The mounting bracket is assumed to be attached to the battery packs. The Tie contact (TYPE2), the connection between two materials that rigidly connects a set of slave nodes (mounting beckets) to master surface (battery packs), was used to determine the contact between the mounting brackets and battery packs. It can be used to connect coarse and fine meshes, model spot-welds, or rivets. The schematic of connection of contact surface is shown in Figure 3.21.

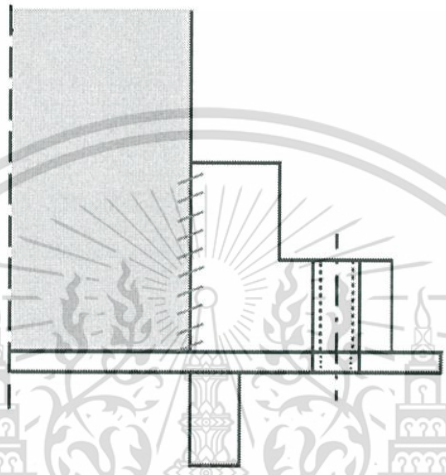

Figure 3.21 The schematic of the connection of mounting brackets to battery packs

The mounting brackets are connected to the battery plate with the same contact, Tie contact (TYPE2). The mounting holes are used as area of nodes that is locked to the battery plate as it had been locked with a fastener as show in Figure 3.22.

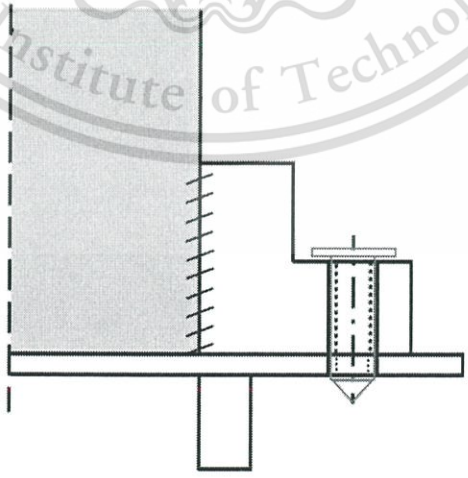

Figure 3.22 The schematic of the area of fastener on the mounting brackets

The final meshed finite element model of the mounting brackets with fastener design and number of elements and nodes are shown in Figure 3.23 and table below.

Figure 3.23 The finite element model of mounting brackets design with battery plate in HyperWorks software

Table 3.6 The number of solid elements and nodes of mounting bracket finite element model

Design	Solid elements	Nodes
Mounting brackets	2,816	5,952

3.5.2 Battery holder

Based on the need of a convenient battery packs replacement and easier than the first design. The second design is another type of battery holder that can support the battery packs and also limit the movement of the battery packs during the traveling of the bus. The design diagram is shown in Figure 3.24. and the properties of the structure bus model is show in Table 3.7.

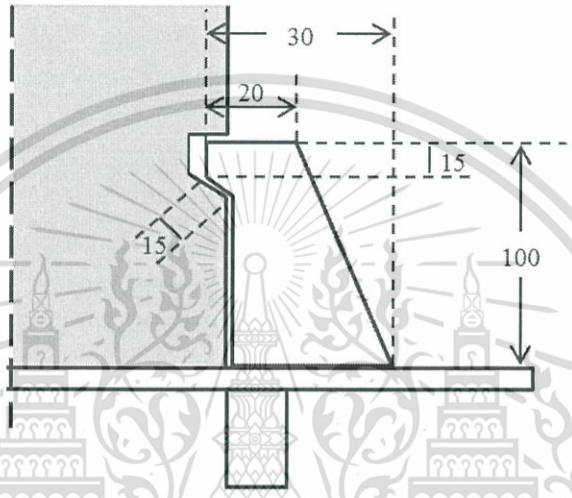

Figure 3.24 The battery holder geometry and dimension (mm.)

Table 3.7 The properties of the bus structure finite element model

Design	Holder mass (Kg.)	Volume (mm^3)	Total Mass (Kg.)
Battery holders	25.17	3.754 E+08	5,063

The battery holder is assumed as perfect connected to a battery plate. Due to the properties of the Tie contact mentioned in the first design, so the function can be used in this case as well, Figure 3.25.

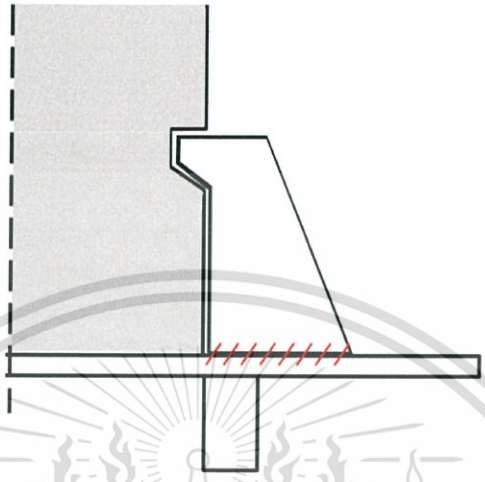

Figure 3.25 The schematic of the connection of battery holder to battery plate

This design allows the battery packs can move slightly without being locked. But the battery holder will limit the movement of the battery packs to avoid excessive movement. The sliding contact (TYPE24) was used between battery holder and battery packs with tolerance in Figure 3.26. This contact has a friction value about 0.2.

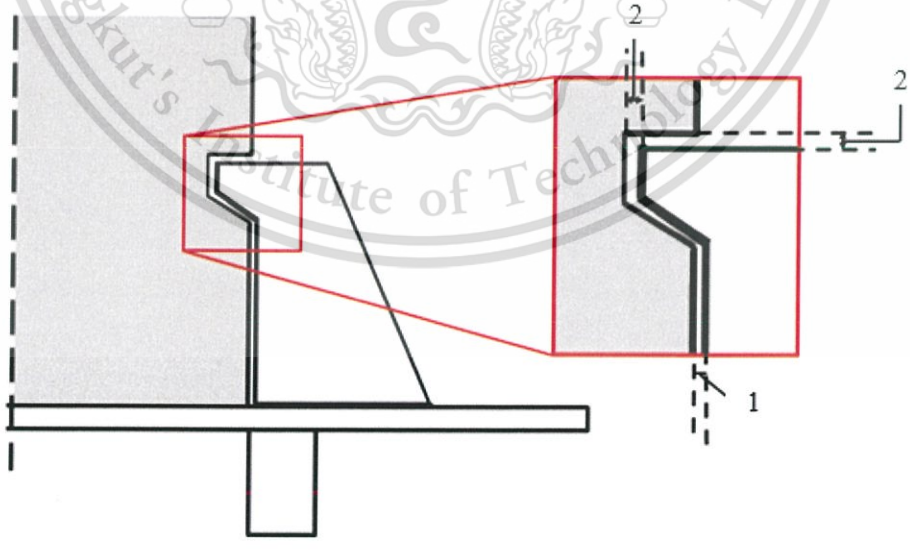

Figure 3.26 The dimension of tolerance of battery holder to battery pack (mm.)

The final meshed finite element model of the battery holder design is shown in Figure 3.27.

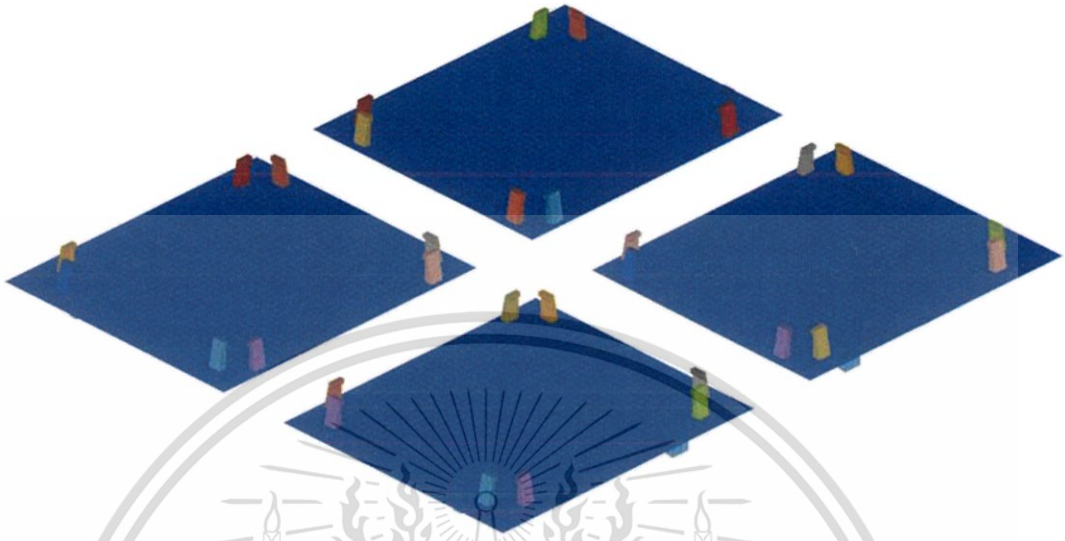

Figure 3.27 The finite element model of battery holder design with battery plate

Table 3.8 The number of solid elements and nodes of battery holder finite element model

Design	Solid elements	Nodes
Battery holder	6,320	10,584

3.5.3 Holder pillar

From the second design mentioned about the convenience of replacing battery packs. This design is chosen as a different battery mounting holder design with different gripping configurations. The battery holder may need more strength. So, in the third design, the pillar is used to replace the holder.

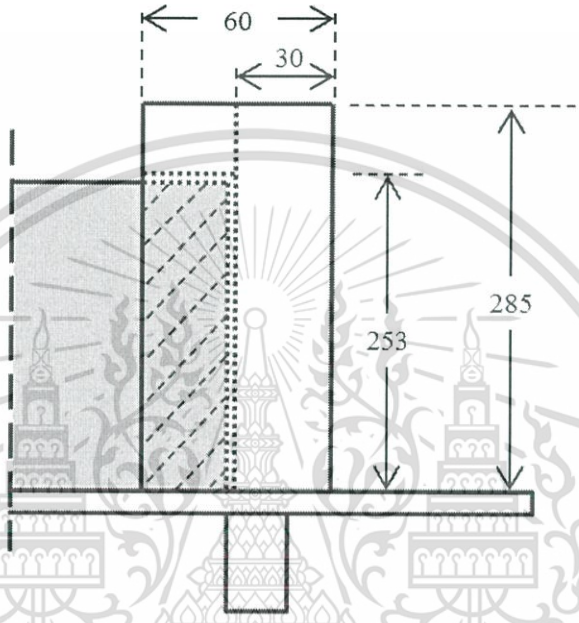

Figure 3.28 The holder pillar geometry and dimension (mm.)

Table 3.9 The properties of the bus structure finite element model

Design	Holder mass (Kg.)	Volume (mm^3)	Total Mass (Kg.)
Holder pillar	76.18	3.824 E+08	5,117

The property of contact type for battery pillar to battery packs and plate is similar to the second design, perfect connected, Tie contact (TYPE2) to battery plate, Figure 3.29 and Sliding contact (TYPE24) to battery packs, Figure 3.30. The only difference is the geometry of the battery holder which makes the contact surface of the battery packs has a greater contact area.

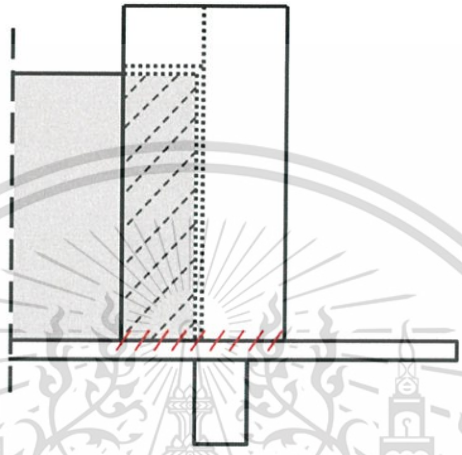

Figure 3.29 The schematic of the connection of holder pillar to battery plate

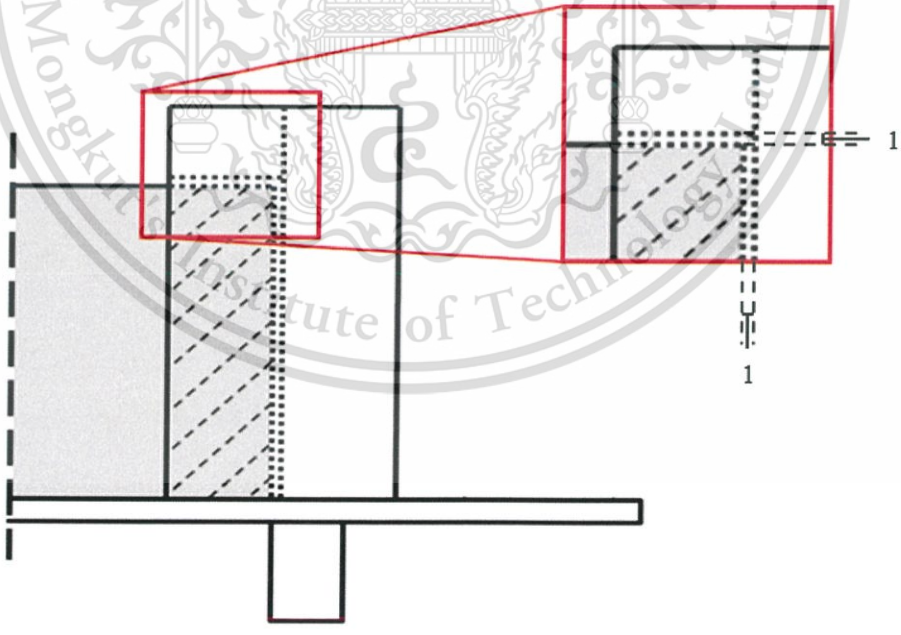

Figure 3.30 The dimension of tolerance of holder pillar to battery pack (mm.)

And the final meshed finite element model of the holder pillar design is shown in Figure 3.31.

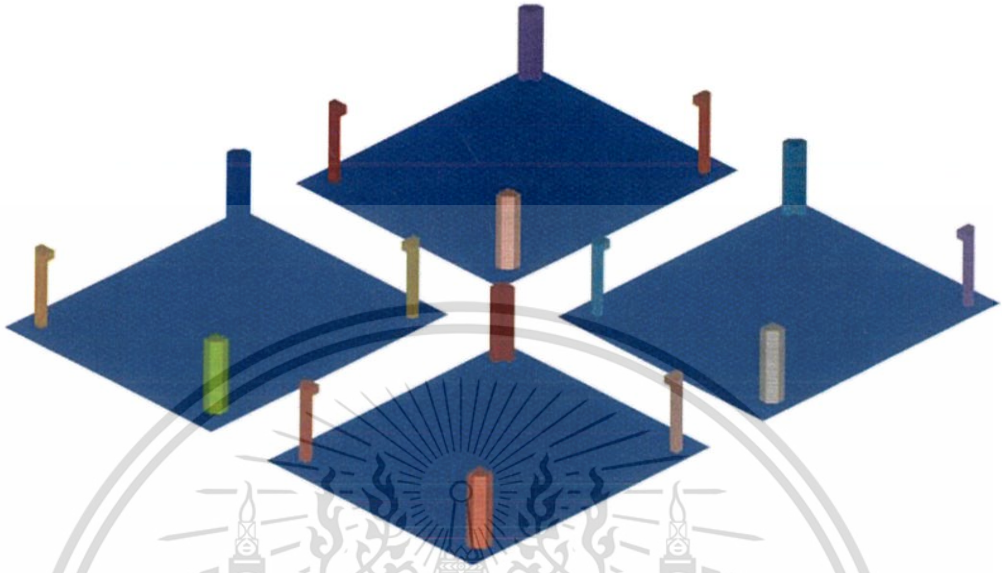

Figure 3.31 The finite element model of holder pillar design with battery plate

Table 3.10 The number of solid elements and nodes of holder pillar finite element model

Design	Solid elements	Nodes
Holder pillar	10,288	15,424

CHAPTER 4

RESULTS

This chapter will present and discuss about the results of simulation under conditions. The simulation results are divided into 2 steps, the virtual proving ground and durability simulation by using finite element method.

4.1 Virtual proving ground simulations

This simulation section, the virtual proving ground simulations of full bus model were carried out the dynamics displacements of suspension mounting point by using nonlinear dynamic software, MSC.ADAMS/Car, while the full bus model was assigned to travel over the single bump 10 cm height with initial velocities 25 km/hr. The dynamic displacements are measured from the location of tire contact with the road surface to front and rear suspension points through the functions of the air-spring and shock absorber. The results set are shown by using MSC.ADAMS/Post processor. The displacements of front left and right of air-spring and shock absorber mounting will show in Figure 4.1 and Figure 4.2.

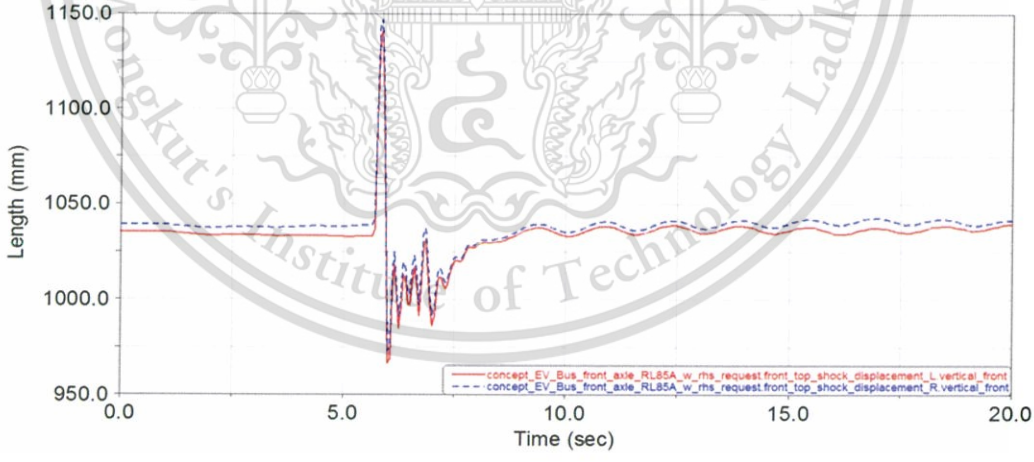

Figure 4.1 The displacement of front left and right shock absorber in vertical direction

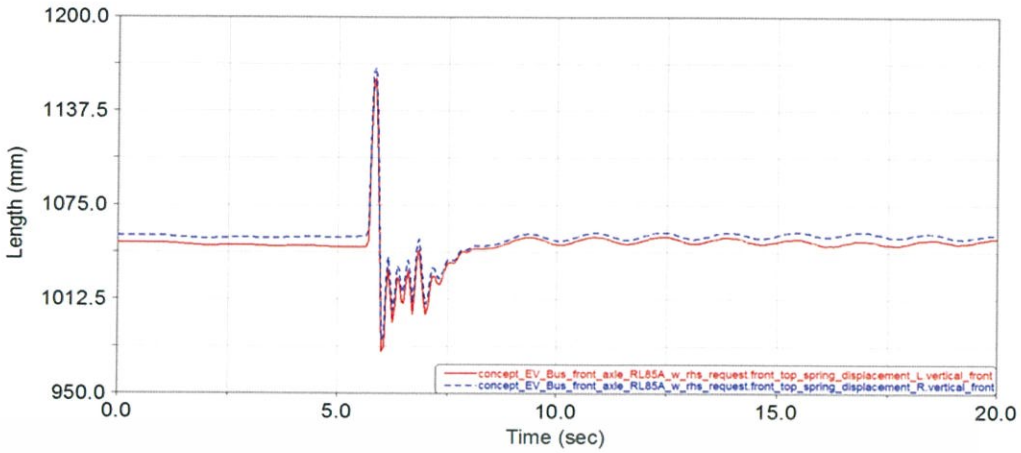

Figure 4.2 The displacement of front left and right air-spring in vertical direction

And the rear suspension systems that contained of 4 air-springs and shock absorber mounting will show in Figure 4.3 and Figure 4.4.

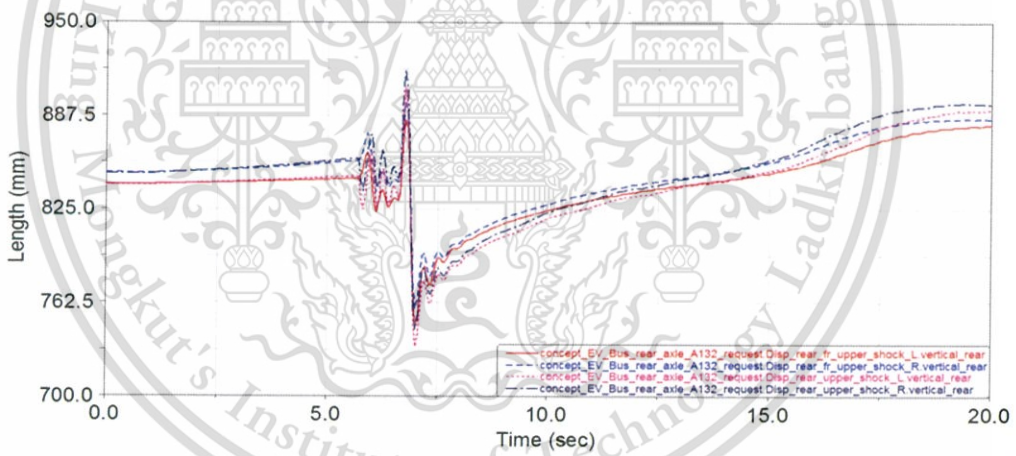

Figure 4.3 The displacement of rear left and right shcok absorber in vertical direction

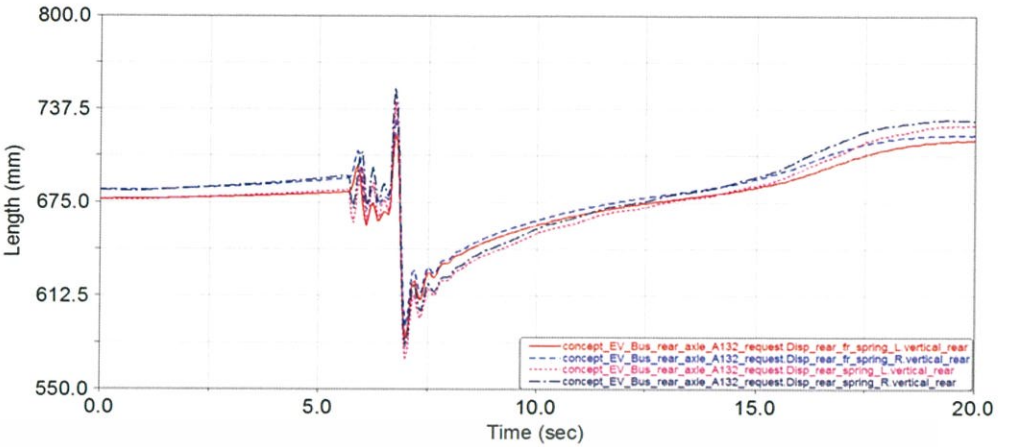

Figure 4.4 The displacement of rear left and right air-spring in vertical direction

The values of displacement derived from the MSC.ADAMS/Car are the positions of the suspension mounting point. In order to get the value of the displacement to apply in the next step of simulation, these values of positions will be edited. According to the objective of this study is to investigate only the excitation time periods which the model was impacted by traveled over the single bump. The simulation time of model in MSC.ADAMS/Car will be filter by cutting down and focus on the excitation time of the bus model only. Other than that, the simulation by the finite element method will takes a long time which depends on the input condition. Therefore, the data of the time interval during the first and after the model passed over the bump can be subtracted from the time interval. Below in Figure 4.5 and Figure 4.6 will show the values of displacement of front and rear suspension mounting in all axis after filtered and recalculated.

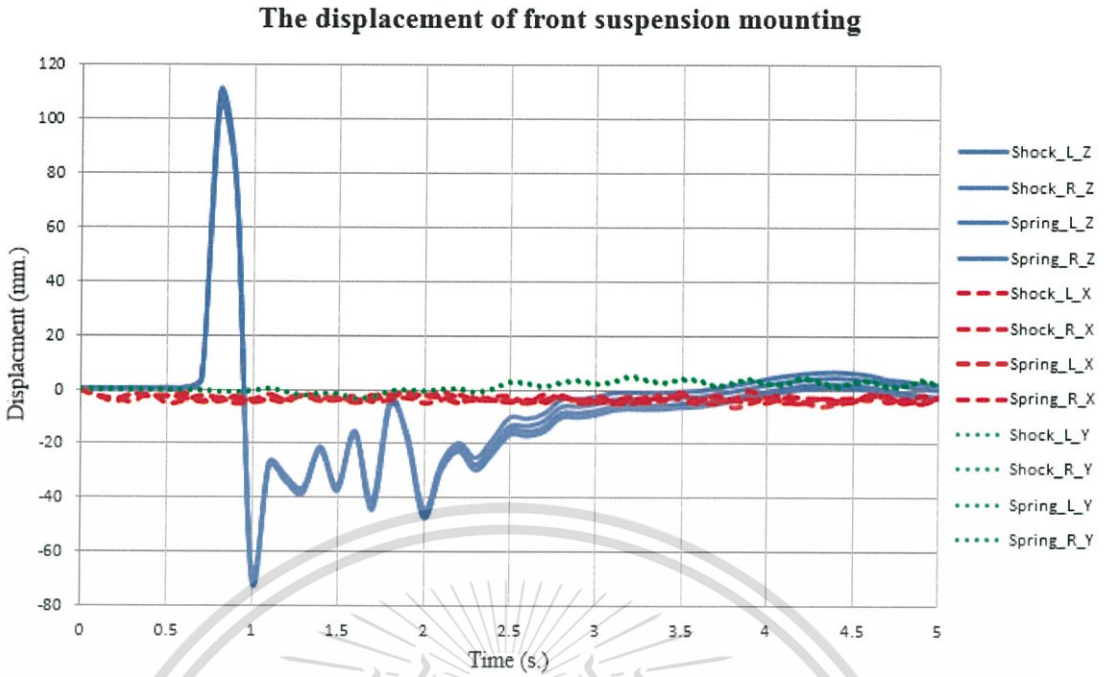

Figure 4.5 The displacement of front suspension mounting in all axis

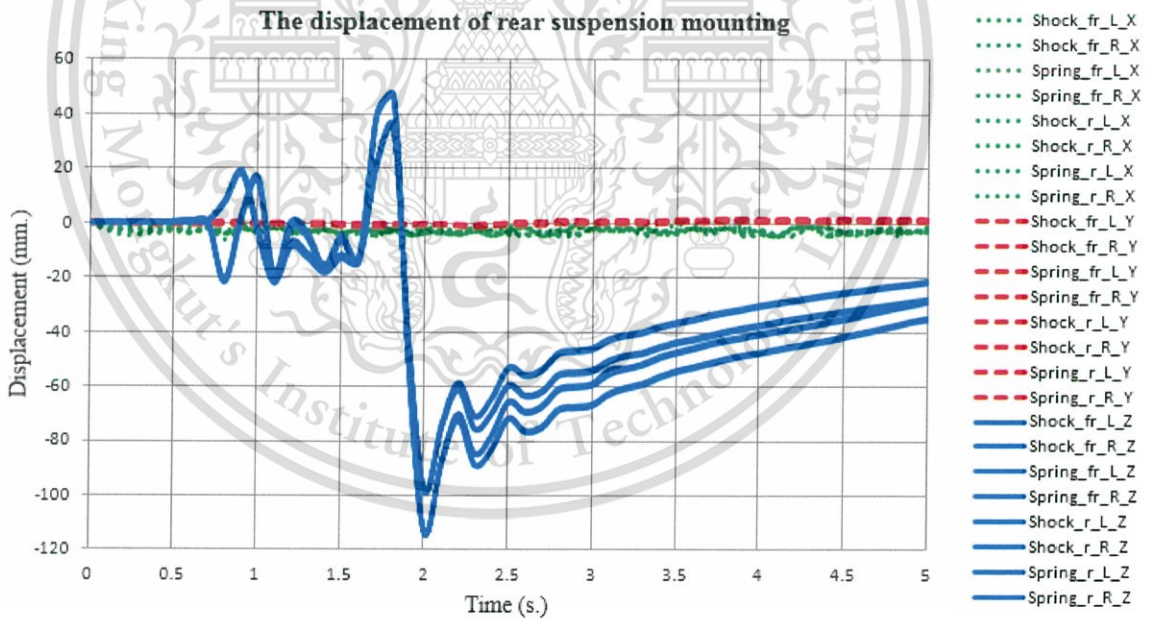

Figure 4.6 The displacement of rear suspension mounting in all axis

From the Figure 4.5 and Figure 4.6 above, it is noticeable that the displacement of suspension mounting point in the longitudinal and lateral directions is very small values when compared to vertical direction. There is no significant difference between the displacements of suspension mounting from the simulations (Kim Bladh, 2012). So, the displacement of suspension mounting point in vertical direction was chosen to apply in finite element method simulation.

4.2 Finite element analysis simulations

This section will present the results of stress from dynamic simulation using finite element method on bus model via HyperMesh; RADIOSS solver, the durability of battery mounting in each design will be discussed. To optimize the results of finite element analysis, the mesh sensitivity was analyzed.

4.2.1 Battery mounting durability

The battery mounting durability of each designs are discussed in this section. The battery mounting has a different strength to withstand the impact form the movement of the battery packs acting to the battery mounting. The characteristics of the mountings are also different for each purpose. In this topic, the stresses will be use to comparing the durability with each battery mounting design due to the continuous repeated load in long term event will causes the greatest damage stress and effect the fatigue of the components (Liu, Yin, Zhang, Zhang, & Zhou, 2015).

4.2.1.1 Mounting bracket with fastener

The finite element model of mounting bracket design was carried out with the dynamic stress distribution. The critical point is located at element 1911946, around the fastener hole shown in Figure 4.8, on the mounting bracket of battery pack number 4, Figure 4.7. and the movement of mounting bracket during maximum occurrence is show in Figure 4.9.

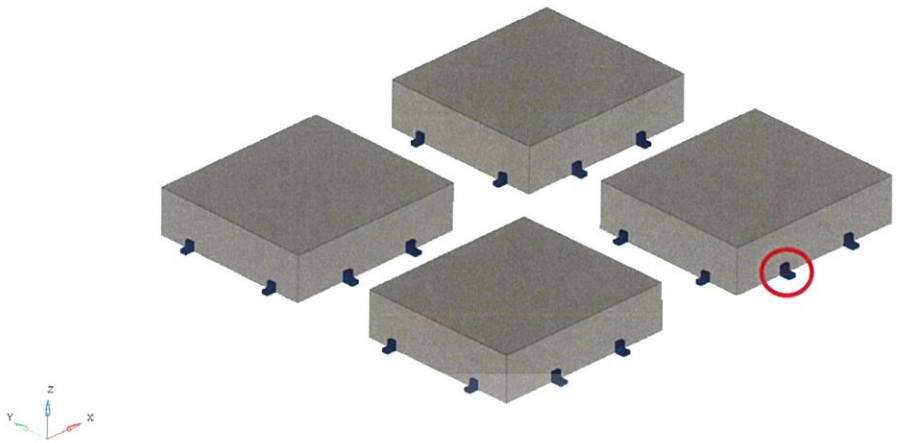

Figure 4.7 Location of maximum stress on the mounting bracket design

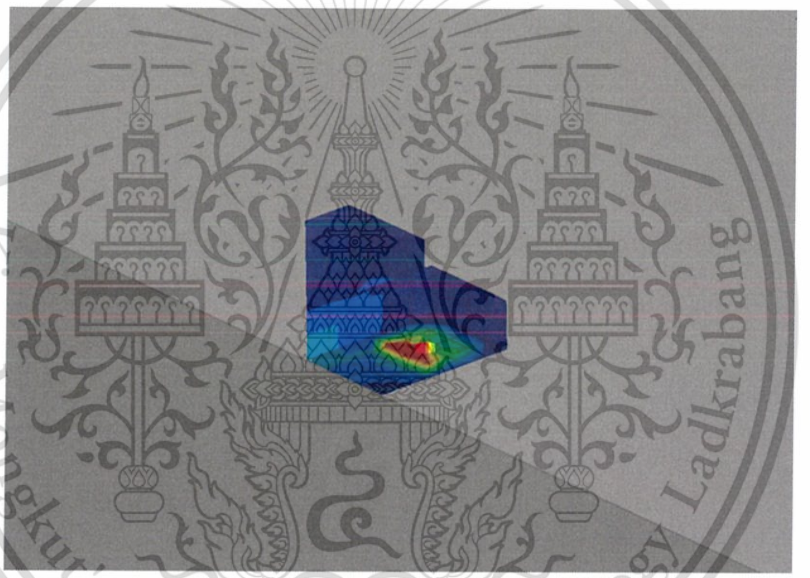

Figure 4.8 The stress distribution of the mounting bracket on battery pack number 4

Figure 4.9 The displacement of battery packs of the mounting brackets design during the moment of maximum stress occurrence

The maximum magnitude of stress on the mounting bracket is 307.78 MPa that show in Figure 4.10.

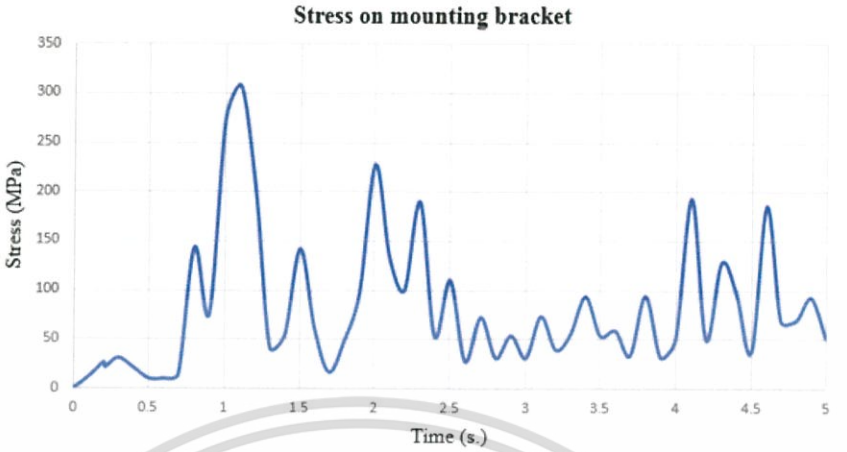

Figure 4.10 The stress of the mounting bracket on battery pack number 4

4.2.1.2 Battery holder

The battery holder design, the condition has changed, the battery packs has movement and rotation in 3-axis directions along with behavior of bus model. The critical point of stress is occurred at element 1497. This element is located at the mounting holder on battery number 1. Figure 4.11 to Figure 4.12 show the location, stress distribution and the movement during maximum stress of the mounting holder.

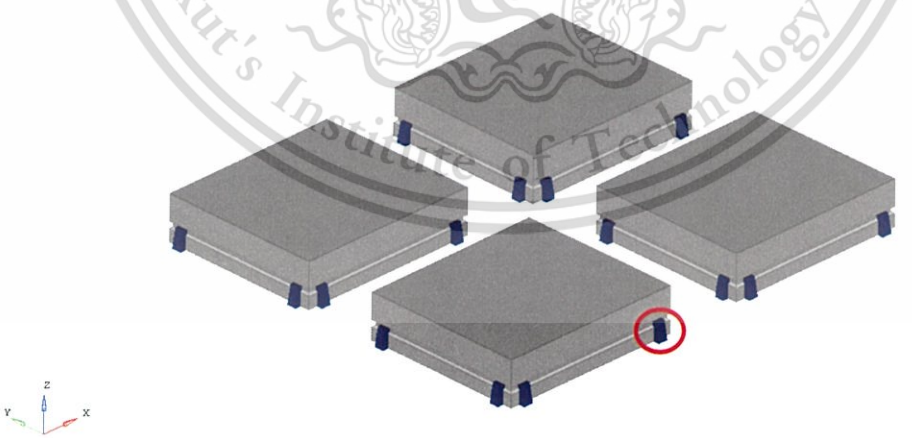

Figure 4.11 Location of maximum stress on the battery holder design

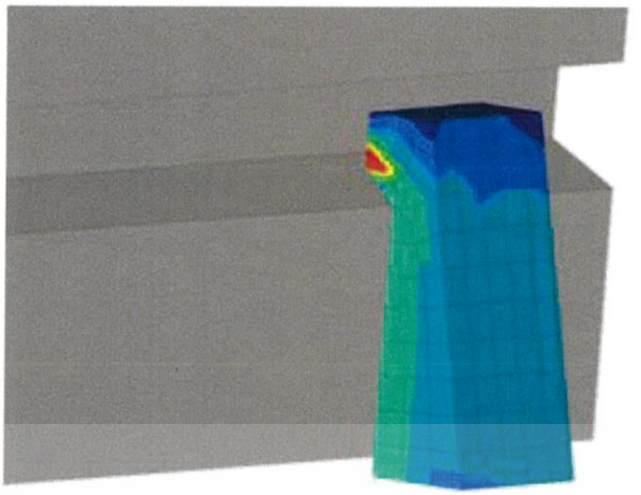

Figure 4.12 The stress distribution of the mounting holder on battery pack number 1

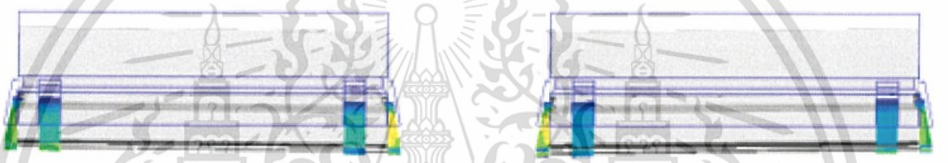

Figure 4.13 The displacement of battery packs of the battery holder design during the moment of maximum stress occurrence

The maximum magnitude of stress on the mounting holder is 304.32 MPa that show in Figure 4.14.

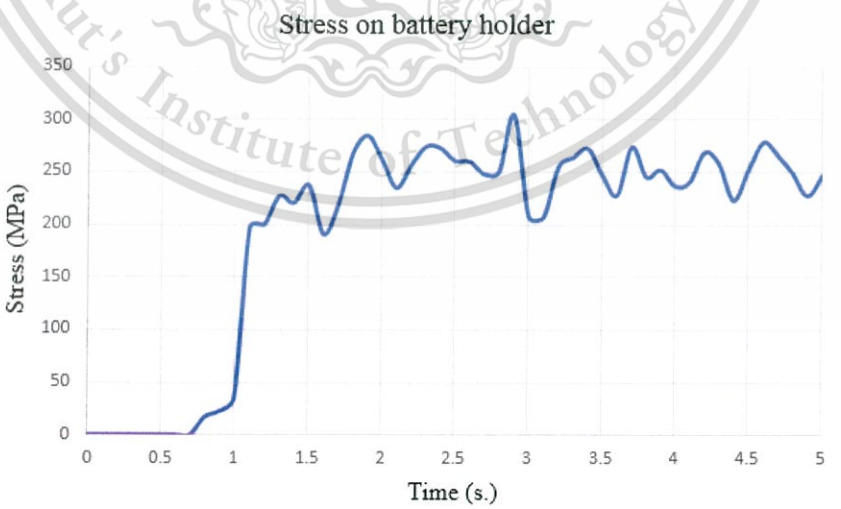

Figure 4.14 The stress of the mounting holder on battery pack number 1

4.2.1.3 Holder pillar

This design a bit differs from the second design of the battery mounting. The movement of the battery is limited in different location, the four holder pillars replace the mounting holder for support the movement of each the battery pack in 3-axis direction. However, the friction of the movement of the battery pack is still the same. After the simulation with the same condition, it was found that the maximum stress occurred at element number 1916659, at the corner under the pillar of battery pack number 3 as Figure 4.15.

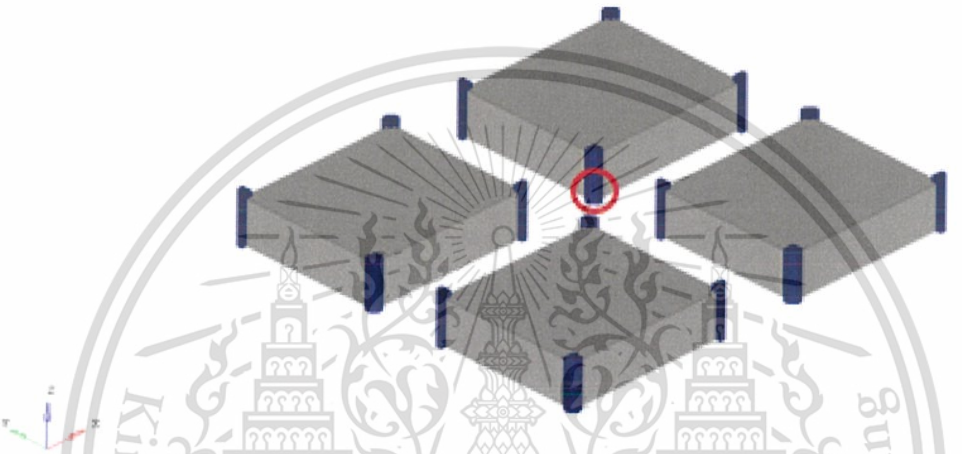

Figure 4.15 Location of maximum stress on the holder pillar design

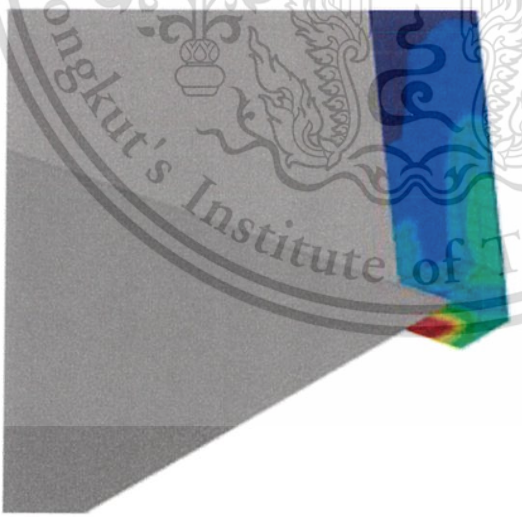

Figure 4.16 The stress distribution of the holder pillar on battery pack number 3

Figure 4.17 The displacement of battery packs of the holder pillar design during the moment of maximum stress occurrence

The maximum magnitude of stress on the holder pillar design is 105.72 MPa that show in Figure 4.18.

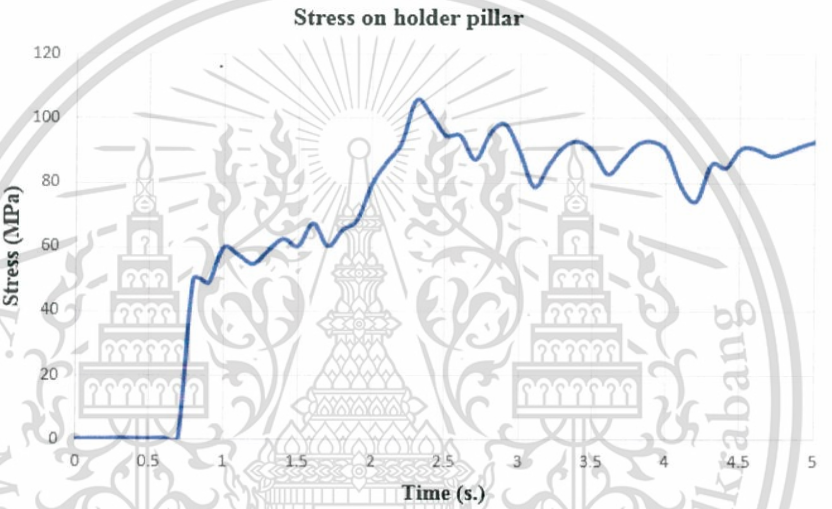

Figure 4.18 The stress of the holder pillar on battery pack number 3

4.2.2 Battery packs

The different design of the battery mounting may need to consider the movement of the battery pack in different directions. Each design has different characteristics of battery mounting to meet the purpose of the design. This makes the movement of the battery pack with different moves. The different characteristics of the battery pack movement will affect the acting force and durability of the battery mounting. So, another aspect of the battery mounting design. The characteristics of the battery packs acceleration and displacement are shown to compare the effect of durability and the maximum stress of the battery mounting from the previous section.

4.2.2.1 Battery packs of the mounting bracket design

The first design of the battery mounting holder is presented by the mounting bracket lock up to battery pack with fastener. This mean that the battery pack is locked to battery plate that connected to the roof structure. When the bus model traveled over the single bump, the suspension will move up which affect through the bus structure to roof structure. Causing the frequency movement of the roof structure to battery plate and battery pack respectively. The acceleration and displacement of each battery pack of mounting bracket design are shown in Figure 4.19 to Figure 4.22.

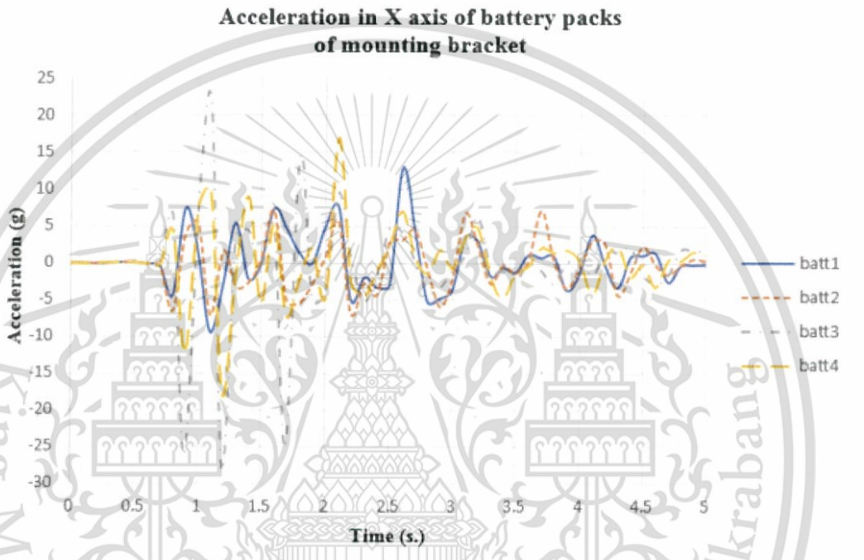

Figure 4.19 Acceleration in X axis of battery packs of mounting bracket

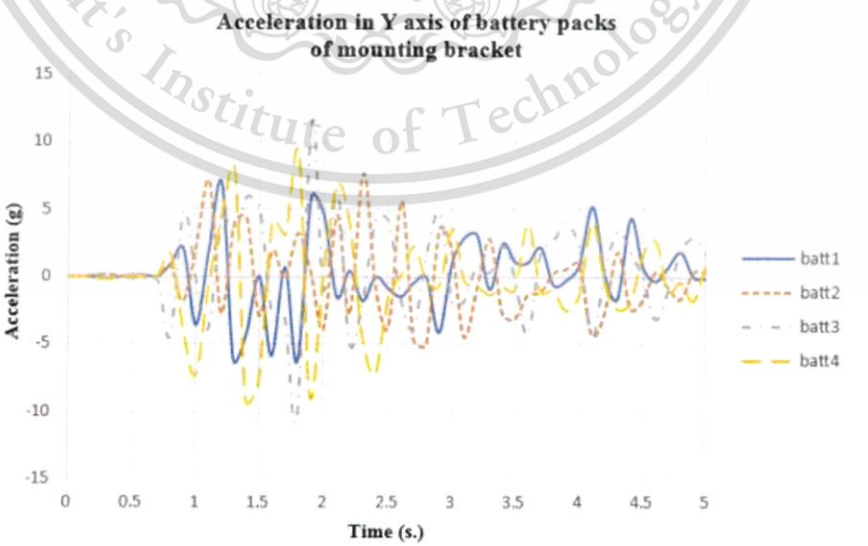

Figure 4.20 Acceleration in Y axis of battery packs of mounting bracket

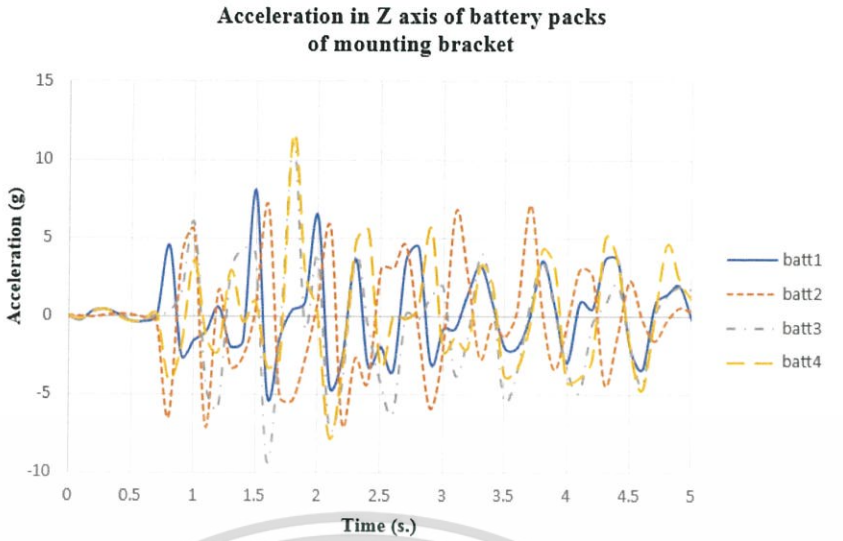

Figure 4.21 Acceleration in Z axis of battery packs of mounting bracket

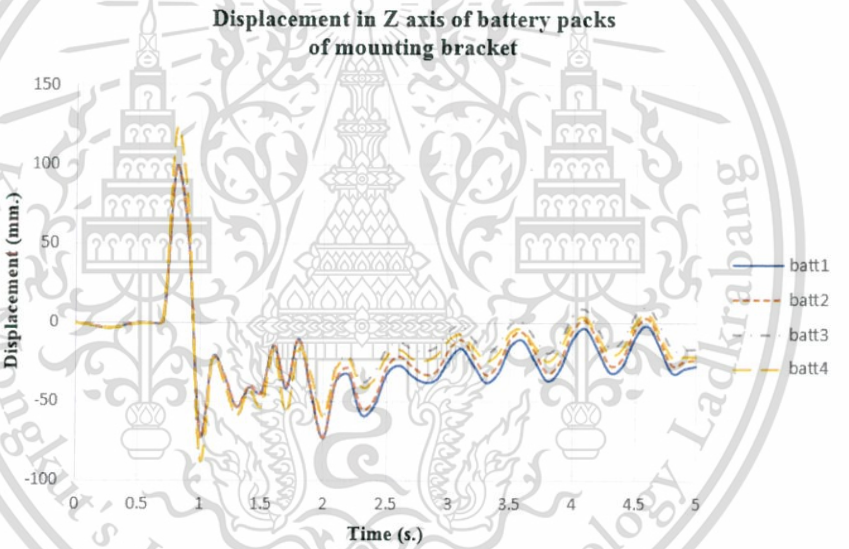

Figure 4.22 Displacement in Z axis of battery packs of mounting bracket

From the Figure 4.21, the maximum acceleration in z axis is occur at battery pack number 4 about 12 g which can be compared with the battery pack displacement as shown in Figure 4.22, It can be seen that the battery pack number 4 has the maximum displacement in z axis. This can explain the maximum stress of the mounting bracket shown in the previous section.

4.2.2.2 Battery packs of the battery holder design

The second design is aim to a convenient battery packs replacement, the battery holder is introduced. This will support and limit the movement of the battery packs during the bus maneuver. The acceleration and displacement of battery pack of the battery holder design is shown in Figure 4.23 to Figure 4.26.

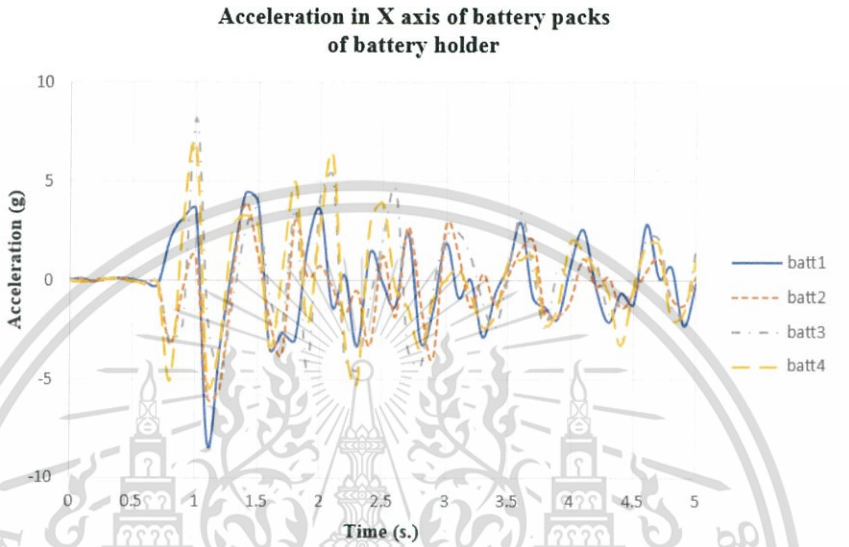

Figure 4.23 Acceleration in X axis of battery packs of battery holder

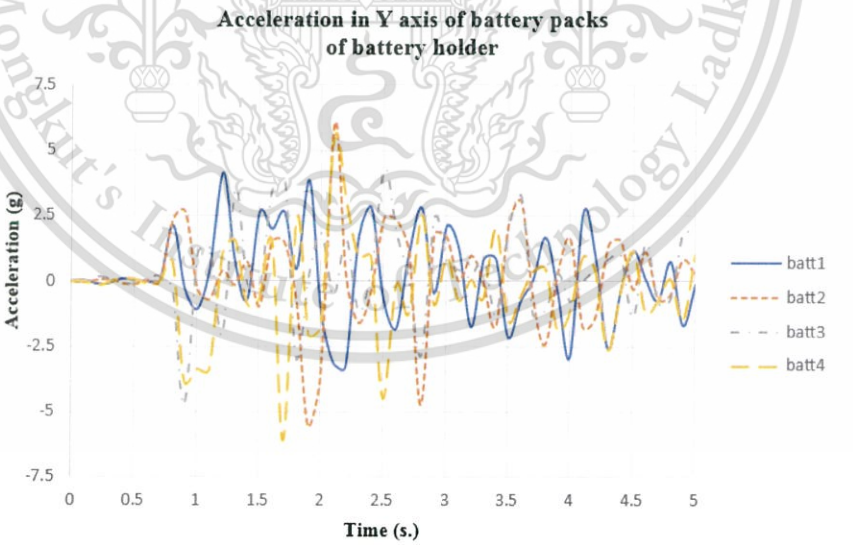

Figure 4.24 Acceleration in Y axis of battery packs of battery holder

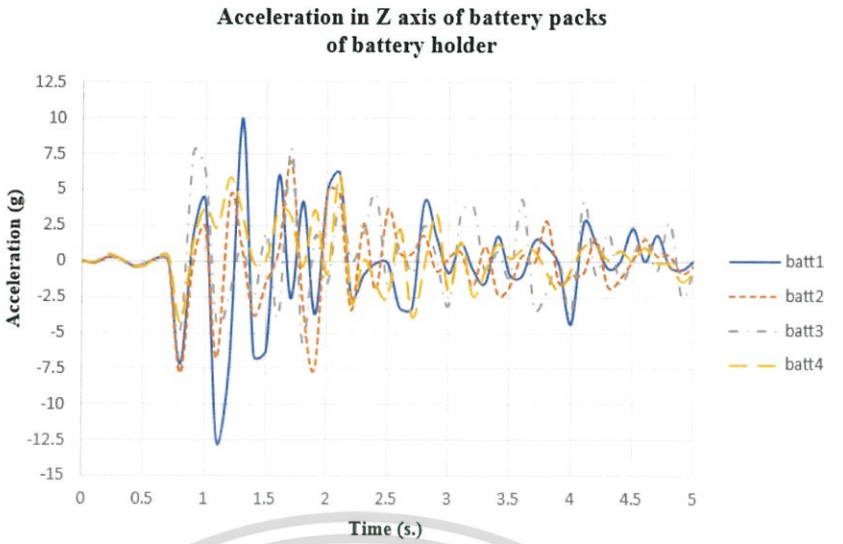

Figure 4.25 Acceleration in Z axis of battery packs of battery holder

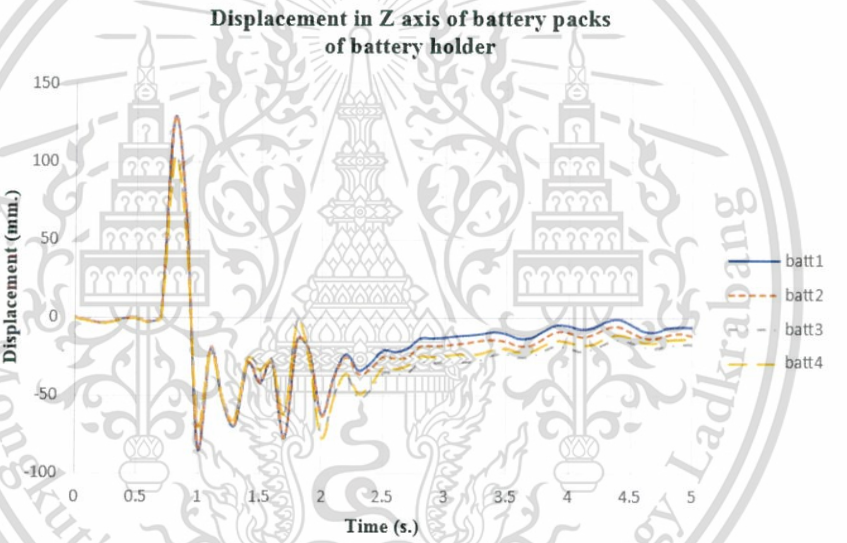

Figure 4.26 Displacement in Z axis of battery packs of battery holder

The Figure 4.25 show the maximum acceleration in z axis is occur at battery pack number 1 about 10 g and Figure 4.26 show the maximum displacement in z axis is at battery pack number 1 which corresponded quite well with the result of maximum stress of the battery holder design in the same way.

4.2.2.3 Battery pack of the holder pillar design

In this design is present the holder with different gripping configurations to introduced as a guideline of the battery mounting design that requires the strength holder to support the battery packs. This design has the same concept of seize the battery pack with a second design. But the battery holder on each side of battery pack is replaced with the pillar that support at corner of battery pack. Figure 4.27 to Figure 4.30 are show the acceleration and displacement of battery pack.

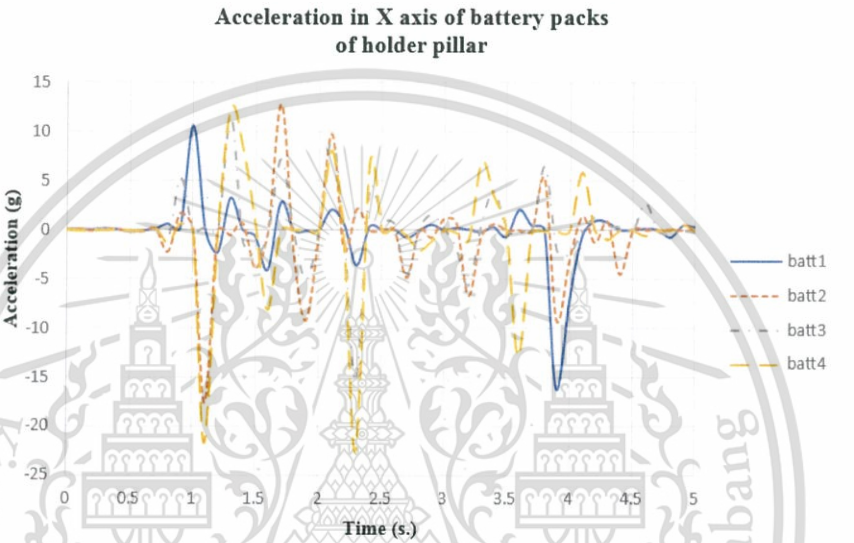

Figure 4.27 Acceleration in X axis of battery packs of holder pillar

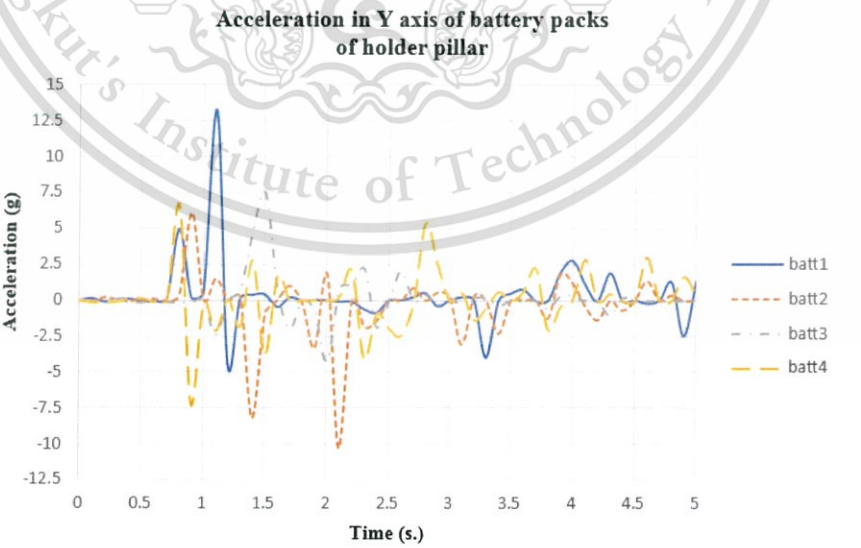

Figure 4.28 Acceleration in Y axis of battery packs of holder pillar

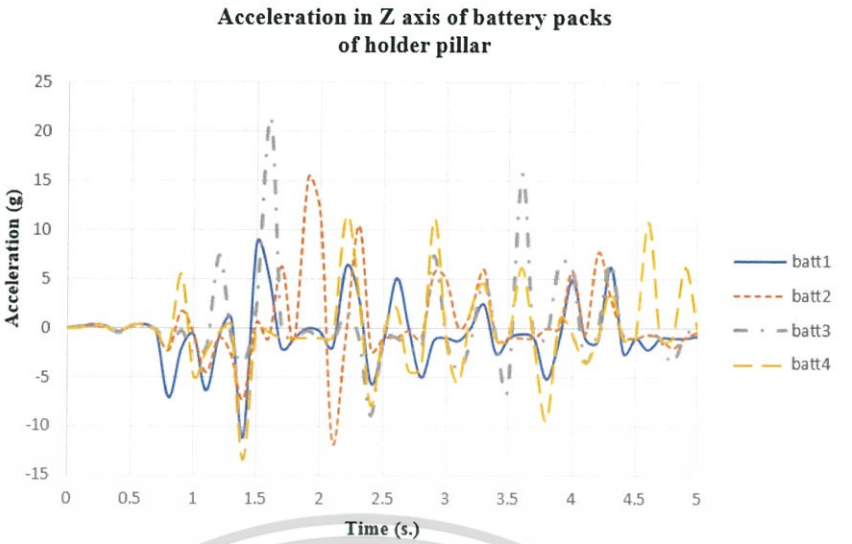

Figure 4.29 Acceleration in Z axis of battery packs of holder pillar

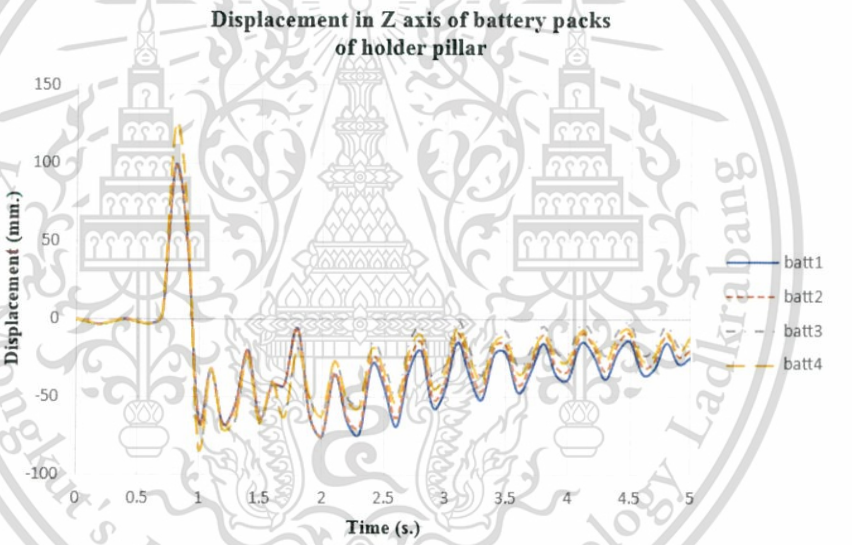

Figure 4.30 Displacement in Z axis of battery packs of holder pillar

The maximum acceleration in z axis is occur at battery pack number 3 about 20 g and the maximum displacement in z axis is at battery pack number 3 that show in Figure 4.29 and Figure 4.30 which corresponded with the result of maximum stress of the holder pillar design.

4.2.3 Roof structure

With the 3 different design of the battery mounting, resulting in the properties of the bus model is different. The main structures of each design are separately considered. The roof structure of each design is discussed. Due to the design of the battery holder affects the model properties. Analysis of the roof structure takes place at 8 elements on the area under the battery packs to compare and consider the trend of stress distribution of each design.

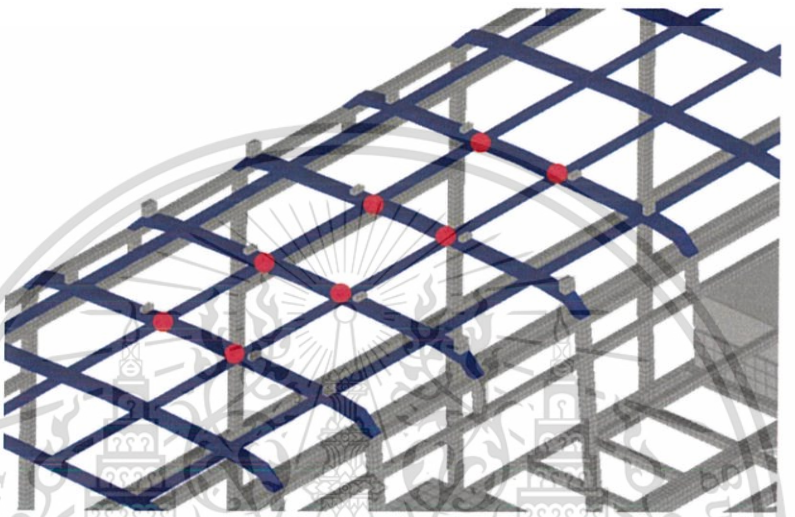

Figure 4.31 The location of 8 elements under the battery pack are being considered

First design of battery mounting, mounting brackets, have magnitude of the maximum stress of 8 elements on roof structure is 535.84 MPa. Occurs under the battery pack number 4.

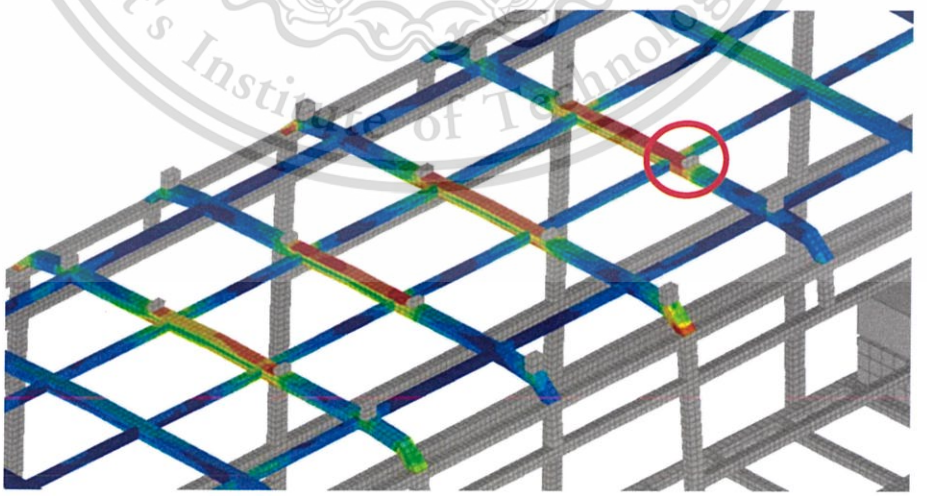

Figure 4.32 The stress distribution on roof structure of mounting bracket design

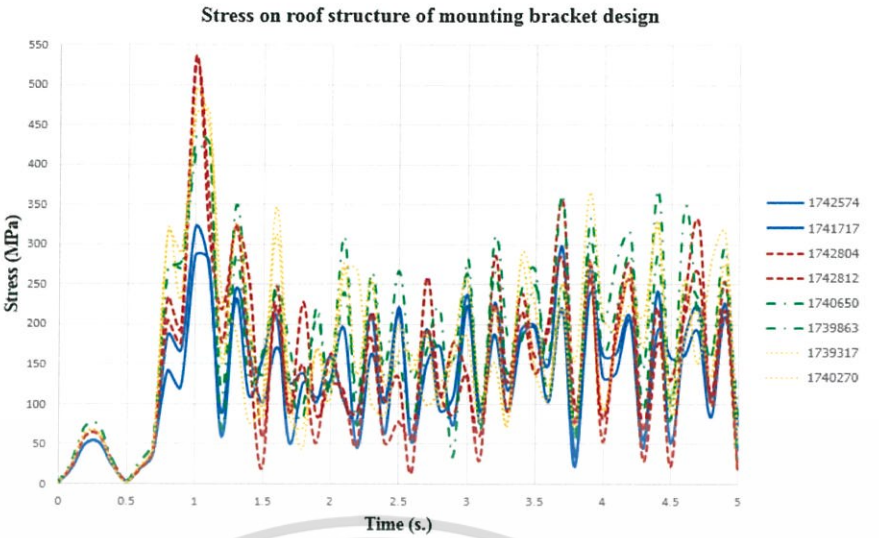

Figure 4.33 The stress on roof structure of mounting bracket design

The second design, battery holder. The maximum stress magnitude of 8 elements on the roof structure is 543.45 MPa. Under the battery packs number 1.

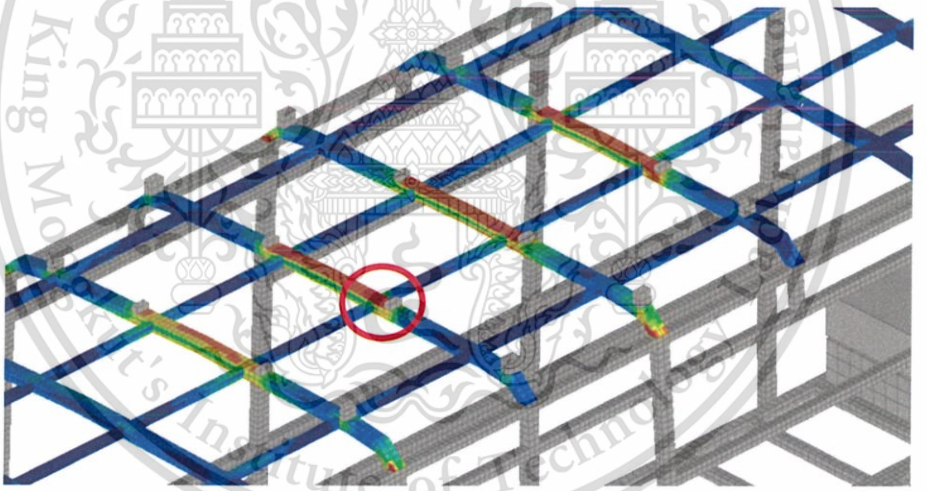

Figure 4.34 The stress distribution on roof structure of battery holder design

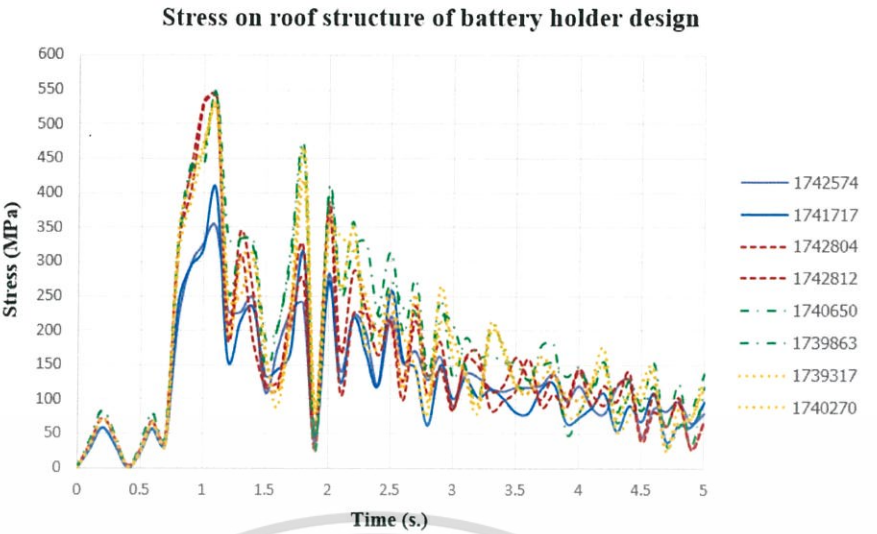

Figure 4.35 The stress on roof structure of battery holder design

And the last design of battery holder, holder pillar. The maximum stress magnitude of 8 elements on the roof structure is 582.14 MPa.

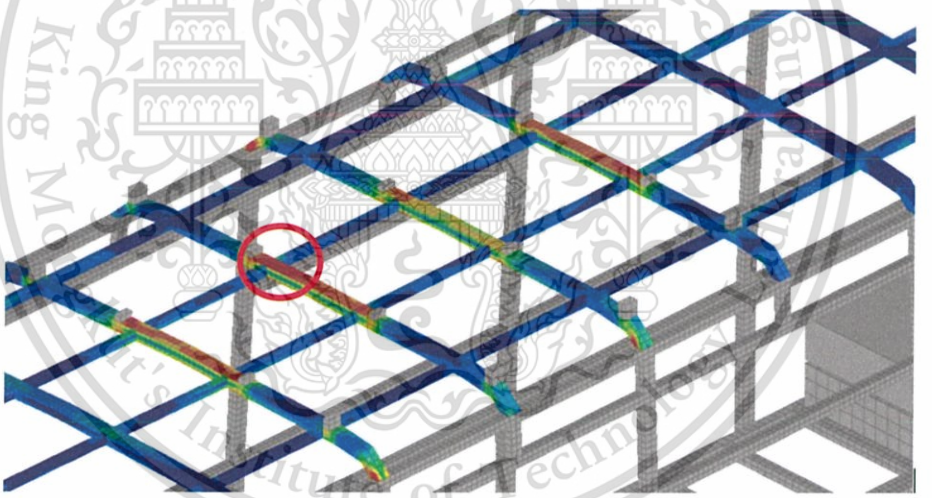

Figure 4.36 The stress distribution on roof structure of holder pillar design

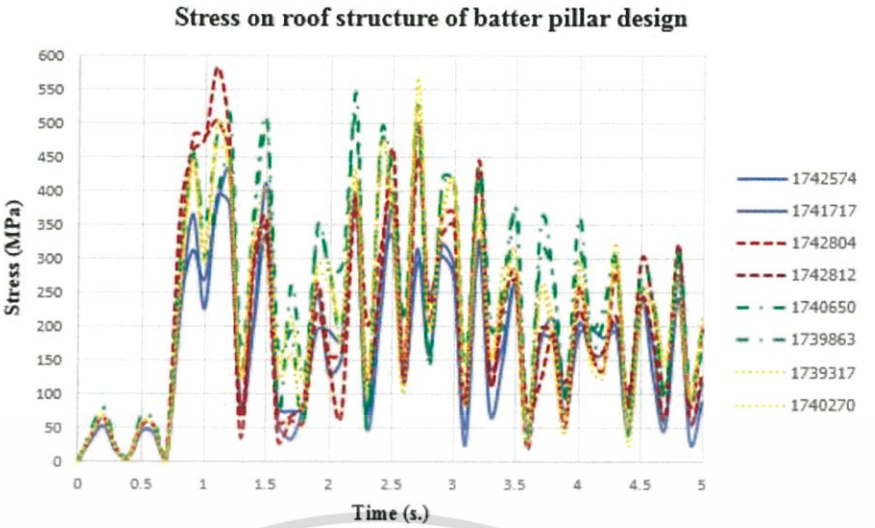

Figure 4.37 The stress on roof structure of holder pillar design

4.2.4 Mesh refinement analysis

To improve the accuracy of finite element results of stress distribution on battery pack mounting in each design, Mesh refinement is introduced. There are three ways of refining a finite element mesh; the H-method, the P-method and the R-method as (Madan G. Kittur & Ronald L. Huston, 1989) described.

The H-method is used in this study. This method depends on the selection of the size of the element. The large element will give a rough result. Replacing this large element with a larger number of smaller elements will result in a higher accuracy of result. (Madan G. Kittur & Ronald L. Huston, 1990) mention that the increasing of the number of elements by the H-method will give the result better than increasing the polynomial order (P & R-method) for the same increase in the number of degrees of freedom. In the same way, the greater the number of elements, the more time consumption in simulation duration. Finding the optimal size of the elements is essential in simulation. The purpose of this study is to investigate the stress on the battery pack mounting. Therefore, this component is analyzed with this method. The size of element is chosen to mesh in 3 different range of sizes: fine, medium and coarse (Ruta & Ozbolt, 2016), with sizes of 10-15 mm., 6-9 mm. and 2-5 mm. The first step, 10-15 mm., was presented in section 4.2.1 already. This section will present other 2 step, 6-9 mm. and 2-5 mm. The result of stress for each design of battery holder after re-mesh will be discussed.

4.2.4.1 Mounting bracket

The mesh refinement of the mounting bracket with 2 steps is presented after mesh refinement. The stress distribution and magnitude of the mounting bracket after mesh refinement is discussed by grid independence method. The results of stress distribution will show in Figure 4.38 to Figure 4.41.

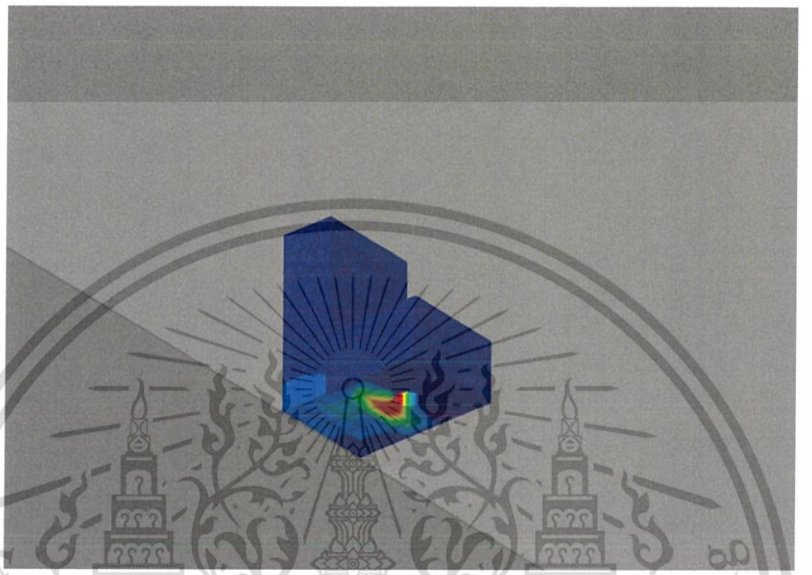

Figure 4.38 The stress distribution of mounting bracket after mesh refinement step 2 (6-9 mm.)

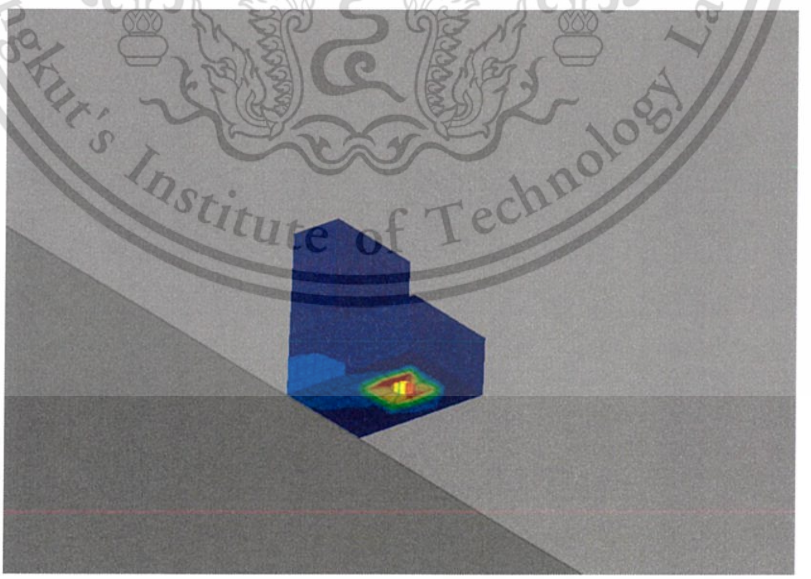

Figure 4.39 The stress distribution of mounting bracket after mesh refinement step 3 (2-5 mm.)

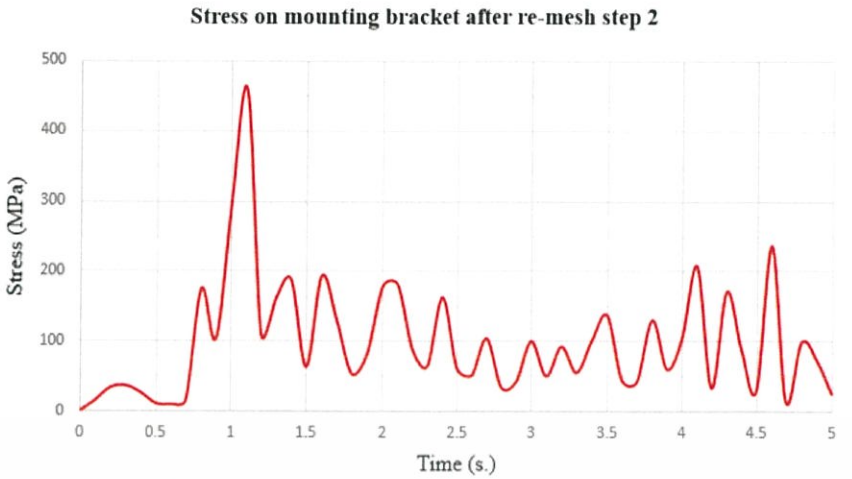

Figure 4.40 The stress of the mounting bracket after re-mesh step 2

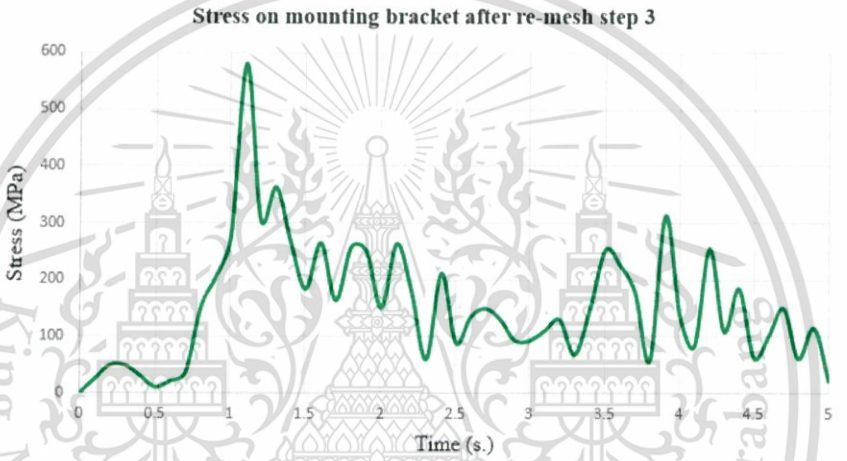

Figure 4.41 The stress of the mounting bracket after re-mesh step 3

The maximum magnitude of stress on the mounting bracket of 3 steps mesh is show in Table 4.1.

Table 4.1 The maximum magnitude of stress on the mounting bracket from 3 steps of meshing

Step of mesh refinement	Maximum stress (MPa)
Mesh step 1 (10-15 mm.)	307.78
Mesh step 2 (6-9 mm.)	459.72
Mesh step 3 (2-5 mm.)	580.10

Table 4.2 The number of solid elements and nodes of mounting bracket finite element model from 3 steps of meshing

Step of mesh refinement	Solid elements	Nodes
Mesh step 1 (10-15 mm.)	2,816	5,952
Mesh step 2 (6-9 mm.)	6,720	11,532
Mesh step 3 (2-5 mm.)	17,160	26,232

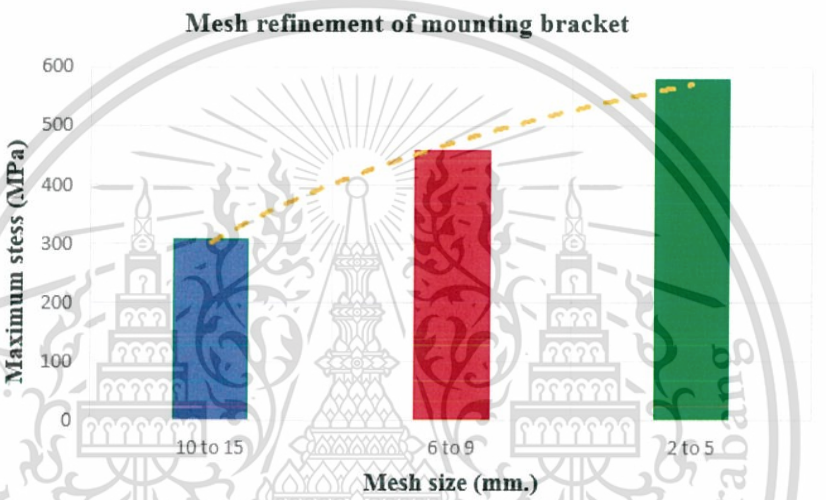

Figure 4.42 The trend of stress of mesh refinement on mounting bracket design

4.2.4.2 Battery holder

The stress distribution and magnitude of the battery holder are shown in Figure 4.43 to Figure 4.46 with maximum magnitude show in Table 4.3 and the trend of stress of mesh refinement in Figure 4.47.

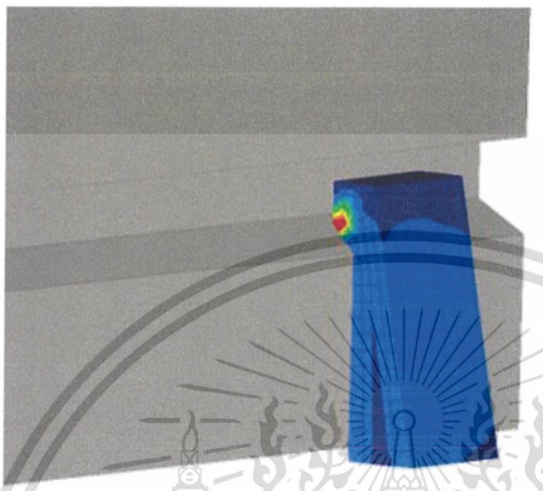

Figure 4.43 The stress distribution of battery holder after mesh refinement step 2 (6-9 mm.)

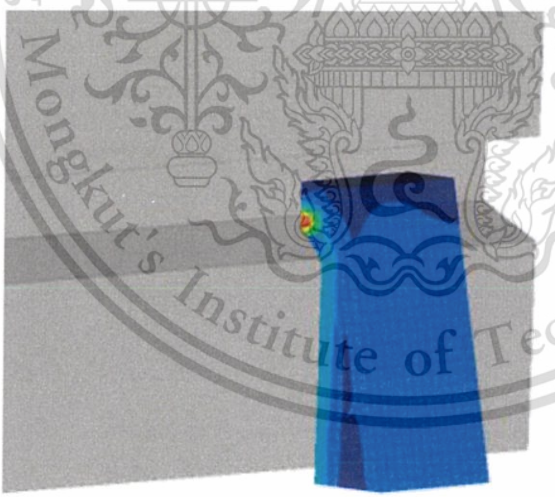

Figure 4.44 The stress distribution of battery holder after mesh refinement step 3 (2-5 mm.)

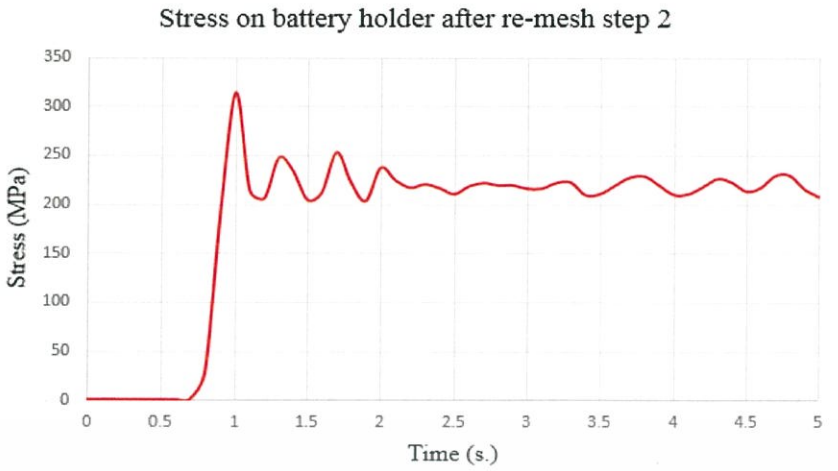

Figure 4.45 The stress of the battery holder after re-mesh step 2

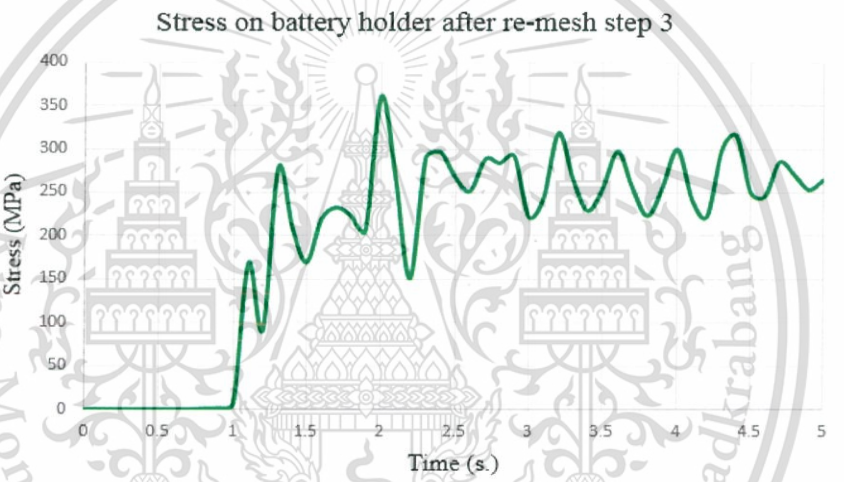

Figure 4.46 The stress of the battery holder after re-mesh step 3

Table 4.3 The maximum magnitude of stress on the battery holder from 3 steps of meshing

Step of mesh refinement	Maximum stress (MPa)
Mesh step 1 (10-15 mm.)	304.32
Mesh step 2 (6-9 mm.)	314.93
Mesh step 3 (2-5 mm.)	359.80

Table 4.4 The number of solid elements and nodes of battery holder finite element model from 3 steps of meshing

Step of mesh refinement	Solid elements	Nodes
Mesh step 1 (10-15 mm.)	6,320	10,584
Mesh step 2 (6-9 mm.)	17,255	25,408
Mesh step 3 (2-5 mm.)	58,800	78,364

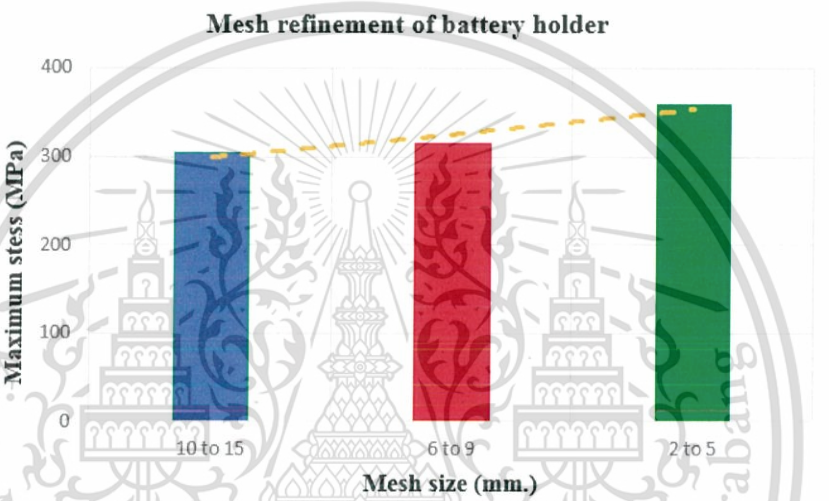

Figure 4.47 The trend of stress of mesh refinement on battery holder design

4.2.4.3 Holder pillar

The trend of stress is also slightly similar with 2 design above. The stress distribution and magnitude are shown in Figure 4.48 to Figure 4.51. The maximum magnitude and trend of stress are shown sequentially.

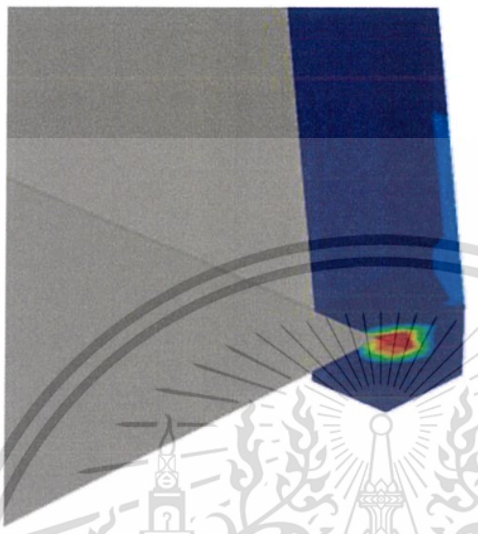

Figure 4.48 The stress distribution of holder pillar after mesh refinement step 2

Figure 4.49 The stress distribution of holder pillar after mesh refinement step 3

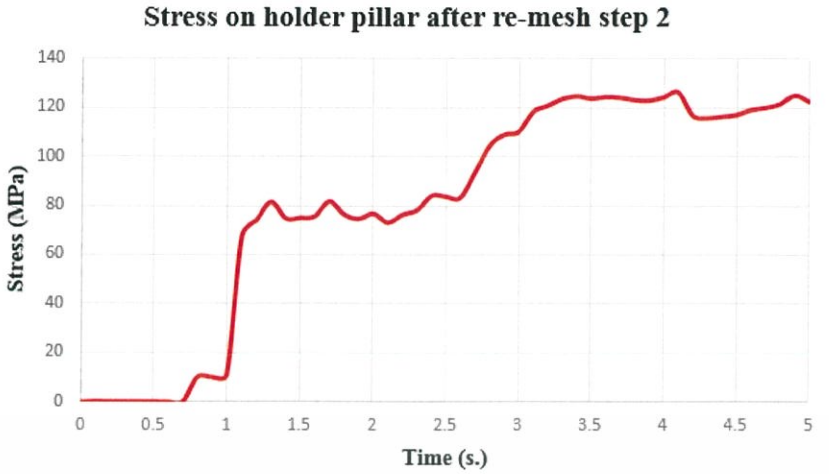

Figure 4.50 The stress of the holder pillar after re-mesh step 2

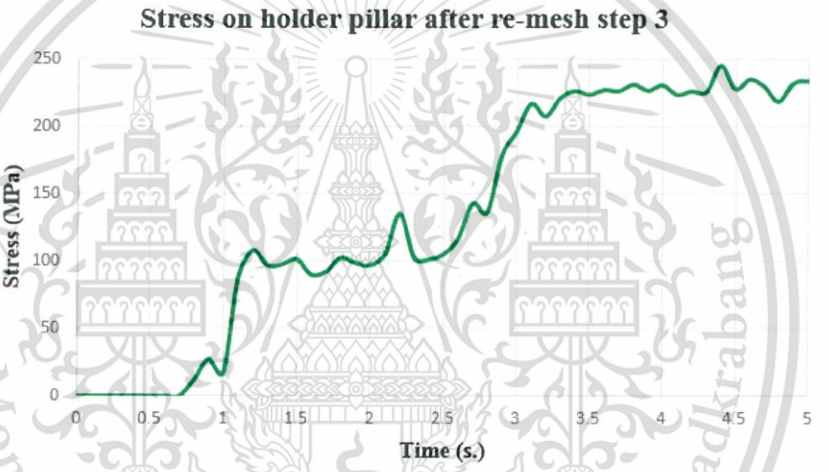

Figure 4.51 The stress of the holder pillar after re-mesh step 3

Table 4.5 The maximum magnitude of stress on the holder pillar from 3 steps of meshing

Step of mesh refinement	Maximum stress (MPa)
Mesh step 1 (10-15 mm.)	105.72
Mesh step 2 (6-9 mm.)	126.46
Mesh step 3 (2-5 mm.)	245.07

Table 4.6 The number of solid elements and nodes of holder pillar finite element model from 3 steps of meshing

Step of mesh refinement	Solid elements	Nodes
Mesh step 1 (10-15 mm.)	10,288	15,424
Mesh step 2 (6-9 mm.)	35,224	46,622
Mesh step 3 (2-5 mm.)	113,876	143,544

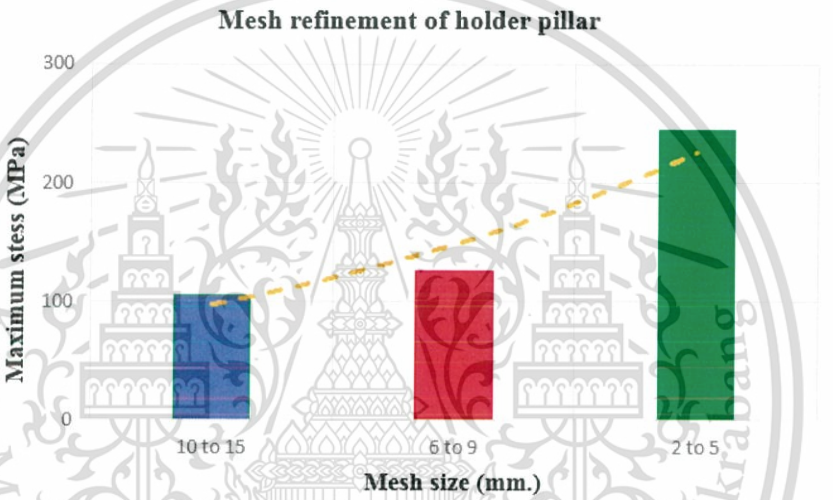

Figure 4.52 The trend of stress of mesh refinement on holder pillar design

From the results of stress above, all of the results showed that the gradient in the mesh refinement analysis was consistent with the theory of H-method. But, in order to analyze thoroughly in mesh refinement, the maximum stress occurring at different times, so using only the highest stress values to analyze may not be enough. The analysis of grid convergence method was presented.

4.2.5 Grid convergence analysis

The mesh refinement performed as nonuniform grid refinement ratio, the mesh refinement ratios greater than 1.3 to obtain good results (Schwer, 2008); $r = \frac{h_2}{h_1} = \frac{15}{9} = 1.6$, $r = \frac{9}{5} = 1.8$. The grid convergence analysis methods can be done independently without a fixed method, the author chooses the mounting holder which the maximum stress occurred and focus on the period of interesting time, the battery pack caused the maximum acceleration in vertical direction. The element has selected by drawing a straight line through the element that maximum stress occurred in order to consider the stress distribution behavior of all 3 mesh refinement steps. In each step of the mesh refinement, there are differences in the number of elements. The position of the elements that are interested is separated into zones for easy comparison. The gird convergence of the battery holder finite element model was discussed below.

4.2.5.1 Mounting bracket

The grid convergence on the mounting bracket design is separate into 4 zones as Figure 4.53. The maximum stress of each element at time t = 1.8 s., the maximum acceleration of battery packs, being brought to focus. The stress distribution on each element of the mounting bracket is show in Figure 4.54.

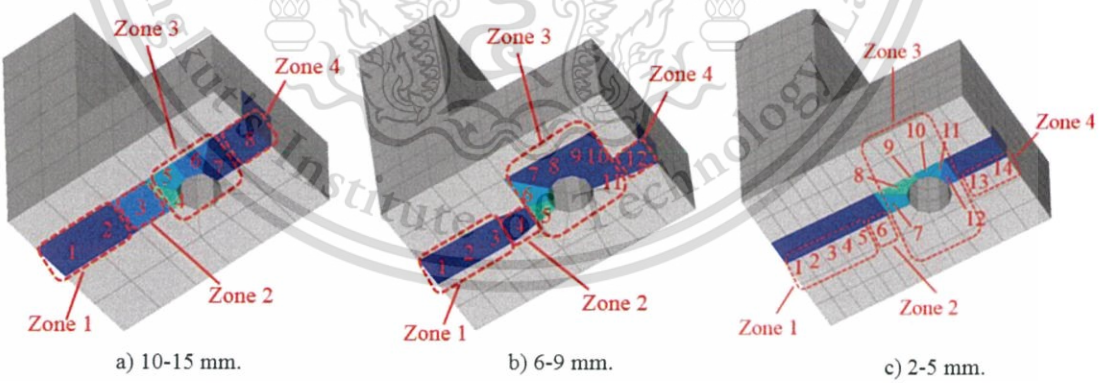

Figure 4.53 The zone area of mounting bracket on each step of mesh refinement

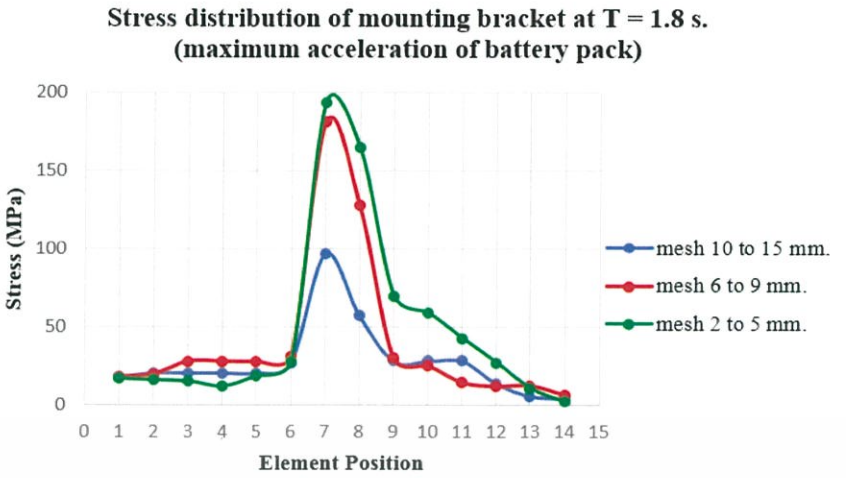

Figure 4.54 The maximum stress of each element of mountin bracket design at time T=1.8 s.

As Figure 4.54, it can be observed that the trend of stress distribution is in the same direction. Therefore, the author chose the maximum value to analyze the differences between each step of mesh refinement, Table 4.7.

Table 4.7 The comparison of maximum stress differences of the mounting brackets from 3 step of meshing

Step of mesh refinement	Max. stress (MPa)	% Gap	Solid elements	Increase in number of element (Times)	Nodes	Increase in number of nodes (Times)
Mesh step 1 (10-15 mm.)	97.02	x	10,288	x	15,424	x
Mesh step 2 (6-9 mm.)	180.85	86	35,224	3.42	46,622	3.02
Mesh step 3 (2-5 mm.)	193.21	7	113,876	3.23	143,544	3.08

From the Table 4.7, it can be noticed that the mesh step 1 to 2, the maximum stress value has increased to 86% with the number of solid elements increasing by 3.4 times. On the other hand, the maximum stress from the mesh step 2 to 3 raise by only 7% with the number of solid elements that have increased by 3.2 times from the mesh 6-9 mm. With the calculation time varies with the number of solid elements, reducing the size of the solid elements in the next order may have not different results which will take more time than necessary.

4.2.5.2 Battery holder

The grid convergence on the battery holder design is also separate into 4 zones. The maximum acceleration of battery packs of this design occurred at t = 1.3 s. The zone area of battery holder design and the stress distribution on each element are show in Figure 4.55 and Figure 4.56.

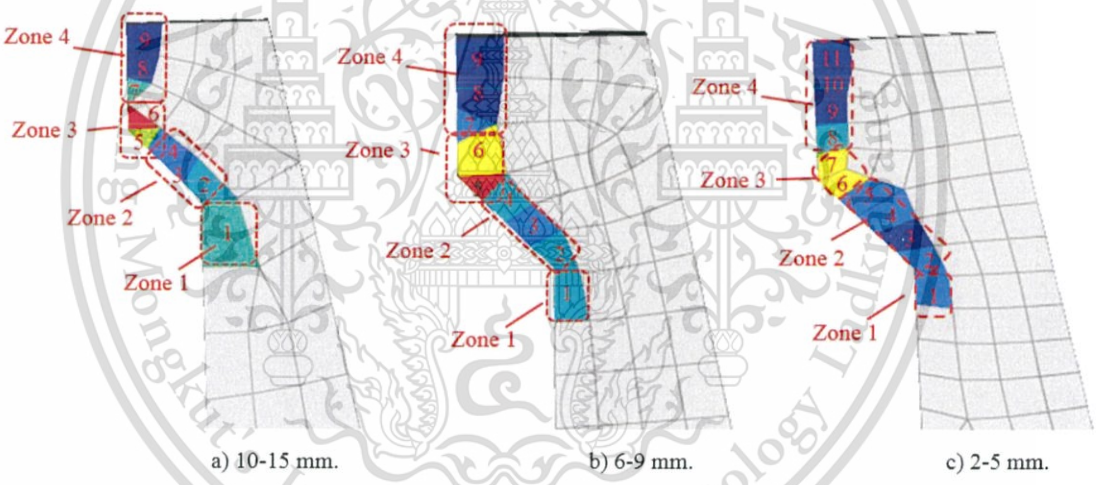

Figure 4.55 The zone area of battery holder on each step of mesh refinement

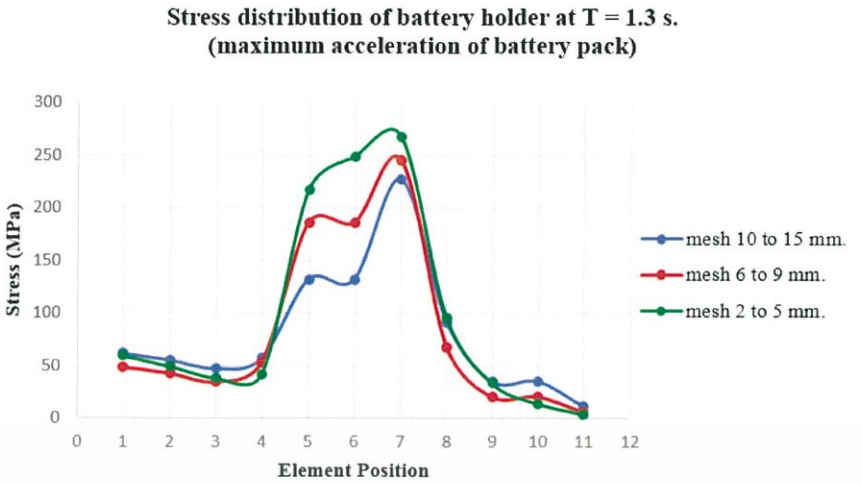

Figure 4.56 The maximum stress of each element of battery holder design at time T=1.3 s.

The maximum stress value chosen will be show in the Table 4.8.

Table 4.8 The comparison of maximum stress differences of the battery holder from 3 step of meshing

Step of mesh refinement	Max. stress (MPa)	% Gap	Solid elements	Increase in number of element (Times)	Nodes	Increase in number of nodes (Times)
Mesh step 1 (10-15 mm.)	226.84	x	6,320	x	10,584	x
Mesh step 2 (6-9 mm.)	245.33	9	17,255	2.73	25,408	2.40
Mesh step 3 (2-5 mm.)	267.74	8	58,800	3.41	78,364	3.08

From the second design, it can be seen that the size of all 3 steps of mesh refinement given quite a similar result of maximum stress. With the number of elements increasing to 2.7 times from the coarse mesh, size 10-15 mm., the maximum stress increases just 9%. More than that, with the fine mesh, 2-5 mm., the elements are increased by 3.4 times from the mesh step 2, but the result of maximum stress increased just only 8%.

Therefore, it can be assumed that with the smaller mesh size, it may not be necessary. With the results that are less than 10% different with greatly increased simulation time.

4.2.5.3 Holder pillar

The grid convergence on the holder pillar design is separate into 3 zones. The maximum acceleration of battery packs of this design occurred at t = 1.6 s. The zone area of holder pillar design and the stress distribution on each element are show in Fig and Fig., and the maximum stress value chosen will be show in the table.

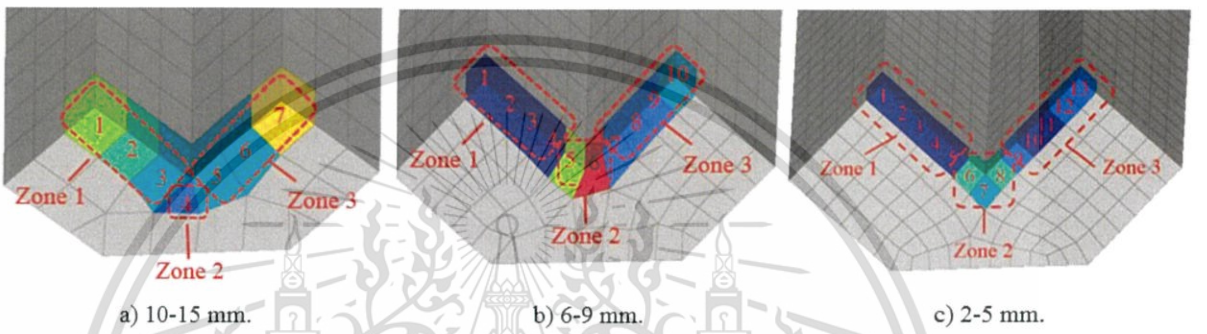

Figure 4.57 The zone area of holder pillar on each step of mesh refinement

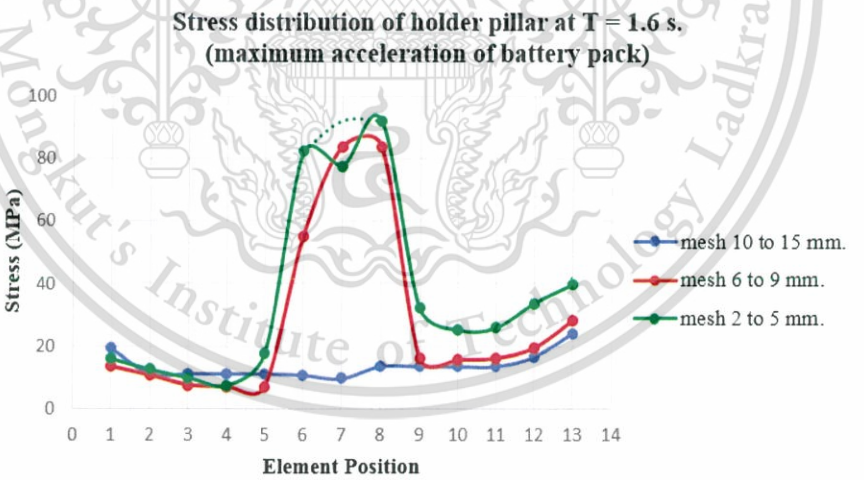

Figure 4.58 The maximum stress of each element of battery holder design at time T=1.6 s.

Table 4.9 The comparison of maximum stress differences of the holder pillar from 3 step of meshing

Step of mesh refinement	Max. stress (MPa)	% Gap	Solid elements	Increase in number of element (Times)	Nodes	Increase in number of nodes (Times)
Mesh step 1 (10-15 mm.)	13.50	x	10,288	x	15,424	x
Mesh step 2 (6-9 mm.)	84.87	528	35,224	3.42	46,622	3.02
Mesh step 3 (2-5 mm.)	92.29	9	113,876	3.23	143,544	3.08

From the analysis of grid convergence methods for this design, it was found that the coarse mesh gave a very different effect. Observed by the stress distribution in mesh step 1, 10-15 mm., there is a very different behavior compared to the finer mesh, mesh step 2 and 3. When observed in the following sequence, it will be found that the size of the finer mesh of the two steps causes the behavior of the stress distribution to be similar. Therefore, it can be interpreted that this mesh size, 10-15 mm., may not be suitable for this geometry of holder. For the mesh step 2 and 3 can be noticed that the trend of maximum stress quite similar, with only 9% difference compared to the number of elements that have increased by 3.2 times.

From all these simulations, the size of the element has chosen as acceptable in both of the results and the duration time to compute. As mentioned above, the calculation of simulation time depends on the number of elements. When the number of elements greater, it will take longer to compute. The accuracy of the calculation should be within the acceptable range of the duration of simulation and the results.

4.2.6 Static Analysis

The study of the durability of the battery holder with dynamic analysis techniques has been presented above. This section is an additional part of the static analysis which can be referenced in the field of initial design. Including to study further the fatigue limit. This static analysis focus to the finite element model is in steady state condition, no external force, only the weight of battery packs. To investigate the initial stress occurring within the finite element model of each design. The analysis on this topic will be consider on the stress of the battery pack mounting and the roof structure.

4.2.6.1 Battery packs mounting

The stress that occurs on the battery packs mounting in each design is different depending on the geometry of the mounting, as well as the different gripping characteristics according to the purpose of each design. The result of static stress of each battery packs mounting is show in Figure 4.59.

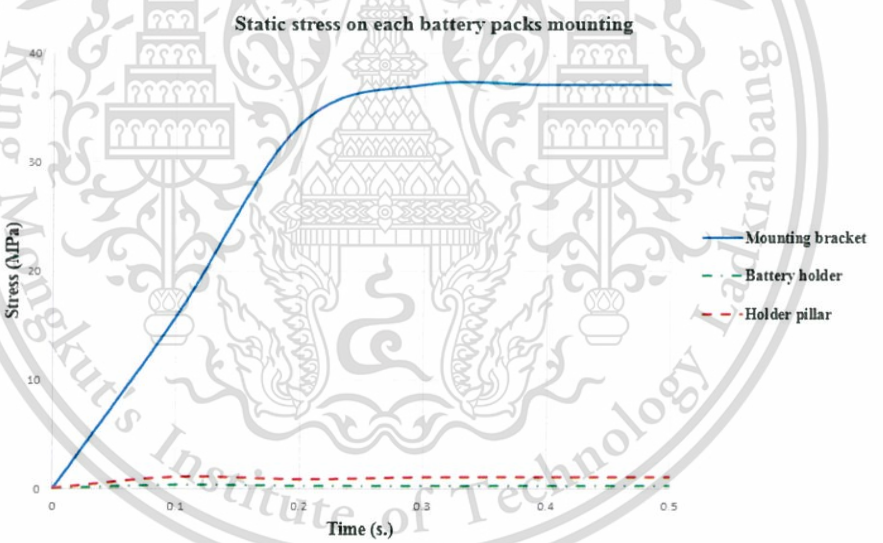

Figure 4.59 The static stress on each battery pack mounting design

From the Figure 4.59, it can be observed that the stress occurs on the mounting bracket design is the highest magnitude due to the characteristic of connection of the bracket causing each bracket carry the weight of the battery. So, it can be seen that in the mounting bracket design has the highest stress about 37 MPa. In the same way, the stress in the battery holder and holder pillar designs quite not occurs, since the two design of battery packs mounting are designed as the holder by eliminating the

movement of the battery pack. In this static way, the battery pack does not move. There is no force act on the holder. The stress on each battery holder hardly happens at all.

4.2.6.2 Roof structure

To study the static behavior of the battery packs mounting on the roof structure. The stress analysis on the roof structure was discussed.

First design of battery packs mounting, mounting brackets, the static stress on the roof structure is about 77.10 MPa. The static stress distribution and magnitude of stress are show in Figure 4.60 and Figure 4.61.

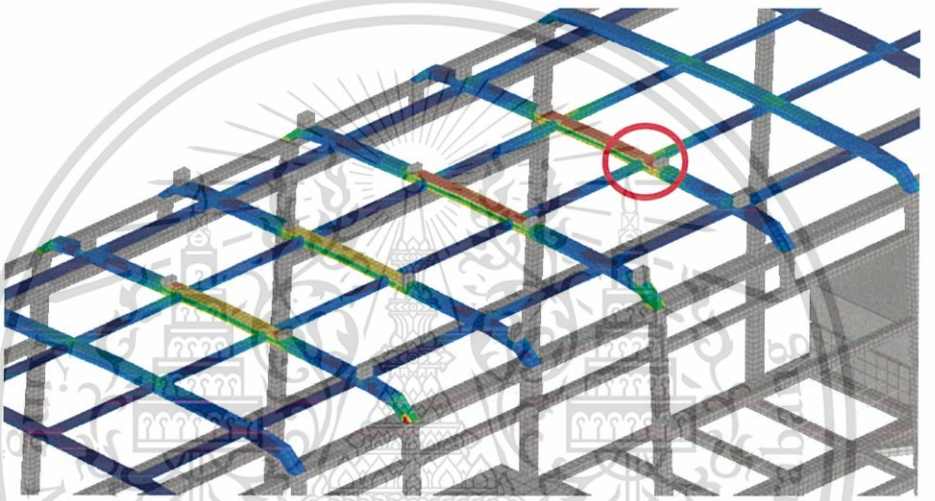

Figure 4.60 The static stress distribution on roof structure of mounting bracket design

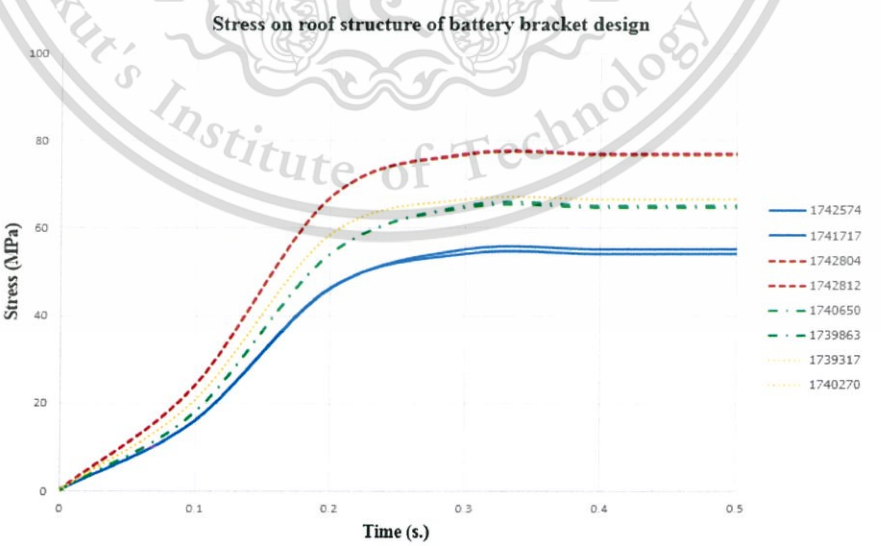

Figure 4.61 The static stress on roof structure of mounting bracket design

The second design, battery holder. The static stress on the roof structure is about 82.58 MPa. As Figure 4.62 and Figure 4.63.

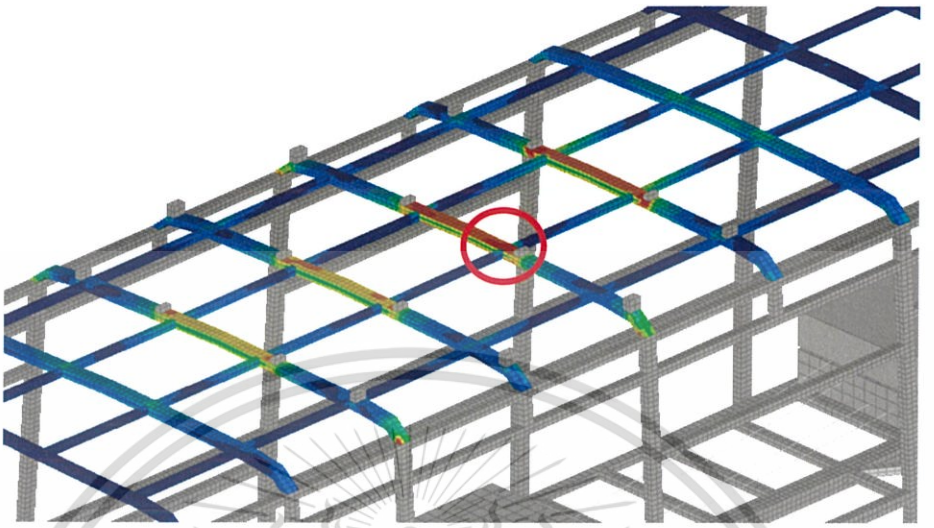

Figure 4.62 The static stress distribution on roof structure of battery holder design

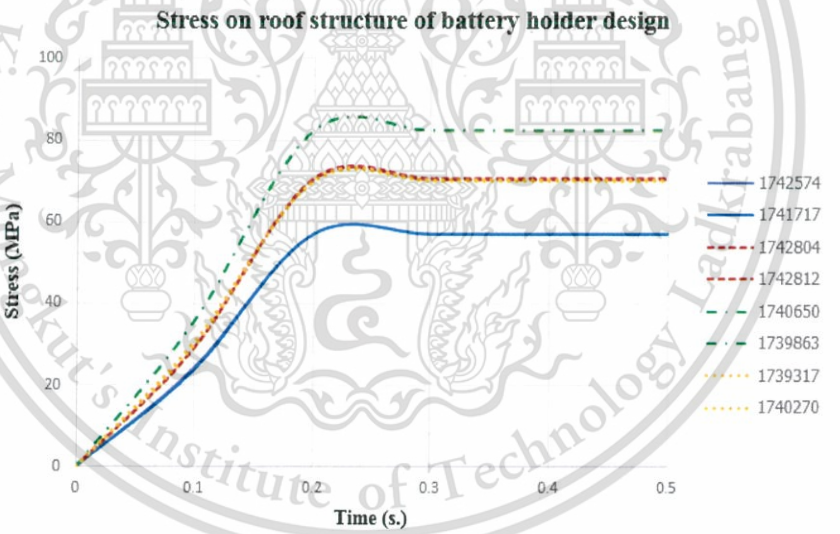

Figure 4.63 The static stress on roof structure of battery holder design

And the last design of battery holder, holder pillar. The static stress on the roof structure is about 81.91 MPa. As show in Figure 4.64 and Figure 4.65.

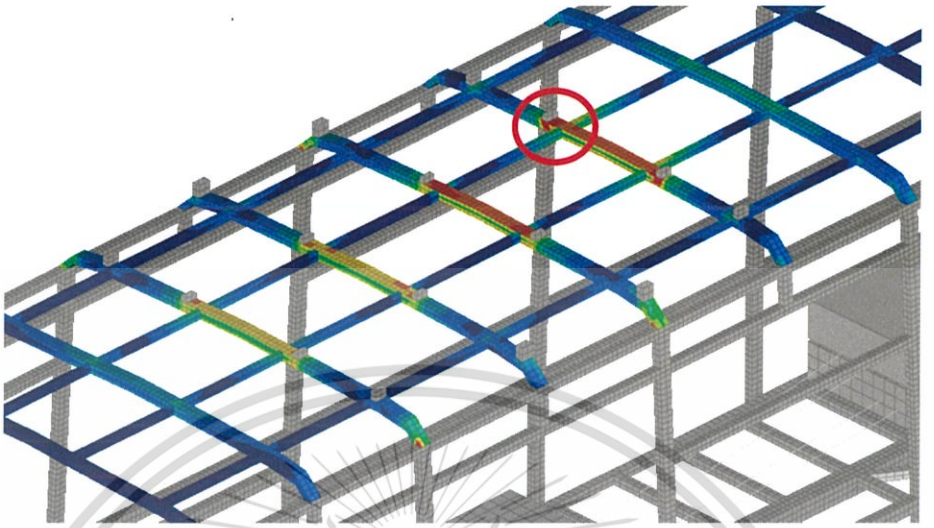

Figure 4.64 The static stress distribution on roof structure of holder pillar design

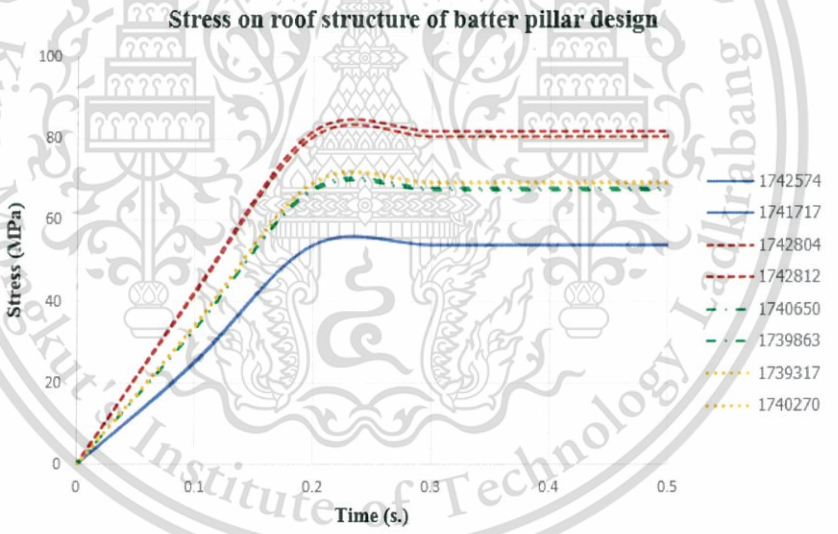

Figure 4.65 The static stress on roof structure of holder pillar design

As a result of stress analysis on roof structure in each design, it is found that the higher the stress depends on the weight of each design. Therefore, resulting in the difference in the stress of 3 different designs. The result of the stress on the roof structure of the 3 designs can be used to calculate the mean value of stress on the roof structure with the weight of the battery packs and the geometry of the battery packs mounting that was presented in this study.

CHAPTER 5

CONCLUSIONS AND DISCUSSIONS

5.1 Conclusions

The study of simulation of a full bus model evaluated the dynamic stress by using the non-linear dynamic analysis. The multi-body system of full 12-metre bus model has been modelled in ADAMS/Car software in order to study the behavior of the force, which appears under the condition through the suspension systems to structure. The full bus model has been simulated by means of a virtual proving ground and an explicit finite element method. The results from a virtual proving ground has been used as desired target responses in the finite element analysis for evaluating the finite element model. The conclusion of this study is discussed in this section.

5.1.1 The vehicle behavior simulation (VPG simulation)

The results from the simulation of multi-body system of full 12-metre bus model by using the virtual proving ground method of ADAMS/Car software is presented. The dynamic displacement of the top mounts of suspension systems model has been measured.

- This analysis gives the demonstration of the complete behavior of the bus vehicle, considering to the non-linear dynamic behavior and multi-body systems of the full bus model.
- The virtual vehicle durability analysis using the virtual proving ground method is highly feasible for the prototype vehicle development process. This method allows the road load input applies to the finite element analysis.
- The simulation of a single bump road profile can predict the location of stress hotspot which were occurred in the actual durability test.
- The longitudinal and lateral displacement were very small values since the digitized road model in this simulation is straight-line road event with the single obstacle. The bump made the longitudinal and lateral displacement as a small frequency. It did not have a significant effect to the vertical direction as mentioned above.

- The simulation of the dynamic displacement of suspension hard point for highly complex structure model, the rigid body model is suitable to both duration time and computational resource. The flexible model represents in the simulation of the finite element analysis.
- The dynamic displacement of suspension top mounts can be used for the reference criteria to design the battery holder.

5.1.2 The large scale of structure model simulation (FEM simulation)

The results of dynamic stresses of the battery pack mounting is explained. The results of battery packs acceleration, the stress on the roof structure, and the mesh refinement analysis are discussed.

- The design of mounting brackets appears the highest stress because the contact of the mounting brackets to battery packs assume as perfect welding, thus the movement of battery packs was directly affected to the mounting brackets.
- With the different contact of the battery packs holders, the free movement of battery packs result in the stress on the battery holder design. They were about 38% lower than the mounting brackets. Moreover, the geometry of this design results in the lowest acceleration of the battery pack.
- The results of stress from the final design revealed that the values obtained were low while comparing to the results of the stress of the two previous designs. The stress distribution decreases about 66%.
- The results of dynamic acceleration and the displacement of battery packs on each design are quite well. The maximum acceleration of the battery packs corresponds to the position of the battery packs because the battery holder causes the maximum stress. The displacement of the battery packs on each design is about 3% different.
- The highest acceleration appears in the holder pillar design due to the geometry of the holder, resulting in the battery packs moving freely in a vertical direction. Whereas, the lowest acceleration appears in the battery holder design because the location of holder is different. Besides, the characteristics of the holder are designed differently from the holder pillar design. It results in the acceleration of the battery pack in the battery holder design decreases by 50% from the holder pillar and different from the mounting brackets about 30%.

- The results of stress on the roof structure also corresponds. The location of stress hotspot occurred at the same position of the battery packs on each design. The magnitude of stress on each design is about 8% differently. It depends on the different of geometry of the battery holder.
- The grid independent method describes the mesh refinement in a good way. The rough mesh as 10-15 mm. gives a rough result of all design. The error of the result may be high and it notices from the holder pillar design. The behavior of stress is very different from the two steps of mesh refinement, 6-9 mm., and 2-5 mm. It notes that this mesh size inappropriate for calculating of the geometry holder pillar.
- The mesh size 6-9 mm provides the results more accurate than the first mesh size. The maximum stress varies up to 86% in the mounting bracket design with the number of elements increasing by 2.4 times. The mesh size 10-15 mm. of the holder pillar design is not interested in the comparison since the behavior of stress obtained from the rough mesh. It is not reasonable while comparing to the mesh size 6-9 mm., and 2-5 mm.
- The increasing number of elements result in more accurate, on the other hand, it increases the duration of calculation time. The grid independent method observes that the maximum stress with mesh sizes 6-9 mm. and 2-5 mm. from the mesh refinement method has a different less than 10% with elements increased up to 3.4 times. As well as, the duration of simulation time is quite raised more than 4 times from mesh size 6-9 mm. Therefore, the mesh size as 6-9 mm. is the most suitable option for the finite element model of these 3 holder designs.

5.2 Discussion

This study presents the method of analysis the durability of vehicles. The results from both the virtual proving ground simulation and the finite element analysis simulation show a quite reliable direction. However, the simulation of this study cannot validate to the virtual vehicle excitation, due to the limitation of research and resource, the set of the results can only be calculated by the computational of commercial software. On the other hand, the results from the excitation or the physical measurements are not always exactly true. Because the inaccuracy of equipment and human error can be influenced. Therefore, the discrepancies may not only derive from the virtual simulations, but also the minor errors related to physical measurements.

The multi-body model of this study is a large scale. The author tries to use his best intentions and the precision in modeling process. The detail of suspension system of the virtual proving ground simulation has a significant impact on the performance of the full vehicle model. The sensitivity of the subsystem affects to the stability of vehicle modal behavior. This method can observe the behavior of the dynamic displacement of the suspension system while travel over the obstacles. The result of dynamic displacement shows a strong correlation with the road profile. In the same way, the large-scale model is a problem in the finite element modeling process. The errors of modelling have different effects on the finite element simulation behavior. In the finite element modeling process, there are an irregularity errors as a result of the size and the complexity of the model. The author tries his best to confirm that the model does not have any serious errors.

The finite element analysis can provide a greater understanding of the full vehicle system under simulated with road load from the virtual proving ground simulation. This method can be applied to study the vehicle model in order to simulate the durability of structure and to identify areas of highest stress including the fatigue life. The results of stress on the battery packs holder give the different behavior of dynamic stress with different geometry. In term of the durability of the roof structure, the result of stress distribution and the dynamic displacement of the battery packs show that the battery holder design has the lowest affect to the strength of the roof structure. Both results will notice that there is approaching to steady. In addition, the acceleration of the battery packs has minimum magnitude. Therefore, this design is the most appropriate to handle the battery packs on the roof structure. From all the results of the grid convergence

analysis, it is obviously that after the 3 steps of the mesh refinement, the result of the maximum stress distribution is less than 10% different with the number of elements increasing more than 3.4 times, then requires more simulation time than necessary. The author considers the difference that occurs within the acceptable range of result. The increasing duration of the simulation time result in difference less than 10% unnecessary. Therefore, the author concludes a recommendation for the 6-9 mm. mesh size appropriates for the design of battery packs holder which has the geometry similar to the presented above only.

Another variation that would have influenced on the result is the actual excitation. As the author mentioned above, this study was unable to perform a real bus experiment due to the limitation of the resources available and it was impossible to compare the simulation results to actual bus with different structure. The author expresses the results in terms of the distribution of stress on the other components and the acceleration of the battery packs. This study explains and verifies the stress behavior on the battery packs mounting which focuses and confirms the analytical method.

However, in order to validate the analytical results, the actual experiment was also imperative to be able to verify the results of computational simulation.

REFERENCES

Aakanksha Gaur, T. E. of E. B. (2014, November 19). Proving ground testing. Retrieved from https://www.britannica.com/technology/proving-ground

Altair Engineering, Inc. (2009). *RADIOSS THEORY MANUAL - 10.0 version - Large Displacement Finite Element Analysis PART 1* (Vol. 2009). Altair Engineering, Inc., World Headquarters: 1820 E. Big Beaver Rd., Troy MI 48083-2031 USA.

Altair Engineering, Inc. (2016). Altair Engineering, Inc.

Arthur Tang. (2000). Virtual Proving Ground – A CAE Tool for Automotive Durability, Ride & Handling and NVH Applications. (Vol. 2000). Presented at the 6th International LS-DYNA Conference.

Ashish Kumar Choudhary, & Rakesh Grover. (2017). Seat belt anchorage CAE correlation & Simulation in Radioss (Vol. 2017, p. 6). Presented at the 12th edition of Altair Technology Conference, Altair Engineering India Pvt. Ltd., Bangalore, India.

Atul Kumar, S. K. A. (2015). Drop Simulation of USB Flash Drive (Vol. 2015). Presented at the The 8th International Conference on High Temperature Capillarity, Bad-Herrenalb, Germany.

Bampton, M. C. C., & Craig, Jr., R. R. (1968). Coupling of substructures for dynamic analyses. *AIAA Journal*, *6*(7), 1313–1319. https://doi.org/10.2514/3.4741

Bishop, N. W. & S. (2012). Finite Element Based Fatigue Calculations., *2012*.

Bonato, M., & Goge, P. (2016). Methods for analysis and comparison of automotive vibration tests (pp. 1–6). IEEE. https://doi.org/10.1109/RAMS.2016.7448011

Brian D. Jensen, & Timothy W. McLain. (n.d.). MeEn 335: System Dynamics.

Burgress, A. (1988). TRANSIENT RESPONSE OF MECHANICAL STRUCTURES USING MODAL ANALYSIS TECHNIQUES.

C. M. Wai, Rivai, A., & Bapokutty, O. (2013). Modelling optimization involving different types of elements in finite element analysis. *IOP Conference Series: Materials Science and Engineering*, *50*, 012036. https://doi.org/10.1088/1757-899X/50/1/012036

Cardona, A., Geradin, M., & Doan, D. B. (1991). Rigid and flexible joint modelling in multibody dynamics using finite elements. *Computer Methods in Applied Mechanics and Engineering*, *89*(1–3), 395–418. https://doi.org/10.1016/0045-7825(91)90050-G

Carlos Felippa. (2017). Solid Elements: Overview. In *Advanced Finite Element Methods (ASEN 6367)* (Vol. April 22, 2017, p. Part 3, Chapter 8: Solid Elements: Overview). Department of Aerospace Engineering Sciences, University of Colorado at Boulder, USA.

Chien, S. I.-J., & Kuchipudi, C. M. (2003). Dynamic Travel Time Prediction with Real-Time and Historic Data. *Journal of Transportation Engineering*, *129*(6), 608–616. https://doi.org/10.1061/(ASCE)0733-947X(2003)129:6(608)

Choi, G. S., Min, H. K., & Paik, S. H. (2000). Dynamic Stress Analysis of Vehicle Using Virtual Proving Ground Approach. https://doi.org/10.4271/2000-01-0121

Conle, F. A., & Mousseau, C. W. (1991). Using vehicle dynamics simulations and finite-element results to generate fatigue life contours for chassis components, *13*(3), 195–205.

Cook, R. D. (2001). *Concepts and applications of finite element analysis*. (R. D. Cook, Ed.) (4th ed). New York, NY: Wiley.

Cray Research Inc. (2008). Minivan CFD simulation. Retrieved from http://www.computerhistory.org/makesoftware/exhibit/car-crash-simulation/

Cray Research Inc. (2018). Real and simulated crash test. Simulation performed on Cray supercomputer. Retrieved from http://www.computerhistory.org/makesoftware/exhibit/car-crash-simulation/

Darshan Vijay Wale. (2015). Modelling and Simulation of Full Vehicle for Analysing Kinematics and Compliance Characteristics of Independent (Macpherson strut) and Semi Independent (Twist Beam) suspension system. *IOSR Journal of Mechanical and Civil Engineering (IOSR-JMCE)*, *2015*(6), PP: 16-20.

Darshan Y. M. Reddy, S. P. (2017). *Virtual Full Vehicle Durability Testing of a passenger car* (Master thesis in Automotive Engineering). CHALMERS UNIVERSITY OF TECHNOLOGY, G¨oteborg, Sweden.

Dassault Systèmes SolidWorks Corporation. (2015). Dassault Systèmes SolidWorks Corporation.

Donald C. Craig. (1996). *Extensible Hierarchical Object Oriented Logic Simulation with an Adaptable Graphical User Interface* (Master of Science). Memorial University of Newfoundland, Department of Computer Science, Newfoundland and Labrador, Canada.

Dr. C. M. Ramesha, A. K. G., Singh, A. R. A., & Chetan S Naik. (2015). Modal Analysis and Harmonic Response Analysis of a Crankshaft (Vol. June 2015). Presented at the International Journal of Emerging Technology and Advanced Engineering.

Edara, R., Shih, S., Tamini, N., Palmer, T., & Tang, A. (2008). 18 Wheel Truck Dynamic and Durability Analysis using Virtual Proving Ground (Vol. 2008, p. 14). Presented at the 10th International LS-DYNA Conference.

Engineering Technology Associates, Inc. (2009, March). VPG/PrePost Tutorial, Fatigue Analysis using eta/VPG.

Farhang Aslani, M. Y. (1994, June). Simulation of Proving Ground Events For Heavy Truck Cabs Using ADAMS, MSC/NASTRAN, and P/FATIGUE.

Ferry, W. B., Frise, P. R., Andrews, G. T., & Malik, M. A. (2002). Combining virtual simulation and physical vehicle test data to optimize durability testing. *Fatigue Fracture of Engineering Materials and Structures*, *25*(12), 1127–1134. https://doi.org/10.1046/j.1460-2695.2002.00605.x

Frost,K. J., V. E. (1976). Metal fatigue. VonN. E. Frost,K. J. Marsh,L. P. Pook, Glasgow. Oxford Engineering Science Series. 1. Auflage, Oxford University Press, London. 1974,499 Seiten, zahlr. Bilder, zahlr. Tabellen. *Materialwissenschaft und Werkstofftechnik*, *7*(8), 304–304. https://doi.org/10.1002/mawe.19760070814

Gi Seob Choi, H. K. M., & Jung, J. A. (2003). Vehicle dynamic analysis using virtual proving ground approach. *KSME International Journal*, *17*(7), 958–965. https://doi.org/10.1007/BF02982980

Granlund, J., & Brandt, A. (2008). Bus Drivers' Exposure To Mechanical Shocks Due To Speed Bumps. In *Bus Drivers Exposure to Mechanical Shocks Due to Speed Bumps* (Vol. 2008, p. 10). Society for Experimental Mechanics, USA.

Halfpenny, A., & Pompetzki, M. (2011). Proving Ground Optimization and Damage Correlation with Customer Usage. *SAE International Journal of Materials and Manufacturing*, *4*(1), 620–631. https://doi.org/10.4271/2011-01-0484

Iyidiker Cagri, C. I., Yilmaz Anil, K. N., & Otokar Otobus Karoseri A.S. (2010). Fatigue Life Prediction of a Bus Body Structure Using CAE Tools (Vol. 1, pp.

319–329). Presented at the FISITA 2010 World Automotive Congress, Budapest, Hungary.
JARI. (2013). Proving Ground. Retrieved from http://www.jari.or.jp/tabid/228/Default.aspx
Jens Wittenburg. (2008). *Dynamics of Multibody Systems* (Vol. 2008). Berlin, Heidelberg: Springer Berlin Heidelberg. https://doi.org/10.1007/978-3-540-73914-2
Kim Bladh. (2012). *Virtual full vehicle durability testing of a coach* (Master of Science Thesis Stockholm). KTH (Kungliga Tekniska Högskolan) Royal Institute of Technology, Stockholm, Sweden.
Kim, H. S., Hwang, Y. S., & Yoon, H. S. (2000). Dynamic Stress Analysis of a Bus Systems. In *Proceedings of 2nd MSC Worldwide Automotive Conference, MSC.* (Vol. 2000, p. 10). Dearbon, Michigan, USA.
Krumm, J. (2008). A Markov Model for Driver Turn Prediction. https://doi.org/10.4271/2008-01-0195
Kuo, E. Y., & Kelkar, S. G. (1995). Vehicle Body Structure Durability Analysis. https://doi.org/10.4271/951096
Kyung-Won Suh, M., Suh, K.-W., & Hong, S.-G. (2000). New Approach in Vehicle Durability Evaluation, Virtual Proving Ground.
Lee, Y.-L., Barkey, M. E., & Kang, H.-T. (2011). *Metal fatigue analysis handbook: practical problem-solving techniques for computer-aided engineering*. Waltham, MA: Butterworth-Heinemann.
Liao, L. (2011). A Study of Inertia Relief Analysis. American Institute of Aeronautics and Astronautics. https://doi.org/10.2514/6.2011-2002
Liu, G., Yin, H., Zhang, T., Zhang, H., & Zhou, M. (2015). Fatigue Life Analysis of One Hybrid Bus Frame Based on Road Spectrum (Vol. 2015). Presented at the 3rd International Conference on Material, Mechanical and Manufacturing Engineering (IC3ME), Atlantis Press. https://doi.org/10.2991/ic3me-15.2015.391
Madan G. Kittur, & Ronald L. Huston. (1989). *Mesh Refinement in Finite Element Analysis by Minimization of the Stiffness Matrix Trace* (Technical Report No. 89-C– 019). Lewis Research Center: National Aeronautics and Space Administration.
Madan G. Kittur, & Ronald L. Huston. (1990). Finite Element Mesh Refinement Criteria For Stress Analysis. *Computers & Structures*, *34*(2), 251–255. https://doi.org/10.1016/0045-7949(90)90368-C
Mahendra A. Petale. (2016). Virtual Durability Simulation for Chassis of Commercial vehicle, *03*(02), 1017.
Mahmoodi-k, M., & Davoodabadi, I. (2014). STRESS AND DYNAMIC ANALYSIS OF OPTIMIZED TRAILER CHASSIS.
Marco W. Holtz, & van Niekerk, J. L. (2008). *Modelling and design of a novel air-spring for a suspension seat* (Master of Science in Engineering). University of Stellenbosch, Department of Mechanical Engineering, Faculty of Engineering, Stellenbosch, South Africa.
MSC.Software Corporation. (2005). ADAMS/Tire Using the PAC2002Tire Model.
MSC.Software Corporation. (2012a). MSC.Software Corporation.
MSC.Software Corporation. (2012b, May). *Vehicle Modeling and Simulation using Adams/Car, ADM740 Course Notes*.
Niemi, E. (1995). *Stress determination for fatigue analysis of welded components*. (International Institute of Welding, International Institute of Welding, & International Institute of Welding, Eds.). Cambridge, England: Abington Publ.

Pacejka, H. B. (2006). *Tyre and Vehicle Dynamics* (2nd ed). Oxford: Butterworth-Heinemann.

Pankaj Chandna, G. B., & V.P. Singh. (2008). Finite Element Analysis Of A Bus Body Structure Using CAE Tools (Vol. 2008). Presented at the HyperWorks Technology Conference 2008 Technical Presentations, Bangalore, India.

Pötter, K. (2012). STRUCTURAL DURABILITY AND INTEGRITY IN VEHICLE DESIGN.

Rayakar, R. S., & Bhat, D. S. (2014). Determination of Strength Analysis of Bus Body Carline through FEA.

Ruta, D., & Ozbolt, J. (2016). Dynamic Fracture of Concrete Compact Tension Specimen: Mesh Sensitivity Study. In *Proceedings of the 9th International Conference on Fracture Mechanics of Concrete and Concrete Structures*. IA-FraMCoS. https://doi.org/10.21012/FC9.248

S. Vizzini. (2014). *CMS methods in complete NVH analysis*. CHALMERS UNIVERSITY OF TECHNOLOGY, G¨oteborg, Sweden.

Schwer, L. E. (2008). Estimating Discretization Error using GCI. . . *LS*, 10.

Siemens Industry Software. (1993). Basic Dynamic Analysis User's Guide, 404.

T. Cain. (2017, March 28). 2015 Honda Odyssey EX Long-Term Test: 19,000 Miles And Counting. Retrieved from https://www.thetruthaboutcars.com/2017/03/2015-honda-odyssey-ex-long-term-test-19000-miles-counting/

Tebbe, J. C., Chidambaram, V., Kline, J. T., Scime, S., Shah, M. P., Tasci, M., & Zheng, D. (2006). Chassis Loads Prediction using Measurements as Input to an Unconstrained Multi-Body Dynamics Model. https://doi.org/10.4271/2006-01-0992

Ulf Sellgren. (2003). *COMPONENT MODE SYNTHESIS - A method for efficient dynamic simulation* (Technical Report) (p. 6). Stockholm, Sweden: KTH (Kungliga Tekniska Högskolan) Royal Institute of Technology.

VETR. (2014, December 10). Multi-axis F1 suspension test rig. Retrieved from http://www.invetr.com/dynamics-and-performance/multi-axis-suspension-test-rig

Wang, D., Lin, G., & Zhang, W. (2015). Design of real-time filter for the wheel force transducer. *Sensor Review*, *35*(2), 174–182. https://doi.org/10.1108/SR-06-2014-657

Zhao, S., Li, Y., & Qu, X. (2014). Vehicle Chassis Integrated Control Based on Multimodel and Multilevel Hierarchical Control. *Mathematical Problems in Engineering*, *2014*, 1–13. https://doi.org/10.1155/2014/248676

Zwaanenburg, K. (2002). Integration of Physical and Virtual Prototypes. https://doi.org/10.4271/2002-01-1290

APPENDIX A

PUBLICATION

The 70th JSAE Annual Spring Congress, 24-26 May 2017, Yokohama, Japan

Simulation of Dynamic Stresses on Electric Bus Structure Using ADAMS/Car

Piyawat Paetanom[1)*], Chi-na Benyajati[2)], Panya Kansuwan[3)], Setthaluth Pangkreung[2)], and Masaaki Okuma[4)]

1) International College, King Mongkut's Institute of technology Ladkrabang, Chalongkrung Rd., Ladkrabang, Bangkok, 10520, Thailand (E-mail: pi_paetanom@hotmail.com)
2) National Metal and Materials Technology Center, National Science and Technology Development Agency
3) Mechanical Engineering, King Mongkut's Institute of technology Ladkrabang
4) Department of Mechanical Science and Engineering, Tokyo Institute of Technology

ABSTRACT: The installation of battery packs on the roof of electric city bus is considered. The method of multi-body system (MBS) was used to study the dynamic stresses on a bus structure using commercial ADAMS/CAR. A full skeletal model of 12-metre bus structure was generated with addition of tires, suspension, and chassis as rigid bodies. The bus model was assigned to travel over and interact with digitized road surface of interest, i.e. a single bump, with different heights at different initial velocities. The simulation results included stress distributions on the structure and the positional behavior of the bus during simulated maneuvers.

KEYWORDS: Vehicle development, CAD/CAE, FEM, Multi-body dynamics, Full-vehicle simulation

1. INTRODUCTION

Nowadays, the design of a vehicle structure is of fundamental importance to the vehicle performance. The structure must be strong and durable. It has to be optimized and testing several times. The automotive companies need to reduce in cost and developing time for a new product. The durability test takes away a lot of time on testing process. It is impossible to be tested on a lot of different road surfaces. Including the cost will be very high and show only visible results. So the CAE method has a role in the design section and durability testing for cutting-down the time and cost of testing process. The finite element method has used in this study; it is a useful method of calculation for stress and strain. This method is clearly and precisely for the numerical solution of a wide range of engineering problems.

Many studies on dynamic stress analysis of vehicle have used the Virtual Proving Ground (VPG) approach to obtain the dynamic stress and distribution. The VPG simulation method can continually observe the stress distribution at every timestep and discern the weak points. In order to predict dynamic stress and fatigue criterion of vehicle frame, Gi Seob Choi and Han Ki Min, Seung Hoon Paik did experimented about single bump run test, road load simulation and field test. The prediction results were compared with experimental results and the feasibility of the integrated life prediction methodology was verified. The simulation of the model was run on a single bump at 40km/h. to calculate the reaction force and torque at each joint of the suspension components [1]. Ramesh Edara, Shan Shih, Nasser Tamini, Tim Palmer and Arthur Tang investigated the 18 Wheel Truck.

Dynamic and Durability Analysis using Virtual Proving Ground. To studies the prediction of durability performance of a trailer suspension frame. LS-DYNA contact analysis is used with contact interfaces defined between the tire and road surface to predict the spindle load as well as the component loads and stress/strain time histories. The providing ground test surfaces were modeled as finite element models. The calibrated bump event is very useful for correlation studies between the test and simulation [3].

From the previous studies that shown above are the examples of application of simulation that use in automotive to validation the vehicle components. This application can use in many fields to improve or develop the design of vehicle and can reduce the time and cost to predict the components life time in the vehicle. This study will apply the methods of multi-body system (MBS) in this work to study the dynamic stresses on an electric bus structure using the commercial ADAMS/CAR software.

The MSC ADAMS/CAR is commercial software, typical of the range of multi-body analysis, developed for a simulation of dynamic nonlinear events and could be employed in conjunction with finite element analysis (FEA) to estimate fully analytical road loads and applied to automotive durability to predict the dynamic stress or strain in structural components. Generally, a model containing various important vehicle components including tires, suspension system, chassis and trimmed body, is created in finite element and then assigned to run on and interact with a digitized road surface of interest. This method gives the fast and accurate results where the structure is under the equal condition in the load and constraint to the durability analysis.

In order to provide enough power for all electrical loads to fulfill the requirements as a city bus, the trend is to install as many battery packs as possible onto an electric bus. Finding appropriate locations to accommodate all these battery packs could become a challenge, in both performance and functionality-wise of the bus. The installation of the battery packs on the roof is considered in this study. The method of multi-body system (MBS) was used in this work to study the

dynamic stresses on an electric bus structure using the commercial ADAMS/CAR software. A full skeletal model of 12-metre bus structure was generated by ADAMS/CAR templates. Additionally, the model also consisted of various important vehicle components including tires, suspension system, chassis and structure. All the vehicle components were assumed as rigid bodies while the flexibility of the structural frame was considered to focus on the stresses generated in the bus body. The bus model was assigned to travel over and interact with a digitized road surface of interest, i.e. the single bump test, with different heights at different initial velocities. The resulting stresses on the bus structure could be calculated via a determination of the acting forces from the contacts of tires with road surface to the structure through suspensions. The simulation results included the stress distributions on the structure displayed in a contour plot to identify the potential weak points as well as the positional behavior of the bus during the simulated maneuvers. The maximum value of the stress on the structure was considered. The obtained simulation results would then be used to determine design suitability, in terms of structure and position, of a battery compartment of a city electric bus.

2. PROCESS METHODOLOGY

Modeling

Full bus model was consisted of tires, front and rear suspension systems, power train, steering systems, chassis and skeleton structure. Front suspension system is Low beam front mount type, with an air spring damper on each side. Rear suspension system is 4-bar type. Using 4 air springs to support the weight of the car and absorb the force from the suspension. The air spring damper suspension, the spring can be changed according to the height of the car that referred to by the ride height sensor that attached to the suspension system; this sensor will measure the height of the car. The K value was generated in the air springs to absorb the force and maintain the height of the car. Reduce the frequency of the structure when the height is changed. Tire was expressed as a subsystem, to calculate the stresses that occurred on the bus structure via determination of the acting forces from the tire contacts with road surface to the structure through suspensions. The installation of the battery packs on the roof is considered. Due to a configuration of this design, an overall center of mass of the bus would be shifting to a higher location A full skeletal model of 12-metre bus structure is focused in this study. It was designed in CAD model and generated to finite element model later.

CAD Model

In this study, CAD model of structure of 12 meter bus model has been generated using Solidworks 2015 software. The CAD model consists of a member of structure and battery housing, which have been assembled to full structure of bus model that shown in Fig 1.

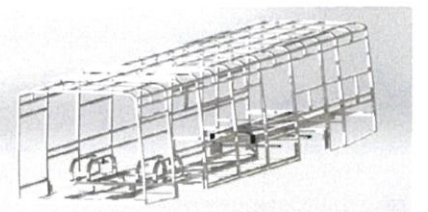

Figure: 1 CAD model in Solidworks

Finite Element Model

The bus structure model in this study was generated by using ViewFlex in Adams/View to generated a Modal Neutral File (MNF) and generate it to the subsystems in Adams/Car to make the rigid part to flexible part. The method of modeling flexibility can be very useful in problems that are characterized by high elasticity and moderate deflections.

The finite element model should imported by the cad model in Parasolid format, in this study will import from Solidworks software. The CAD model has been processes of geometric checkup and remodel in order to get better mesh quality. The size of all the element has been taken not over 15 mm. for maximum size and 10 mm. for minimum size with growth rate 1.5. The sensitive region has been re-meshed automatically by software. The shape of elements is quadrilateral elements and mixed of edge shape, have been used in the analysis. The finite element model of complete bus structure consists of 874,873 elements, 877,412 nodes and 5,264,376 degree of freedoms. All the meshed structure has been created as shell type elements. The complete meshed of bus structure is shown in Fig.2. The model is a 12 meter high floor city bus.

Figure: 2 The finite element model meshing by Adams/View

Road Surface Model

The road surface used in this approach is three-dimensional finite element models of actual road surfaces. The road surface used to perform the Adams/Car road builder module; it is represent the structural strength of the vehicle. The road chosen for this analysis was a single bump condition, to show the period that the force exerted on the structure that caused the highest stress. The model was assigned to travel

over the bump at different initial velocities to discern the stresses that will occurred on the structure of bus model. The bump height 10 is focused. The example of single bump road surface is shown in Fig.3.

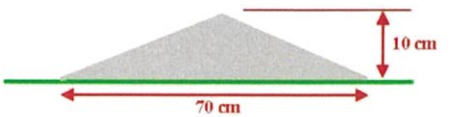

Figure: 3 The single bump road surface model

Boundary Conditions

To determine the stress on the bus structure, the forces that act to the model is essential to identify correctly. The force is the dynamic force that acting to the vehicle at all times, while the model is running on the stress test roads, single bump road. In this study were did two simulations with different condition. First simulation, the initial velocity is defined at 25 km/hr., according to an appropriate speed to run over the bump for the normal case. In additional, the weight of battery has assumed added into the bus model with four different weights, 40 kg, 200 kg, 400 kg and 600 kg. The model assigned to travel over the single bump height 10 cm. The second simulation will upheld the model as the same, bus model with battery 400 kg. And vary the initial velocity defined from 25 to 35 km/hr., according to an appropriate speed to run over the bump for the worse case, assigned to travel over the single bump height 10 cm. The acting forces from the contacts patch of tires with road surface to the structure through suspensions. The properties of 4 models are show in table.1 and table.2 to illustrate the different of weight and the movement of the position of the model CG. And the location of the battery on the structure, which affects the stress that occurs, was located at the roof of the bus structure due to a configuration of this design and investigates the effect of the stress on the bus structure. The weight of the bus model was assumed as only the weight of structure and components not include the weight of passengers to demonstrate the actual stress occurring on the bus structure including the period and location of the critical damage on the structure.

The mass of model

Model	Mass (kg.)
Model with battery 40 kg.	1.4210 E+004
Model with battery 200 kg.	1.4370 E+004
Model with battery 400 kg.	1.4570 E+004
Model with battery 600 kg.	1.4770 E+004

Table.1 Mass of model

The center of mass of model

Model	Location (X,Y,Z) (mm.)	Orientation (X,Y,Z) (deg.)
Model with battery 40 kg.	6165.2686, -4.0500, 697.5604	263.4324, 0.1540, 98.9371
Model with battery 200 kg.	6126.5172, -4.0049, 720.2743	271.5841, 0.7260, 91.6051
Model with battery 400 kg.	6079.2749, -3.9499, 747.9652	274.7511, 1.7530, 90.7705
Model with battery 600 kg.	6033.3120, -3.8964, 774.9061	287.3282, 2.7062, 90.5638

Table.2 Center of mass of model

3. RESULTS

The analysis results show the model with real time stresses and deflection of the vehicle structure. These stresses vary with respect to time. The calculation in this method was done by ADAMS/Car software. The simulation results include the stress distributions on the structure using ADAMS/Post processor and will be plotted in a contour format. This will show the stress distribution by contour plot to discern the potential weak points by using graphic animation, shown in Fig.4. And the results will show the behavior of the vehicle over the condition. The identification of high stress areas design helped to reinforce the structure at high stress areas.

Figure: 4 Von Mises stress contour plot show in graphic animation

First result of stress from simulation, the model traveled over 10 cm. single bump with the same initial velocity, 25 km/hr. The result show that the stress occurred at the same distance in Fig.7 and table 3, shown the result of stress vs distance on different bus model run over the single bump with velocity 25 km/hr.

The result show the maximum Von Misses stress that occurs mostly on the structure takes place at the location of the battery pack number 1 at the node 803040 shown in Fig.5. Therefore, this node will be focused because it is a critical point and to compare the stress with different condition.

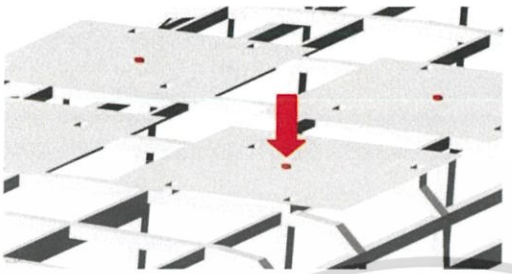

Figure: 5 Location of the battery pack number 1

Figure: 6 Location area of node 803040

Comparison

The comparison of two results of simulation in case of 25 km/hr. traveled over 10 cm. single bump and the same model with 3 initial velocities over 10 cm. single bump.

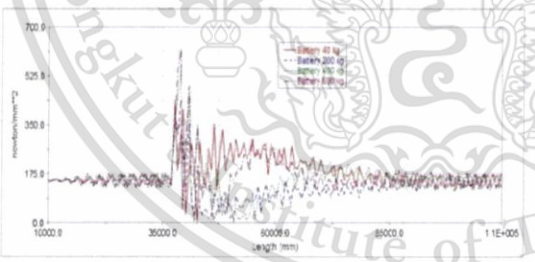

Figure: 7 The results of stress vs distance

Model	Stress (Mpa)
Model with battery 40 kg.	435.460
Model with battery 200 kg.	437.291
Model with battery 400 kg.	551.202
Model with battery 600 kg.	624.987

Table.3 The results of stress

The stress on the bus structure was predicted in this study. The maximum of stress was found to be about 624.987 N/mm^2 in model with battery 600 kg. run over 10 cm. single bump height with initial velocity 25 km/hr. occur at 5.8 seconds. From the result of stress on 4 models, It observed that the stress that occurs is increasing, which is based on the theory of stress.

Another case, the same model with 3 initial velocities over 10 cm. single bump, the model is bus model with battery 400 kg. This case shows the result of stress vs distance in Fig.8.

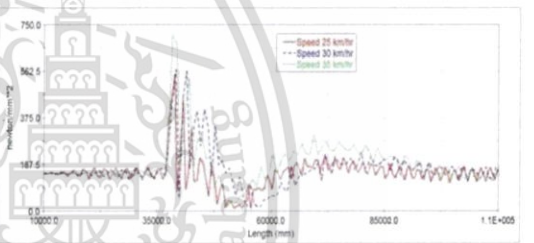

Figure: 8 Stress on bus model with battery 400 kg. travel over 10 single bump with 25, 30 and 35 km/hr.

From the result of stress that show above, it can be seen that the same model with same properties runs on the same road condition but with different initial velocity. The Von Misses stress occurs with different values. When the velocity is increases, the force caused the contacts of tire to structure through the suspension systems while running over the single bump will be increase. These force is affect the stress on the bus structure. It causes stress that occurring at a higher velocity. The result show the maximum of stress was about 707.057 N/mm^2 in case run with 35 km/hr.

4. CONCLUSION

It was not possible to compare quantitatively the results of the bump run on real ground test. However because normally the damage of a vehicle structure comes from the acting forces and loading, so can determine the weak points of vehicle structure by analyzing a single bump condition.

The comparison of the simulation results, there is a clear indication that the model and the method are feasible and reliable. This methodology can be applied to several models of vehicles to identify areas of high stress or reduced fatigue life of components in real road driving conditions. This simulation may make use of different types of road surface can be effectively simulated. The results can be evaluated and analyzed using a fatigue life analysis, which fatigue failure will occurs from the highest stress point. So, it will recommend reducing the stress at this point. The method presented here demonstrates that one model could be used for various functions that are typically completed using several different analyses. Thus, these will give the complete behavior of the vehicle, considering the nonlinear dynamic behavior and multibody systems. This method can save time and money used in the developing the models and experiment durability test.

ACKNOWLEDGEMENT

The authors gratefully acknowledge the financial support from Thailand Advanced Institute of Science and Technology and Tokyo Institute of Technology (TAIST-Tokyo Tech) by National Science and Technology Development Agency (NSTDA)

REFERENCES

1. Gi Seob Choi and Han Ki Min, Seung Hoon Paik., "Dynamic Stress Analysis of Vehicle Using Virtual Proving Ground Approach"., SAE paper number 2000-01-0121.,2000.
2. Kyong-Hwan Mo, Kyung-Won Suh, Seog-Gil Hong., "New Approach in Vehicle Durability Evaluation, Virtual Proving Ground"., Seoul 2000 FISITA World Automotive Congress., June 12-15, 2000, Seoul, Korea.
3. Ramesh Edara, Shan Shih, Nasser Tamini, Tim Palmer, Arthur Tang., "18 Wheel Truck Dynamic and Durability Analysis using Virtual Proving Ground"., 10th International LS-DYNA Users Conference, Simulation Technology (3).
4. Arthur Tang, Nasser Tamini, David Yang., "Virtual Proving Ground – A CAE Tool for Automotive Durability, Ride & Handling and NVH Applications"., 6th International LS-DYNA Users Conference.
5. Marcelo Prado, Rodivaldo H. Cunha, Alvaro C. Neto, Argemiro Costa, Jose E. D'Elboux., "Bus Handling Validation and Analysis Using ADAMS/Car"., 20 April 2016.
6. Mancosu, F. ;Savi, C., "Vehicle sensitivity to tyre characteristics both in open and closed loop maneuvers"., Pirelli Pneumatic, 2000 ADAMS Conference – Rome, November 15-16.
7. Yuan Zhang, Pual Xiao, Tim Palmer and Akbar Farahani., "Vehicle Chassis/Suspension Dynamic Analysis – Finite Element Model vs. Rigid Body Model"., Paper number 980900.
8. Chang-Ro Lee and Jeong-Won Kim, John O. Hallquist, Yuan Zhang and Akbar D. Farahani., "Validation of a FEA Tire Model for Vehicle Dynamic Analysis and Full Vehicle Real Time Proving Ground Simulations"., Paper number 971100.
9. O Kurdi, R Abd-Rahman, M N Tamin., "Stress Analysis Of Heavy Duty Truck Chassis Using Finite Element Method"., Faculty of Mechanical Engineering, Universiti Teknologi, Malaysia.
10. Iyidiker Cagri, Cokal Izzet, Yilmaz Anil, Kilic Namik., "Fatigue Life Prediction of a Bus Body Structure Using CAE Tools"., Otokar Otobus Karoseri A.S, Turkiye., F2010-C-221., June 2010.

The 31st International Electric Vehicle Symposium & Exhibition & International Electric Vehicle Technology Conference, September 30-October 2018, Kobe, Japan.

Simulation of Dynamic Stresses on Battery Pack Holder from Different Road Topologies

Piyawat Paetanom[1)*], Chi-na Benyajati[2)], Panya Kansuwan[3)], and Masaaki Okuma[4)]

1) International College, King Mongkut's Institute of technology Ladkrabang, Chalongkrung Rd., Ladkrabang, Bangkok, 10520, Thailand (E-mail: pi_paetanom@hotmail.com)
2) National Metal and Materials Technology Center, National Science and Technology Development Agency
3) Mechanical Engineering, King Mongkut's Institute of technology Ladkrabang
4) Department of Mechanical Science and Engineering, Tokyo Institute of Technology

Presented at EVS 31 & EVTeC 2018, Kobe, Japan, October 1 - 3, 2018

ABSTRACT: The designing of battery pack holder was the main purpose of this study. The method of multi-body system (MBS) was used in this work to study the resulting dynamic displacement from road topology using the ADAMS/CAR software. The bus model was assigned to traverse over and interact with a digitized road surface, i.e. a single bump. The resulting dynamic on the battery packs during the speed bump maneuvers were translated to non-linear quasi-static software, HyperWork, to calculate the dynamic stress on the battery pack holders. The overall of design aspect for a low-floor electric city bus will be discussed.

KEY WORDS: Electric bus, Energy storage system, Multi-body dynamics analysis, Structural analysis

1. INTRODUCTION

Nowaday, there are many ways of public transport. Buses feature as one of the common choice in many countries throughout the world. With a trend of reducing carbon dioxide emissions from a transportation sector, companies and factories are more involved and coorperative. The electric bus is becoming more and more attractive to contribute. In the field of automobile industry, the most difficult technical problem for electric vehicle is the research on electric vehicle battery[1)], the main challenge faced by the electric vehicle industry is the maximum distance that vehicle can operate per charging cycle. This leads to a wide range of electric bus concepts ranging from large batteries to fast-charging systems with high charging power. Overall, the trend is to install as many battery packs as possible onto an electric bus. Consequently, finding appropriate locations to accommodate all these battery packs becomes a challenge in both performance and functionality-wise of the bus. Furthermore, due to the demand for providing services for the disabled and the elderly people, a low-floor bus has gain preference as a choice for public transport. Nevertheless, a low-floor bus has a limited internal space for installation of the configuration, as well as the number of the battery packs in the lower area of the structure due to the minimum capacity of seats required. For this reason, the battery packs are added into other available space as much as possible including on the roof in order to provide enough power for all electrical loads to fulfill the requirements as a city bus.

According to the battery packs being placed on the roof, the functional of the battery pack holder is required to support the weight of each battery pack and also the movement of the battery packs during various driving conditions. The design of the battery pack holder was the main purpose of this study. The design aspects were evaluated comprehensively according to the strength and durability of the battery pack holder with a dynamic behavior of a electric bus. To reduce in cost and cutting-down in the developing time of a design, as well as minimizing the time required for an eventual time on testing process, the CAE methods were employed in this study.

In this study, the method of multi-body system (MBS) was used to calculate the resulting dynamic displacements resulting from acting with a road topology which, in turn, will affect the battery pack holders. The calibrated bump event is very useful for correlation and durability studies of the vehicle[2)]. The commercial software ADAMS/CAR (MSC Software Corporation,

USA), developed for a simulation of dynamic nonlinear events, was used to estimate fully analytical road loads and to study on dynamic behavior of electrical bus model. The bus model including tires, suspension system, chassis and trimmed body allowed understanding of the loads transmitted to bus structure under different circumstances and to understand the impact of design decisions on these loads in a straightforward way[4].

Furthermore, the finite element method was employed as a mean to calculate corresponding stress and strain. The commercial software, HyperWork RADIOSS (Altair, 2017), was used to solve a large number of high non-linear dynamics problems, with large displacements, large strains, contact and material non-linearity to calculate the dynamic stress. The resulting dynamic displacement on the bus structure during the speed bump maneuvers obtained from the MBS simulation were translated to the Finite Element model of structure of electric bus. To study the dynamic stresses on the battery pack holders located on the roof of bus structure by Finite Element Analysis, a non-linear quasi-static analysis was carried out to find the location of highest stress occurred on different designs of the battery pack holder. The obtained simulation results would then be used to determine design suitability of a roof-top battery compartment of a city electric bus.

2. PROCESS METHODOLOGY

2.1. CAD Modeling

The CAD model of a full skeletal model of 12-metre bus infrastructure was built first in a computer-aided design (CAD) software. The CAD model consists of member of beam structure with different thickness depends on area of structure and thin plates. The CAD model of other compartments were not in a scope of this study. The complete CAD model of electric bus structure is shown in Fig.1

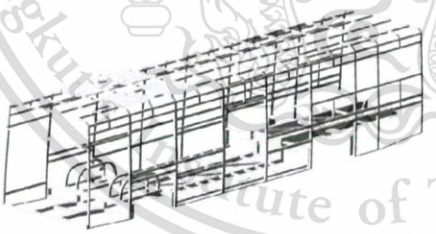

Fig.1 CAD model of electric bus structure

2.2. Full bus modeling

The model of full bus consisted of chassis, skeleton structure, front and rear suspension systems, power train, steering systems, and tires. Front suspension system was a low beam front mount type with air-spring systems, where there were 3 functional components i.e. air-spring, damper and bump stopper, on each side. A rear suspension system was 4-bar type with double air-spring systems. The functional components had 6 functional components (double components) on each side using 4 air springs to support the weight of the car and absorb the force from the suspension. The function of air-spring damper suspension systems, the K value of the spring could be adjusted as appropriate value based on the height of the vehicle which is measured by the ride height sensor that attached on the suspension axle of front and rear suspension systems. Tire was expressed as a subsystem, to calculate the stresses that occurred on the battery packs holder via determination of the acting forces from the tire contacts with road surface to the structure through suspensions.

According to the objective of this study, the full bus model had 12 battery packs, among which 4 packs were located on the roof and 8 packs were inside the bus structure. The installation of the battery packs on the roof was considered and the battery packs holder of battery packs on the roof were investigated. The full assemble bus model of EV is show in Fig.2.

Fig.2 Full bus model assembly in ADAMS/Car

The other components of the electric bus such as doors, seats, windshield, and various interior were excluded. However, their effective mass have been included to the bus structure subsystem already. The properties of the full bus model is show in table 1;

Table.1 Properties of full bus model

Full bus model	Properties		
Mass (kg)	1.4608 E+04		
	X	Y	Z
Location of center of mass (mm.)	7296.44	-3.93	1520.93
Orientation (deg.)	90.62	1.63	269.80

2.3 Road Profile Modeling

A road model was constructed by using Road Builder in ADAMS/Car software. The single bump road profile was chosen in this study to predict the dynamic stress and critical region on the roof structure and nearby battery compartment through suspension systems[3]. The full bus model was assigned to travel over the bump at initial velocity of 25 km/hr. The single bump geometry is show in Fig.3

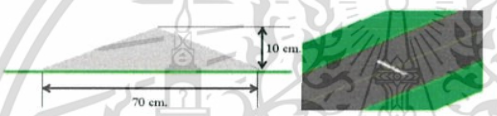

Fig.3 Overall geometry and digitized road of single bump

2.4 Finite Element Model

The CAD of full bus model was imported to the HyperWorks software. The model was extracted to mid-surface and some through processes of geometric checkup and remodel in order to obtain good better mesh quality. The finite element model consisted of 2 different element types; 1D-element (Shell element) on the bus structure and 3D-element (Solid element) on the battery packs holder. The size of solid element on the battery packs holder was around 5-15 mm while the shell element on the other components were not over 35 mm. The shape of elements was quadrilateral elements with mixed of edge shape. The finite element model of full bus structure is show in Fig.4. The material was applied as elastic plastic linear materials. The material properties are shown in table 2.

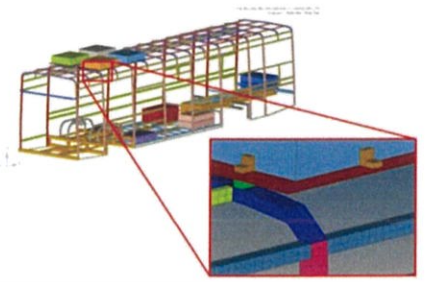

Fig.4 Finite Element model and mesh quality of full bus structure

Table.2 The material properties of finite element model

Material	Steel
Density (kg/m^3)	7.80 E+03
Poisson's Ratio	0.3
Modulus of Elasticity	2.10 E+05

2.5 The battery packs holder design

Three different designs of the battery packs holder were investigated in this study under the same simulation condition.

First design of battery packs holder had the mounting brackets that were attached to the battery packs and locked up to the battery plate on the roof of structure with fastener such as bolts and nuts. There were 8 mounting brackets on each battery pack. The geometry and finite element model of the first design is shown in Fig.5 and 6.

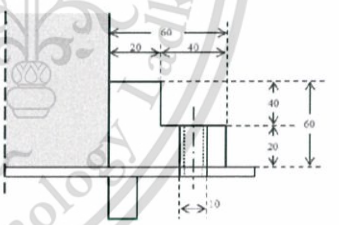

Figure.5 The geometry and dimension (mm.) of the mounting brackets

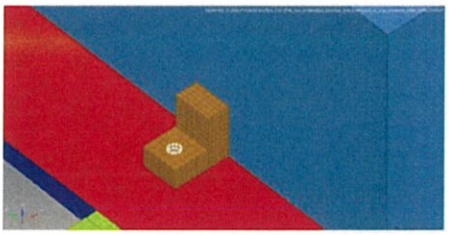

Figure.6 The finite element model of the mounting brackets

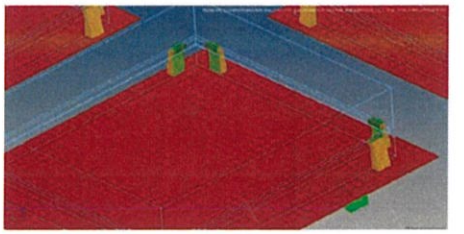

Figure.9 The finite element model of the battery pack holder

A second design concerned about a convenience of replacing of the battery packs. The fasteners were replaced by a set of swing-arm-like configurations to limit the movement of the battery packs such that the battery packs had free movement in 3-axis, Fig.7. The geometry and finite element model of these battery pack holders in second design are shown in Fig.8 and 9.

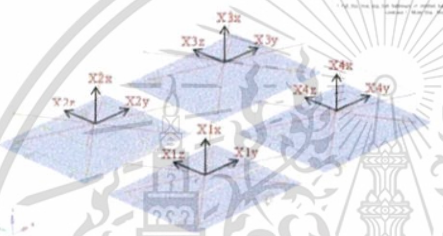

Figure.7 The battery packs free-body diagram

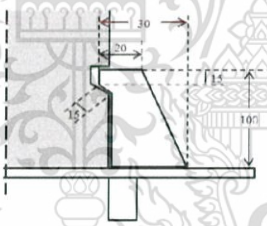

Figure.8 The geometry and dimension (mm.) of battery pack holder

The final design still adhered to the concept of convenience in replacing the battery packs.a set of pillar-shaped holders was introduced to contain the battery pack at all four corners as displayed in Fig.10 and 11.

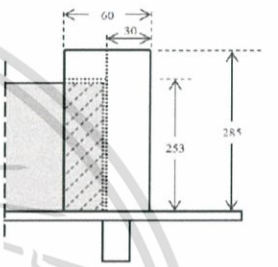

Figure.10 The geometry and dimension (mm.) of the holder pillar

Figure.11 The finite element model of the holder pillar

2.6 Boundary Conditions

In the simulation of proving ground, the full bus model was travelled over and interacted with a digitized road surface of interest, single bump, at an initial velocity of 25 km/hr. The simulation would provided the dynamic displacements of suspension top mount with respect to time. The dynamic displacements of front and rear suspension were then assigned as input to the finite element model to calculate the dynamic stress generated on battery packs holder during the meneuver condition.

3. RESULTS

The simulation results of virtual proving ground were comprised of the dynamic displacements of all front and rear suspension top mounts of full bus model Fig.12. The results were filtered and converted into boundary conditions of finite element analysis.

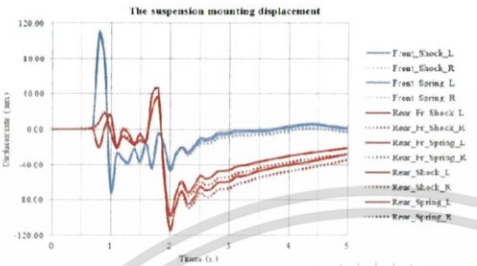

Fig.12 The dynamic displacement curve of front and rear suspension

The obtained dynamic displacements were used as input to the finite element model to calculate the stresses that would occur on the battery packs holders. The trend of resulting stress -that occurred on each design is shown in Fig.13-15. The maximum values of stress determined on each design of battery packs with respect to time are shown in table.3.

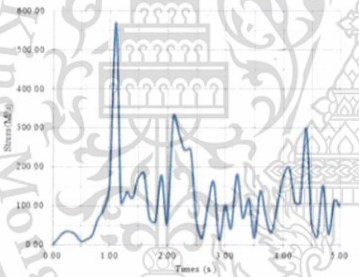

Figure.13 The stress on the mounting brackets design

Figure.14 The displacement of battery packs of the mounting brackets design during the moment of maximum stress occurrence

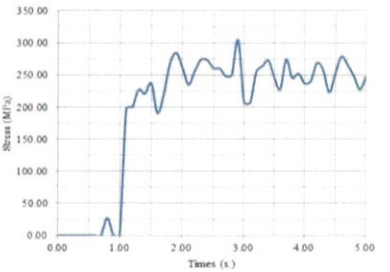

Figure.15 The stress on the battery packs holder design

Figure.16 The displacement of battery packs of the battery packs holder design during the moment of maximum stress occurrence

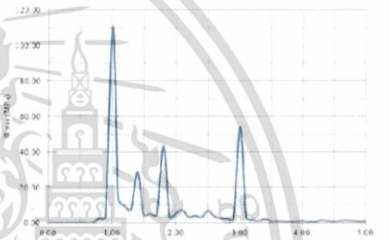

Figure.17 The stress on the holder pillar design

Figure.18 The displacement of battery packs of the holder pillar design during the moment of maximum stress occurrence

Table.3 The maximum stress on each design

Design	Max.Stress (MPa)	Time Step (s.)
Mounting brackets	569.410	1.1
Battery packs holder	304.321	2.9
Holder pillar	110.031	1.0

From the simulations of three different designs of battery packs holder, The resultant maximum stress on the bus structure always occurred at the same location i.e. on the corner of roof structure to side wall panel. The maximum stress occurs when the front suspension systems of the bus model travel over the bump is about 603.083 MPa at 1.1 s. as illustrated on Fig.20 The location of maximum stress is shown in Fig.19.

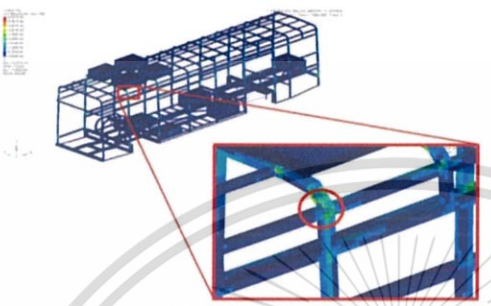

Figure.19 The location of maximum stress on bus structure

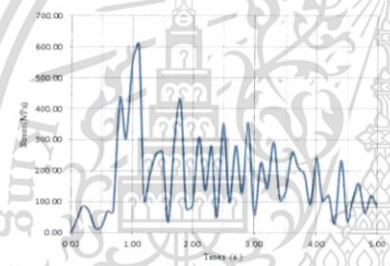

Figure.20 The dynamic stress on bus structure at the location of maximum stress

4. CONCLUSION

From the results of stress shown above, the third design of battery packs holder, holder pillar concept, was subjected to the lowest stress under have the same meneuver condition. Apart from that, the variations in the different design also caused the different location of the stress on the battery pack holders.

However, the simulation technique used in this study demonstrated and the appropriate design of battery mounts that could be applied in the future. The results of stress could also be evaluated and analyzed further in a fatigue life analysis, in which fatigue failure would likely to occur at the highest stress location. In addition, the effect of different types of the road profile i.e. potholes, Belgian blocks road surface could studied further. This method can save time and money used in the developing the models and experiment durability test.

ACKNOWLEDGEMENT

The authors gratefully acknowledge the financial support from Thailand Advanced Institute of Science and Technology and Tokyo Institute of Technology (TAIST-Tokyo Tech) by National Science and Technology Development Agency (NSTDA) and Lightweight Engineering Laboratory, National Metal and Material Technology Center (MTEC).

REFERENCES

(1) Meishi zhou, Huaixian Yin, Tiezhu Zhang, Hongxin Zhang, Gaojun Liu: The Fatigue Life Analysis of the Battery Bracket, International Conference on Advances in Energy and Environmental Science (ICAEES 2015)

(2) Ramesh Edara, Shan Shih, Nasser Tamini, Tim Palmer, Arthur Tang., "18 Wheel Truck Dynamic and Durability Analysis using Virtual Proving Ground"., 10th International LS-DYNA Users Conference, Simulation Technology (3)

(3) Gi Seob Choi and Han Ki Min, Seung Hoon Paik., "Dynamic Stress Analysis of Vehicle Using Virtual Proving Ground Approach", SAE paper number 2000-01-0121.,2000

(4) Ricardo R. Teixeira, S´ergio R. D. S. Moreira and S. M. O. Tavares. Multibody dynamics simulation of an electric bus, 1st International Conference on Structural Integrity, Procedia Engineering 114 (2015) 470 – 477

(5) Kyong-Hwan Mo, Kyung-Won Suh, Seog-Gil Hong., "New Approach in Vehicle Durability Evaluation, Virtual Proving Ground"., Seoul 2000 FISITA World Automotive Congress., June 12-15, 2000, Seoul, Korea.

(6) O. Kurdi, R. Abd-Rahman, M. N. Tamin., "Stress Analysis Of Heavy Duty Truck Chassis Using Finite Element Method"., Faculty of Mechanical Engineering, Universiti Teknologi, Malaysia.

(7) Iyidiker Cagri, Cokal Izzet, Yilmaz Anil, Kilic Namik., "Fatigue Life Prediction of a Bus Body Structure Using

CAE Tools"., Otokar Otobus Karoseri A.S, Turkiye., F2010-C-221., June 2010.

(8) Arthur Tang, Nasser Tamini, David Yang., "Virtual Proving Ground – A CAE Tool for Automotive Durability, Ride & Handling and NVH Applications"., 6th International LS-DYNA Users Conference.

(9) Gaojun Liu, Huaixian Yin, Tiezhu Zhang, Hongxin Zhang, Hongxin Zhang: Fatigue Life Analysis of One Hybrid Bus Frame Based on Road Spectrum, 3rd International Conference on Material, Mechanical and Manufacturing Engineering (IC3ME 2015)

(10) Jostna Ingalea, Prof. A. B. Dighewarb: Design and Optimization of Car Battery Tray, International Journal of Research in Advent Technology, Vol.5, No.2, February 2017, E-ISSN: 2321-9637

(11) Dittapoom Shinabuth, Chi-na Benyajati, Sittikorn Lapapong, Monsak Pimsarn, Masaaki Okuma: Finite Element Analysis of an Electric Bus Body Structure in Real Driving Conditions, The 3rd TSME International Conference on Mechanical Engineering, October 2012, CST 1020

(12) Woongchul Choi1, Jeongyong Kim: Electric Bus with a Battery Exchange System, EVS28 KINTEX, Korea, May, 2015

AUTHOR BIOGRAPHY

Author:	Mister Piyawat Paetanom
Degree:	Master of Engineering
Date of Graduation:	17th December 2018
Date of Birth:	28th August 1992
Place of Birth:	Chiang Mai,Thailand

Undergraduate and Graduate Education:

Master of Engineering in Automotive Engineering,
King Mongkut's Institute of Technology Ladkrabang, Bangkok, 2018

Bachelor degree in Mechanical Engineering,
Mahidol University, Nakhonpathom, 2014

Major: Automotive Engineering

Presentations and Publications:

[1] Piyawat Paetanom, Chi-na Benyajati, Panya Kansuwan, Setthaluth Pangkreung and Masaaki Okuma "Simulation of Dynamic Stresses on Electric Bus Structure Using ADAMS/Car", Technical Paper, 2017, The 70th JSAE Annual Spring Congress, 24-26 May 2017, Yokohama, Japan.

[2] Piyawat Paetanom, Chi-na Benyajati, Panya Kansuwan, and Masaaki Okuma, "Simulation of Dynamic Stresses on Battery Pack Holder from Different Road Topologies", Technical Paper, 2018 The 31st International Electric Vehicle Symposium & Exhibition & International Electric Vehicle Technology Conference, September 30-October 2018, Kobe, Japan.